

**INDOOR POSITIONING SYSTEM USING  
VISIBLE LIGHT COMMUNICATION**

**LEE WILSON**

**UNIVERSITY TUNKU ABDUL RAHMAN**

**INDOOR POSITIONING SYSTEM USING VISIBLE LIGHT  
COMMUNICATION**

**LEE WILSON**

**A project report submitted in partial fulfilment of the  
requirements for the award of the degree of  
Bachelor (Hons.) of Electrical and Electronics Engineering**

**Lee Kong Chian Faculty of Engineering and Science  
University Tunku Abdul Rahman**

**September 2015**

## DECLARATION

I hereby declare that this project report is based on my original work except for citations and quotations which have been duly acknowledged. I also declare that it has not been previously and concurrently submitted for any other degree or award at UTAR or other institutions.

Signature : \_\_\_\_\_

Name : Lee Wilson

ID No. : 10UEB02673

Date : \_\_\_\_\_

## APPROVAL FOR SUBMISSION

I certify that this project report entitled “**INDOOR POSITIONING SYSTEM USING VISIBLE LIGHT COMMUNICATION**” was prepared by **LEE WILSON** has met the required standard for submission in partial fulfilment of the requirements for the award of Bachelor of Degree (Hons.) Electrical and Electronic Engineering at Universiti Tunku Abdul Rahman.

Approved by,

Signature : \_\_\_\_\_

Supervisor : Mr. See Yuen Chark  
\_\_\_\_\_

Date : \_\_\_\_\_

The copyright of this report belongs to the author under the terms of the copyright Act 1987 as qualified by Intellectual Property Policy of Universiti Tunku Abdul Rahman. Due acknowledgement shall always be made of the use of any material contained in, or derived from, this report.

© 2015, Lee Wilson. All right reserved.

Specially dedicated to  
my beloved grandmother, mother and father

## **ACKNOWLEDGEMENTS**

I would like to thank everyone who had contributed to the successful completion of this project. I would like to express my gratitude to my research supervisor, Mr. See Yuen Chark for his invaluable advice, guidance and his enormous patience throughout the development of the research.

## **INDOOR POSITIONING SYSTEM USING VISIBLE LIGHT COMMUNICATION**

### **ABSTRACT**

LED lighting has become popular due to its high efficiency and low power consumption as compared to Fluorescent light. This has led to the Visible Light Communication (VLC) research which opens a dimension in Indoor Positioning System (IPS). In this project, a new method of VLC-IPS is proposed. This method uses four LEDs as transmitter and a photodiode as receiver. The photodiode will receive signals from the transmitters and the current coordinate will be estimated. In this system, unique frequency modulation (F-ID) method is used on the transmitter to prevent interference; while on the receiver, Fast Fourier Transform (FFT) is used to retrieve the transmitted signal. In the meantime, the received signal strength (RSS) and trilateral methods are used to estimate the distance between transmitters and receiver which will then estimate the coordinates of the receiver. The experiments are conducted on situations where there are interferences such as sunlight, fluorescent light and Gaussian noise in the proposed system. The results show that both the performance and the efficiency of the proposed method are competitive and better than the state-of-the-art system; Basic Framed Slotted Addictive – Received Signal Strength strategy and Frequency Division Multiplex – Time Different of Arrival strategy.

## TABLE OF CONTENTS

|  |              |
|--|--------------|
| <b>DECLARATION</b>                     | <b>iii</b>   |
| <b>APPROVAL FOR SUBMISSION</b>         | <b>iv</b>    |
| <b>ACKNOWLEDGEMENTS</b>                | <b>vii</b>   |
| <b>ABSTRACT</b>                        | <b>viii</b>  |
| <b>TABLE OF CONTENTS</b>               | <b>ix</b>    |
| <b>LIST OF TABLES</b>                  | <b>xii</b>   |
| <b>LIST OF FIGURES</b>                 | <b>xiii</b>  |
| <b>LIST OF SYMBOLS / ABBREVIATIONS</b> | <b>xvii</b>  |
| <b>LIST OF APPENDICES</b>              | <b>xviii</b> |

### CHAPTER

|          |   |          |
|----------|---|----------|
| <b>1</b> | <b>INTRODUCTION</b>   | <b>1</b> |
|          | 1.1 Visible Light Communication (VLC) based Indoor Positioning System (IPS) | 1        |
|          | 1.2 Problem Statement   | 3        |
|          | 1.3 Aims and Objective  | 5        |
| <b>2</b> | <b>LITERATURE REVIEW</b>  | <b>6</b> |
|          | 2.1 Visible Light Communication (VLC)                                       | 6        |
|          | 2.2 VLC-IPS Overview  | 8        |
|          | 2.3 VLC-IPS Position Estimation   | 8        |
|          | 2.3.1 Receiver Signal Strength (RSS) Position Estimation                    | 8        |
|          | 2.3.2 Time Different of Arrival (TDOA) Position Estimation                  | 10       |

|          |   |           |
|----------|---|-----------|
| 2.3.3    | Phase Different of Arrival (PDOA) Position Estimation   | 12        |
| 2.4      | VLC-IPS Coordinate Calculation                          | 12        |
| 2.5      | Transmitter Modulation                                  | 13        |
| 2.5.1    | Time Division Multiple Access (TDMA)                    | 14        |
| 2.5.2    | Dual-Tone Multiple Frequency (DTMF)                     | 15        |
| 2.5.3    | Unique Frequency Address (F-ID)                         | 16        |
| 2.5.4    | Carrier Allocation (CA)                                 | 17        |
| <b>3</b> | <b>METHODOLOGY</b>                                      | <b>19</b> |
| 3.1      | Proposed VLC-IPS System Overview                        | 19        |
| 3.2      | Details of Proposed VLC-IPS                             | 20        |
| 3.2.1    | Unique Frequency Modulator (F-ID)                       | 20        |
| 3.2.2    | LED Transmitter   | 21        |
| 3.2.3    | Photodiode Receiver                                     | 21        |
| 3.2.4    | ADC Sampling and Signal Extraction                      | 22        |
| 3.2.5    | Received Signal Strength (RSS) Distance Estimation      | 22        |
| 3.2.6    | Trilateration Coordinate Estimation                     | 24        |
| 3.2.7    | Noise for Visible Light Communication (VLC) System      | 24        |
| 3.3      | Simulation Environment                                  | 27        |
| 3.3.1    | F-ID Modulator, LED and Interferences                   | 29        |
| 3.3.2    | Photodiode (PD) and Analogue to Digital Convertor (ADC) | 32        |
| 3.3.3    | Signal Extracting or Fast Fourier Transform (FFT)       | 34        |
| 3.3.4    | Distance Estimation                                     | 36        |
| 3.3.5    | Trilateral Coordinate Estimation                        | 38        |
| 3.3.6    | Optical Signal Attenuation Computational Model          | 39        |
| 3.3.7    | Others Models in Simulink                               | 40        |
| <b>4</b> | <b>RESULTS AND DISCUSSION</b>                           | <b>42</b> |

|          |  |           |
|----------|--|-----------|
| 4.1      | Result and Discussion of Individual Module                                     | 42        |
| 4.1.1    | Signal Generation  | 42        |
| 4.1.2    | Signal Received  | 47        |
| 4.1.3    | Signal Filtering and Selection   | 49        |
| 4.1.4    | Distance Estimation  | 50        |
| 4.2      | VLC-IPS Performance  | 51        |
| 4.2.1    | Performance with All Interference  | 51        |
| 4.2.2    | Performance without Fluorescent Light Interference                             | 59        |
| 4.2.3    | Comparison between the Performance with<br>Fluorescent and without Fluorescent | 62        |
| 4.2.4    | Performance Comparison with Others Work  | 63        |
| <b>5</b> | <b>CONCLUSION AND RECOMMENDATIONS</b>  | <b>69</b> |
| 5.1      | Conclusion   | 69        |
| 5.2      | Recommendation   | 70        |
|          | <b>REFERENCES</b>  | <b>71</b> |
|          | <b>APPENDICES</b>  | <b>73</b> |

**LIST OF TABLES**

| <b>TABLE</b> | <b>TITLE</b>  | <b>PAGE</b> |
|--------------|---|-------------|
| <b>4.1</b>   | <b>Comparison Table for with or w/o Fluorescent</b>               | <b>62</b>   |
| <b>4.2</b>   | <b>Methods and Environment Setup (Zhang et al., 2014)</b>         | <b>64</b>   |
| <b>4.3</b>   | <b>Summary of Proposed System and Zhang et al. (2014) System</b>  | <b>65</b>   |
| <b>4.4</b>   | <b>Method and Environment Setup (Nadeem et al., 2014)</b>         | <b>66</b>   |
| <b>4.5</b>   | <b>Summary of Proposed System and Nadeem et al. (2014) System</b> | <b>68</b>   |

## LIST OF FIGURES

| FIGURE | TITLE  | PAGE |
|--------|--|------|
| 1.1    | LED Efficiency and Cost per Bulb (Owen Comstock, 2014) | 2    |
| 1.2    | Price Trend Prediction of a 60W LED (Haruyama, 2013)   | 2    |
| 1.3    | World Lighting Trend (Haruyama, 2013)                  | 3    |
| 2.1    | VLC Navigation for Visually Disable Person             | 7    |
| 2.2    | VLC based Robot Control System                         | 7    |
| 2.3    | Orientation of Transmitter and Receiver                | 10   |
| 2.4    | TDOA System Configuration (Jung et al., 2011)          | 11   |
| 2.5    | TDOA System Configuration (Nadeem et al., 2014)        | 12   |
| 2.6    | TDMA Scheme for three LEDs (Yasir et al., 2014)        | 14   |
| 2.7    | DTMF System with Two LEDs (Luo et al., 2014)           | 16   |
| 2.8    | F-ID Transmitter Block Diagram (Jung et al., 2011)     | 17   |
| 2.9    | RF Modulation for LED Transmitter (Kim et al., 2013)   | 18   |
| 2.10   | CA-VLC System (Kim et al., 2013)                       | 18   |
| 3.1    | Basic Block Diagram of Proposed VLC-IPS                | 19   |
| 3.2    | Practical Model of the proposed VLC-IPS                | 20   |

|             |  |           |
|-------------|--|-----------|
| <b>3.3</b>  | <b>Complete VLC-IPS Simulation Model in Simulink</b>   | <b>28</b> |
| <b>3.4</b>  | <b>Continuous Sampling Sine Wave Generator, Discrete Sampling Sine Wave Generator and Square Wave Generator.</b> | <b>30</b> |
| <b>3.5</b>  | <b>System for Sine to Square and Negative Components Elimination</b>   | <b>30</b> |
| <b>3.6</b>  | <b>Simulation Model for F-ID and LED module</b>  | <b>30</b> |
| <b>3.7</b>  | <b>Simulation Model for Fluorescent Interference</b>   | <b>30</b> |
| <b>3.8</b>  | <b>Gaussian Noise Block Diagram in MATLAB</b>  | <b>31</b> |
| <b>3.9</b>  | <b>Overall Optical Transmitter Model for Proposed System</b>   | <b>31</b> |
| <b>3.10</b> | <b>Complete Transmitter Model in Simulink</b>  | <b>32</b> |
| <b>3.11</b> | <b>Default “Gain” model in MATLAB (left) and Photodiode Model in MATLAB (right)</b>                              | <b>33</b> |
| <b>3.12</b> | <b>Simulation Model for ADC Saturation (left) and ADC Quantizer (right)</b>                                      | <b>33</b> |
| <b>3.13</b> | <b>Overall System for Photodiode Receiver</b>  | <b>33</b> |
| <b>3.14</b> | <b>Combine PD and ADC Model in Simulink</b>  | <b>34</b> |
| <b>3.15</b> | <b>Fast Fourier Block Diagram (left) and Complex to Magnitude or Angle Block Diagram (right)</b>                 | <b>35</b> |
| <b>3.16</b> | <b>One to Two Demultiplexor in Simulink</b>  | <b>35</b> |
| <b>3.17</b> | <b>Full Diagram of Signal Conditioning and Extracting Process</b>  | <b>36</b> |
| <b>3.18</b> | <b>Combined FFT Model in Simulink</b>  | <b>36</b> |
| <b>3.19</b> | <b>MATLAB Function in Simulink Environment</b>   | <b>37</b> |
| <b>3.20</b> | <b>Schematic Layout for Distance Estimation Block</b>  | <b>37</b> |
| <b>3.21</b> | <b>Combined Distance Estimation Model</b>  | <b>38</b> |
| <b>3.22</b> | <b>Trilateral Coordinate Estimation Model</b>  | <b>39</b> |

|             |   |           |
|-------------|---|-----------|
| <b>3.23</b> | <b>Optical Signal Attenuation Computational Model</b>                               | <b>40</b> |
| <b>3.24</b> | <b>Sub-model in Simulink</b>  | <b>41</b> |
| <b>4.1</b>  | <b>Time Spectrum for the four F-ID generator</b>                                    | <b>43</b> |
| <b>4.2</b>  | <b>Frequency Spectrum of 1 kHz, 1.25 kHz, 1.75 kHz and 2 kHz F-ID Modulator</b>     | <b>45</b> |
| <b>4.3</b>  | <b>Frequency Spectrum for Fluorescent Lamp with Inductive / Electronics Ballast</b> | <b>46</b> |
| <b>4.4</b>  | <b>Gaussian Noise Spectrum</b>  | <b>47</b> |
| <b>4.5</b>  | <b>Photodiode at Coordinate (3, 3, 1)</b>   | <b>48</b> |
| <b>4.6</b>  | <b>Photodiode Received Signal in Time Spectrum</b>                                  | <b>48</b> |
| <b>4.7</b>  | <b>Photodiode Received Signal in Frequency Spectrum</b>                             | <b>49</b> |
| <b>4.8</b>  | <b>1 kHz, 1.25 kHz, 1.75 kHz and 2 kHz in FFT Result Array</b>                      | <b>50</b> |
| <b>4.9</b>  | <b>Setup for Lambertian Characteristic Determination</b>                            | <b>51</b> |
| <b>4.10</b> | <b>Lambertian Gain with Different Distance between TX and RX</b>                    | <b>51</b> |
| <b>4.11</b> | <b>VLC-IPS Setup for Performance Testing</b>  | <b>52</b> |
| <b>4.12</b> | <b>Result of Estimated and Reference Coordinate in XY plane</b>                     | <b>53</b> |
| <b>4.13</b> | <b>Image on VLC-IPS Accuracy Description</b>  | <b>53</b> |
| <b>4.14</b> | <b>Positioning Error of VLC-IPS</b>   | <b>54</b> |
| <b>4.15</b> | <b>SNR graph of PD Receiver with respect to LED 1 (1, 1)</b>                        | <b>55</b> |
| <b>4.16</b> | <b>SNR graph of PD Receiver with respect to LED 2 (1, 5)</b>                        | <b>56</b> |
| <b>4.17</b> | <b>SNR graph of PD Receiver with respect to LED 3 (5, 1)</b>                        | <b>56</b> |

|             |  |           |
|-------------|--|-----------|
| <b>4.18</b> | <b>SNR graph of PD Receiver with respect to LED 4 (5, 5)</b>                                 | <b>57</b> |
| <b>4.19</b> | <b>SNR graph (Average) of PD receiver in VLC-IPS</b>   | <b>57</b> |
| <b>4.20</b> | <b>Histogram of Positioning Error</b>  | <b>58</b> |
| <b>4.21</b> | <b>Cumulative Distribution Function (CDF) of Positioning Error</b>                           | <b>58</b> |
| <b>4.22</b> | <b>Positioning Error w/o Fluorescent Light</b>   | <b>60</b> |
| <b>4.23</b> | <b>Average SNR w/o Fluorescent Light</b>   | <b>60</b> |
| <b>4.24</b> | <b>Histogram of Positioning Error w/o Fluorescent Light</b>                                  | <b>61</b> |
| <b>4.25</b> | <b>Cumulative Distribution Function (CDF) of Positioning Error w/o Fluorescent Light</b>     | <b>61</b> |
| <b>4.26</b> | <b>Cumulative Distribution Function (CDF) for Positioning Error with and w/o Fluorescent</b> | <b>62</b> |
| <b>4.27</b> | <b>Positioning Error (Zhang et al., 2014)</b>  | <b>64</b> |
| <b>4.28</b> | <b>Positioning Error of Proposed System with Zhang et al. (2014) Environment Setup</b>       | <b>66</b> |
| <b>4.29</b> | <b>Positioning Error (Nadeem et al., 2014)</b>   | <b>67</b> |
| <b>4.30</b> | <b>Positioning Error of Proposed System with Nadeem et al. (2014) Environment Setup</b>      | <b>68</b> |

## LIST OF SYMBOLS / ABBREVIATIONS

|                           |   |
|---------------------------|---|
| $\emptyset$               | Transmitter Angle, degree (°)                 |
| $\varphi$                 | Receiver Angle, degree (°)                    |
| $d$                       | Distance between Transmitter and Receiver, m  |
| $\emptyset_{\frac{1}{2}}$ | Half Angle of Transmitter, degree (°)         |
| $\varphi_{\frac{1}{2}}$   | Half Angle of Receiver, degree (°)            |
| $\Phi_T$                  | Transmitter Optical Flux, lumens              |
| $A$                       | Photodiode Effective Area, m <sup>2</sup>     |
| $N$                       | Total Variance of Gaussian Noise              |
| $\sigma_{shot}^2$         | Variance of Shot Noise                        |
| $\sigma_{thermal}^2$      | Variance of Thermal Noise                     |
| $\gamma^2$                | Responsivity of Photodiode, Ampere/Watt       |
| $P_{ISI}$                 | Intersymbols Interference                     |
| $q$                       | Electron Charge                               |
| $B$                       | Bandwidth of the System                       |
| $k$                       | Boltzmann Constant                            |
| $T_k$                     | Temperature, degree celcius (°C)              |
| $\eta$                    | Fixed Capacitance per unit area of Photodiode |
| $G$                       | Open-loop Voltage Gain                        |
| $\Gamma$                  | FET Channel Noise Factor                      |
| $g_m$                     | FET Transconductance                          |

**LIST OF APPENDICES**

| <b>APPENDIX</b> | <b>TITLE</b> | <b>PAGE</b> |
|-----------------|--------------|-------------|
|-----------------|--------------|-------------|

## CHAPTER 1

### INTRODUCTION

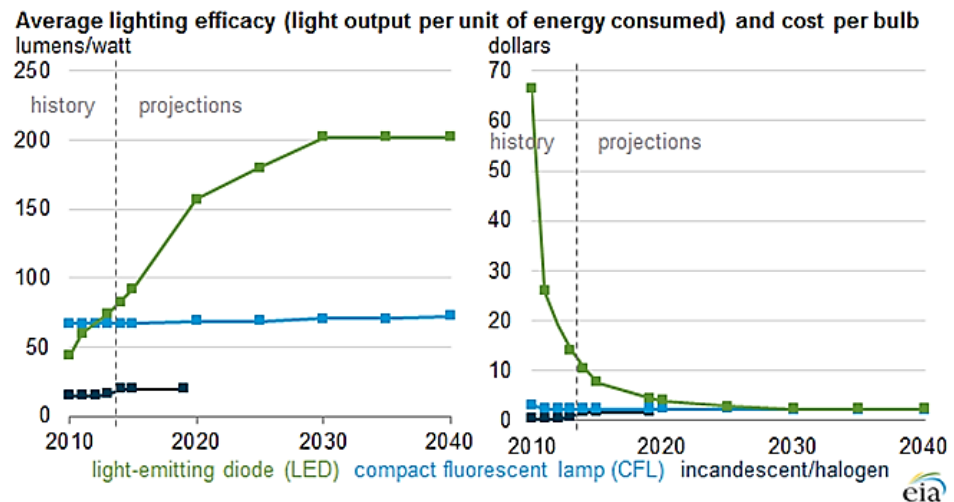
#### 1.1 Visible Light Communication (VLC) based Indoor Positioning System (IPS)

Research on Visible Light Communication (VLC) was begun about 10 years ago according to the published date of Tanaka et al. (2003). During that time, the research on VLC was not popular mainly because of the high production cost of LED. Henceforth, the VLC development is starting to slow down. There have been limited developed appliances in the past ten years. The led research by Tanaka et al. (2003) in the earlier days of VLC is on the VLC based data communication and Komine and Nakagawa (2004) analyses the influences on the reflection and interference in the VLC system.

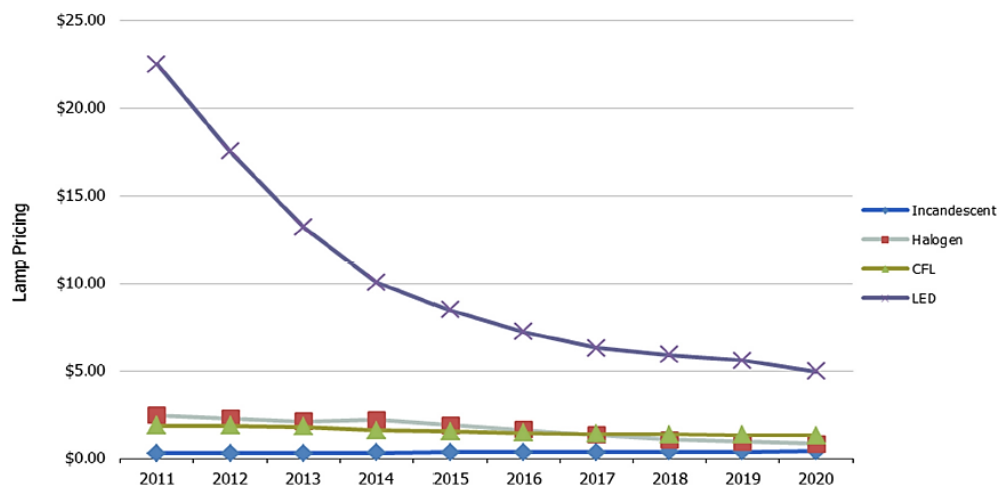
Nowadays, LED lighting is popular because of its high energy efficiency and consumption of less power than incandescent light. This is shown in Figure 1.1. Based on this figure, the implementation of LED light in residential or commercial areas have become more feasible partially due to the low power consumption which reduces the electricity cost. This drives the research on VLC. For example VLC based data communication and VLC based indoor positioning system (IPS).

Figure 1.2 and Figure 1.3 shows the downtrend of LED cost and an increase in market demand on LED lighting system. Based on these figures, switching to LED lighting system becoming more affordable. Hence, this will drive the research on VLC-IPS and its appliances such as indoor navigation for visually impaired persons, VLC

based customer flow analysis in supermarket and robot navigation (Haruyama, 2013). VLC is expected to be the cost effective solution for IPS as it utilizes the existing LED lighting infrastructure in the building for communication.



**Figure 1.1: LED Efficiency and Cost per Bulb (Owen Comstock, 2014)**



**Figure 1.2: Price Trend Prediction of a 60W LED (Haruyama, 2013)**

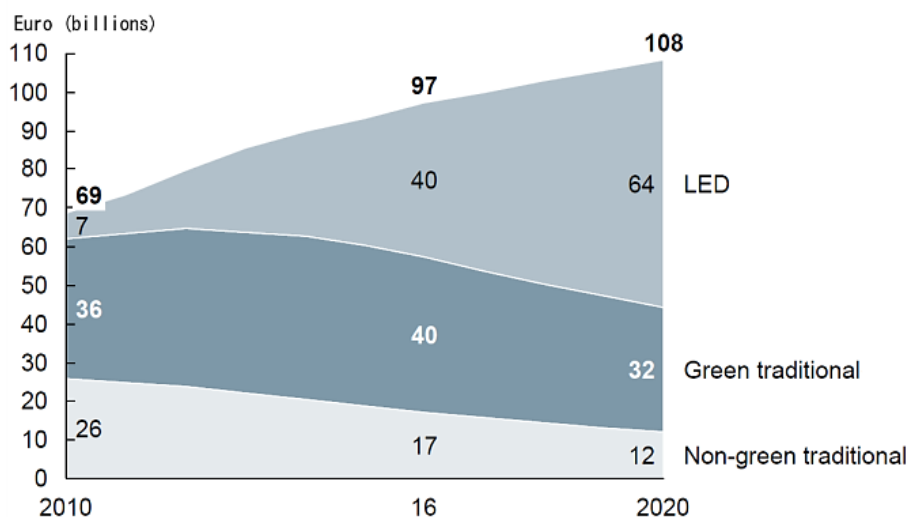


**Figure 1.3: World Lighting Trend (Haruyama, 2013)**

## 1.2 Problem Statement

There are two categories of positioning system, Global Positioning System (GPS) and Indoor Positioning System (IPS). GPS is commonly used in the outdoors for the applications such as smartphone positioning, mobile robot navigation, vehicle navigation system and so on. Although, GPS has been widely used in many appliances but as noted by Yasir et al. (2014) it is not suitable for indoor positioning. One of the reasons is the absence of Line-of-Sight (LOS) between the satellite and the receiver. The absence of LOS may cause the failure in the GPS operation. This is mainly due to the attenuation of GPS signals when traveling through tall buildings, walls or roofs. According to Drane et al. (1998), a GPS signals only have an accuracy of several meters. Based on the research by Barrios and Motai (2011), GPS that uses WAAS-capable GPS receiver offer the accuracy to approximate of 3 meters in 95% of the time but these are not sufficient for Indoor Positioning purposes.

Indoor Positioning System (IPS) is another category of positioning system which mainly aims for indoor appliances. Several method of IPS have been introduced, namely Visible Light, Global Navigation Satellite System (GNSS), Infrared (IR), Ultrasonic, Wi-Fi and Bluetooth. In GNSS positioning method, GPS repeater are installed at the location that necessary for positioning and this method can achieve the

accuracy of 2 meters (Chang et al., 2010). In ultrasonic position method, ultrasonic transmitter and receiver is installed, the time of arrival is used to calculate the position of a person or object and the system accuracy is 10 to 30 millimetres (Yazici et al., 2011). The RF positioning system such as Wi-Fi and Bluetooth, are unlike visible light, IR and ultrasonic system as line-of-sight is not required due to the penetration ability of RF signal. Receive Signal Strength (RSS) is used as a method of sensing in RF positioning system and it is offered accuracy of 3 meters (Lee et al., 2010). Furthermore, RF based IPS is used for internet accessing and positioning but it rises concerns when come to the privacy or use in RF prohibited places such as hospital and airplane (Gu et al., 2009).

Most of the Visible Light Communication (VLC) based technologies in IPS are using LED due to its fast response time, longer life expectancy and consume less power compared to conventional lighting devices such as Incandescent Lamp or old types of Fluorescent Lamp (T-12 or T-8 tubular fluorescent lamp). These LEDs are normally mounted on a ceiling in an enclosed room to ensure a good coverage. Changing of all the existing fluorescent lighting system in a functional area to LED lighting system is costly. Therefore, it is better to mix different lighting technology in an area. Mixing fluorescent lamp with LED can cause interference to the visible light communication (VLC). This might cause the VLC-IPS system fail to operate. This is because, different lighting technology emits light of different frequencies may distort the modulated visible light signals. For example, an inductive powered fluorescent light emits visible light at 100 Hz and electronic powered fluorescent light emit visible light at 20 kHz (Moreira et al., 1995). The interference cause by fluorescent light is important when designing the VLC-IPS.

### **1.3 Aims and Objective**

The objectives of this of project are

1. To develop a method of Visible Light Communication (VLC) based Indoor Positioning System (IPS) that can work with other lighting technologies such as fluorescent light.
2. To present a simulation on the interference from external light source.
3. To develop a VLC-IPS using Frequency Division Multiplexing (FDM) and Receive Signal Strength (RSS).
4. To determine the accuracy and performance of the proposed VLC-IPS.

## **CHAPTER 2**

### **LITERATURE REVIEW**

#### **2.1 Visible Light Communication (VLC)**

Visible Light Communication (VLC) is used for data communication. According to Haruyama (2013), VLC communication required a Line-of-Sight (LOS) communication between transmitter and receiver. The major VLC disadvantages are the distance and data rate. The maximum distance that VLC can have is approximately 100 meter which relatively less compared with Radio Frequency (RF) communication. Further, the data rate of VLC is typically between kilobits to 10 megabits per second.

Although, VLC suffers of distance and data rate problem but it is still valuable in some of the appliances such as VLC navigation system or positioning system. Figure 2.1 and Figure 2.2 show the VLC based Indoor Navigation System for visually disable and robot control system using VLC. Furthermore, some prototype developed for VLC navigation and VLC robot controlling (Haruyama, 2013).



**Figure 2.1: VLC Navigation for Visually Disable Person**

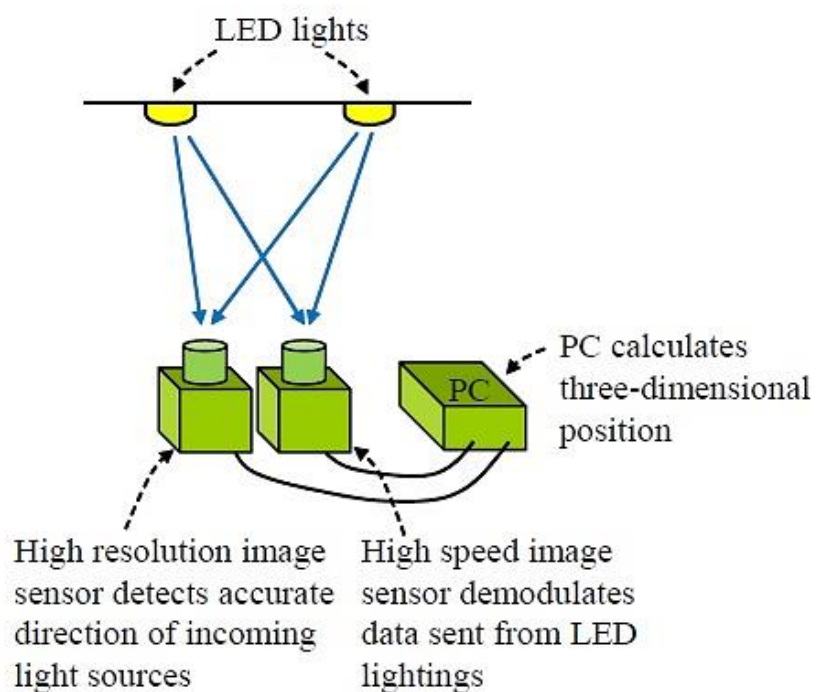


**Figure 2.2: VLC based Robot Control System**

## 2.2 VLC-IPS Overview

Visible Light Communication (VLC) based Indoor Positioning System (IPS) recently become popular due to the advantages of LED. ByteLight is the first company that use VLC, Bluetooth Low Energy (BLE) and Sensors to provide indoor navigation feature by leveraging the existing LED infrastructure inside a building (ByteLight, 2015).

## 2.3 VLC-IPS Position Estimation

There were several method of determine distance between single Visible Light Communication (VLC) signal transmitter and receiver. According to Wang et al. (2013), three method available to determine the distance between transmitter and receiver. These are Receiver Signal Strength (RSS), Time Difference of Arrival (TDOA) and Phase Difference of Arrival (PDOA).

### 2.3.1 Receiver Signal Strength (RSS) Position Estimation

Receiver Signal Strength (RSS) positioning algorithm need to have at least 2 LEDs fixed at the same height and with Line-Of-Sight (LOS) to the receiver. According to Yasir et al. (2014) and Kim et al. (2013), RSS distance estimation algorithm can be express in Lambertian source which can be described by Lambertian equation as below

$$G_{LOS} = \frac{(m+1)A}{2\pi d^2} \cos^m(\emptyset) T(\varphi) g(\psi) \cos^M(\psi) \quad (2.1)$$

where  $T(\psi)$  is the filter gain,  $g(\psi)$  is the concentrator gain,  $\emptyset$  and  $\varphi$  are the transmitter angle and receiver angle by respect to normal respectively,  $m = \frac{-\log 2}{\log(\cos(\frac{\emptyset_1}{2}))}$

and  $M = \frac{-\log 2}{\log(\cos(\frac{\psi_1}{2}))}$ . Further,  $\emptyset_{\frac{1}{2}}$  given by half-angle of the LED transmitter and  $\varphi_{\frac{1}{2}}$

given by half-angle of the photodiode receiver. Figure 2.3 show the orientation of transmitter and receiver. The Eq. 2.1 can further be simplified to Eq. 2.3 by substituting Eq. 2.1 into Eq. 2.2.

$$P_{LOS} = \Phi_T G_{LOS} \quad (2.2)$$

where  $P_{LOS}$  is the received optical power and  $\Phi_T$  is transmitter optical flux.

$$P_{LOS} = \frac{\Phi_T(m+1)A}{2\pi d^2} \cos^m(\varnothing) T(\varphi) g(\psi) \cos^M(\psi) \quad (2.3)$$

By applying the Eq. 2.3, the distance ( $d$ ) between the LED transmitter and the photodiode receiver can be approximated with the knowledge of receiver power strength ( $P_{LOS}$ ), receiver ( $\varnothing$ ) orientation and transmitter ( $\psi$ ) orientation.

Since, concentrator or filter is not implemented in the proposed design, Eq. 2.3 can be further simplified into Eq. 2.4 by substitute filter gain,  $T(\psi)$  and concentrator gain,  $g(\psi)$  to 1 and replace all the constant with a variable 'C'.

$$P_{LOS} = \frac{C}{d^2} \cos^m(\varnothing) \cos^M(\psi) \quad (2.4)$$

$$\text{where } C = \frac{\Phi_T(m+1)A}{2\pi}.$$

According to Kim et al. (2013) RSS IPS design, three LEDs were used as transmitter and a photodiode is used as receiver. Initially, the three LEDs were connected to Arbitrary Waveform Generator (AWG) to get frequency modulated in order to prevent inter-cell interferences. The transmitted signal then recovered by using photodiode with trans-impedances and low noise amplifier. The received signal power is varied according to distance and angle. This is shown in Eq. 2.4. Increase of distance and angle from  $0^\circ$  to  $90^\circ$  will decrease the received signal power. Furthermore, the signal to noise ratio (SNR) will be reduced when the distance increased. Lastly, the received signal which used to model using Lambertian property. The signal strength is used to calculate for the distance and estimate for coordination.

Based on the experiment done by Kim et al. (2013), the RSS positioning algorithm achieved the accuracy of 7cm.

After review RSS position estimation, RSS position estimation have less complexity compared to Time Different of Arrival (TDOA) and Phase Different of Arrival (PDOA). Further, RSS position estimation also does not required synchronization for all the transmitter. Moreover, RSS position estimation method less immune to noise and less accuracy as compared to TDOA and PDOA method.

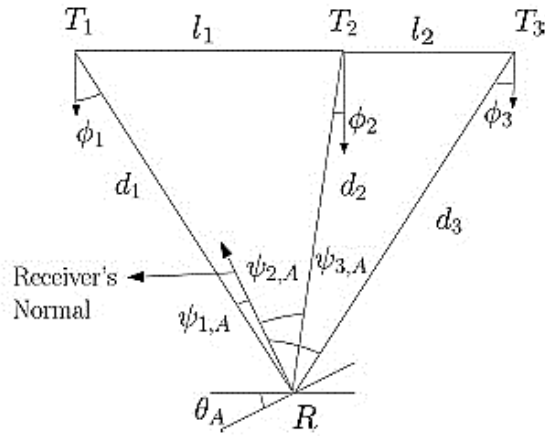


**Figure 2.3: Orientation of Transmitter and Receiver**

### 2.3.2 Time Different of Arrival (TDOA) Position Estimation

Time Different of Arrival (TDOA) positioning algorithm is required three LEDs determine the position of the object. According to Jung et al. (2011) and Nadeem et al. (2014), the TDOA can be calculated by detecting the phase different of the signal. Figure 2.4 and Figure 2.5 shows the typical systems configuration for TDOA system. According to Jung et al. (2011) TDOA system, three LEDs transmitter had been modulated with 3 different frequencies with unique frequency address (F-ID). After the transmitter had been assigned with F-ID, these transmitters will emit their own frequency modulated light and the power of the modulated light can be represented by Eq. 2.5.

$$\begin{aligned}
 P_{LED1} &= P_{CONT} + P_{MOD} \cos(2\pi f_1 t + \varphi_0) \\
 P_{LED2} &= P_{CONT} + P_{MOD} \cos(2\pi f_2 t + \varphi_0) \\
 P_{LED3} &= P_{CONT} + P_{MOD} \cos(2\pi f_3 t + \varphi_0)
 \end{aligned} \tag{2.5}$$

which  $P_{CONT}$  is the power of the continuous optical signal,  $P_{MOD}$  is the power of the modulated optical signal and  $\varphi_0$  is the initial signal phase.

The modulated light is received by photodiode. The output of photodiode is feed into a Band-Pass Filter to retrieve the signal. Band-Pass Filter is needed to

eliminate unwanted signal and LED inter-cell interference. The signal output of the band-pass filter can be represented by Eq. 2.6.

$$E = L \cos\left(2\pi f \left(t - \frac{d}{c}\right) + \varphi_0\right) \quad (2.6)$$

where  $d$  is the distance between transmitter and receiver,  $c$  is the speed of light,  $f$  is the transmitter frequency and  $L = 2KRH(0)P_{CONT}P_{MOD}$ .  $K$  is the proportionality constant,  $R$  is photodiode responsivity,  $H(0)$  is the impulse response. The distance between the transmitter and receiver is determined by the detected phase different.

Based on the simulation performance of TDOA system by Jung et al. (2011), the TDOA system is having the maximum location error of 4.5mm and with average location error of 1.8mm.

After review TDOA positioning estimation method, TDOA method having advantages of stronger noise immunity and more precise estimation compared with RSS method whereas TDOA method is necessary synchronization for all the transmitters. Because of that, TDOA method is more complex and high performance processor is needed to detect and differentiate the phase different between two or more received signals.

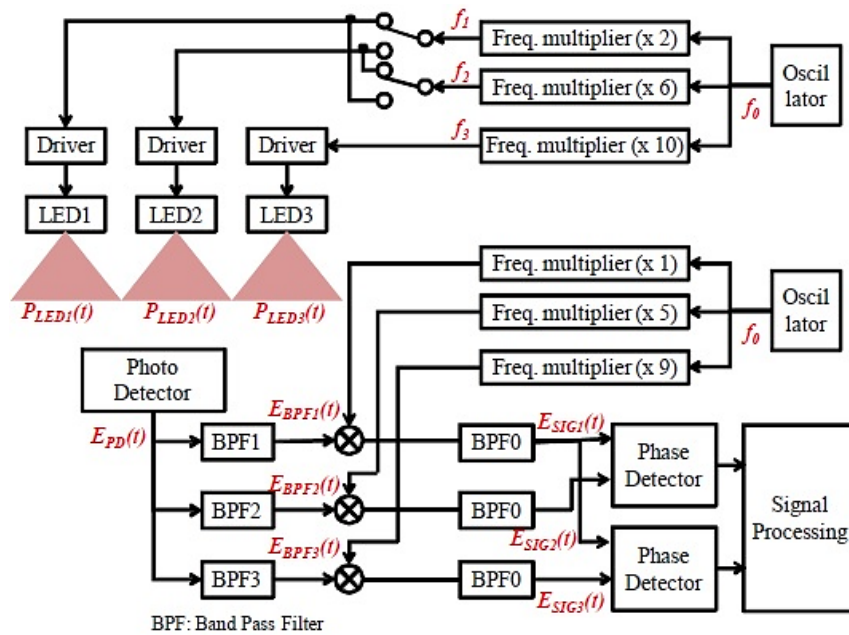


**Figure 2.4: TDOA System Configuration (Jung et al., 2011)**

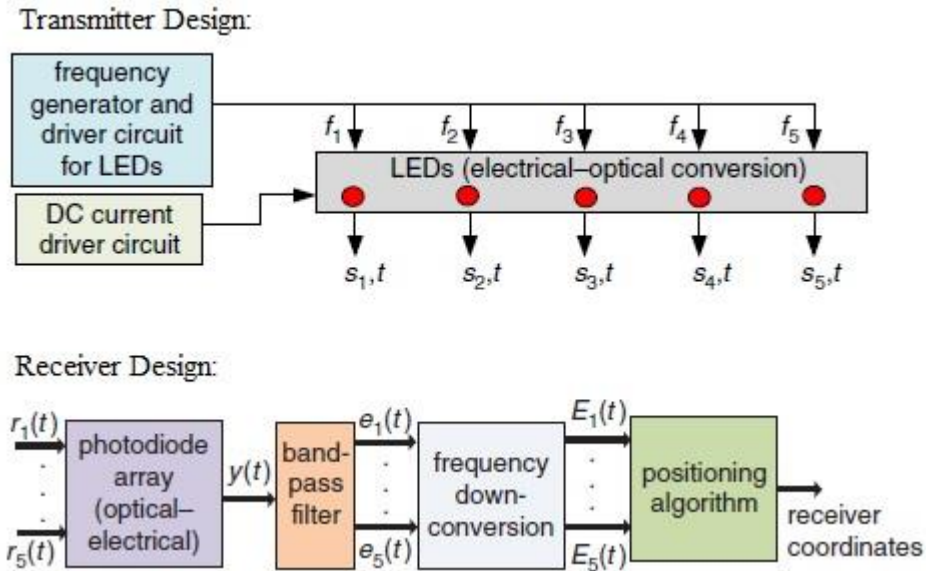


**Figure 2.5: TDOA System Configuration (Nadeem et al., 2014)**

### 2.3.3 Phase Different of Arrival (PDOA) Position Estimation

Phase Different of Arrival (PDOA) algorithm needs to work with Time Different of Arrival (TDOA) to obtain the distance between transmitter and receiver. According to Jung et al. (2011) and Nadeem et al. (2014), the PDOA algorithm were initially used for phase different detection and TDOA algorithm is used to determine the distance between transmitter and receiver by processing the phase different of received signal.

## 2.4 VLC-IPS Coordinate Calculation

Coordinate Calculation is the important in Indoor Positioning System (IPS). Received Signal Strength (RSS), Time Different of Arrival (TDOA) and Phase Different of Arrival (PDOA) are only used as a method to determine the distances between transmitter and receiver. Hence, coordinate calculation is needed to utilize the distance calculated by RSS, TDOA or PDOA method to form coordination as a part of positioning system. According to Kim et al. (2013), the coordinate can be calculate

using Trilateration method and distance data from RSS calculation. Trilateration method can be express in Eq. 2.7.

$$(x_e - x_i)^2 + (y_e - y_i)^2 + (z_e - z_i)^2 = d_{c_i}^2 \quad (2.7)$$

where  $i = 1, 2, 3 \dots$ ,  $x_e, y_e, z_e$  are the estimated coordinate,  $x_i, y_i, z_i$  are the transmitter coordination and  $d_{c_i}$  is the measured distance between the transmitter and receiver. If three transmitter is used Eq. 2.7 can be expanded as Eq. 2.8.

$$\begin{aligned} (x_e - x_1)^2 + (y_e - y_1)^2 + (z_e - z_1)^2 &= d_{c_1}^2 \\ (x_e - x_2)^2 + (y_e - y_2)^2 + (z_e - z_2)^2 &= d_{c_2}^2 \\ (x_e - x_3)^2 + (y_e - y_3)^2 + (z_e - z_3)^2 &= d_{c_3}^2 \end{aligned} \quad (2.8)$$

estimated position  $(x_e, y_e)$  can be obtained by using two of the linear equation in Eq. 2.8 and  $z_1 = z_2 = z_3$ .

If the estimated position is obtained by subtracting the second and third equation in Eq. 2.8, the equation can be express in matrix form shown in Eq. 2.9.

$AX = B$  where

$$\begin{aligned} A &= \begin{bmatrix} x_2 - x_1 & y_2 - y_1 \\ x_3 - x_1 & y_3 - y_1 \end{bmatrix}, X = \begin{bmatrix} x_e \\ y_e \end{bmatrix} \\ B &= \begin{bmatrix} (d_{c_1}^2 - d_{c_2}^2 + x_2^2 + y_2^2 - x_1^2 - y_1^2)/2 \\ (d_{c_1}^2 - d_{c_3}^2 + x_3^2 + y_3^2 - x_1^2 - y_1^2)/2 \end{bmatrix} \end{aligned} \quad (2.9)$$

The Eq. 2.9 can be solve by using the linear least mean square method which given by

$$X = (A^T A)^{-1} A^T B \quad (2.10)$$

Finally, by using Eq. 2.10 the coordinate is approximately estimated by measured signal strength.

## 2.5 Transmitter Modulation

There have several methods that use as transmitter modulation for Visible Light Communication based Indoor Positioning System (VLC-IPS) to prevent inter-cell interferences such as Time Division Multiple Access (TDMA) method, Dual-Tone Multiple Frequency (DTMF) method, Unique Frequency Address (F-ID) method and Carrier Allocation (CA) VLC method.

### 2.5.1 Time Division Multiple Access (TDMA)

Time Division Multiple Access (TDMA) method consist of a cycle of multiple time slots with equal duration for LEDs lighting to prevent inter-cell interference. According to Yasir et al. (2014), three LEDs is used in the VLC-IPS design. The Received Signal Strength (RSS) is measured in each lighting sequences. The LEDs lighting sequences is separated into four time slot in a cycle with equal duration of 12.5ms. Each LEDs have a unique coordinate and different sequences used for measurement. During first sequences, all LEDs light is turned off and background light is measured. During second sequences, first LED turned on and others remain off. The first LED intensity was measured. During third sequences, second LED turned on and second LED was measured. The sequences is show is Figure 2.6 and the sequence is repeats until all LEDs is at least lighten up once in a cycle. More details, the LED transmitter  $T_i$  is only turned on at  $(i + 1)$ th where  $i = 1 \leq i \leq 3$ . Since, the LEDs light in turned on in different period and the LEDs intensity can be measured by photodiode receiver separately.

After reviewing TDMA method, TDMA method have an advantages of easy setup of the TDMA system because the LEDs sequences can be programmed and controlled by centralized microcontroller. TDMA method, each LEDs have unique coordinate and sequences. It is no extra filtering needed for signal separation. Moreover, TDMA method suffers interferences when the background light intensity is flicking. For example, the TDMA method is used with Fluorescent Lamp which have a flicking frequency of about 100Hz. Furthermore, TDMA method also required synchronization between all the LEDs in order follow sequences hence it necessary to have communication between the LEDs and increase the system complexity.

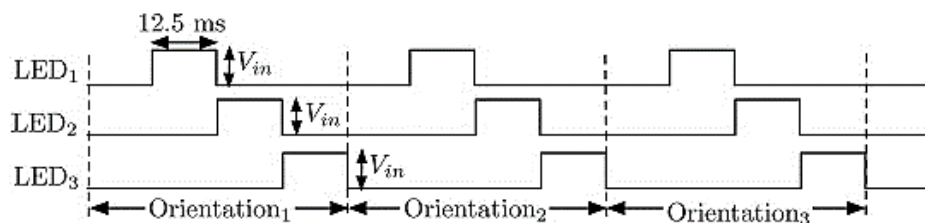


**Figure 2.6: TDMA Scheme for three LEDs (Yasir et al., 2014)**

### 2.5.2 Dual-Tone Multiple Frequency (DTMF)

Dual-Tone Multiple Frequency (DTMF) method consists of one high frequency and one low frequency for the represent of a words in LEDs identity. According to Luo et al. (2014) DTMF system, DTMF is a multi-frequency method which can employ 8 different frequency to represent 16 characters or symbols. DTMF is widely used in telecommunication. For example, voice mail, telephone dialling and electronic banking system. In DTMF system, each transmitter LEDs is assigned with a unique and transmit its ID at the same time periodically. The received DTMF signal with the highest Received Signal Strength (RSS) is used to decode the nearest LED lamp. Example of DTMF system of two LEDs is show in Figure 2.7 where the Tx1 and Tx2 LEDs are transmitting its address “123A” and “0#D\*” respectively and DTMF for symbol ‘1’ contain high frequency of 1200Hz and low frequency of 680Hz whereas DTMF for symbol ‘0’ contain high frequency of 1320Hz and 960Hz of low frequency. Lastly, the receiver need to perform time-frequency analysis to analysis the received frequency in order to retrieve back the DTMF information, threshold detection method to determine the nearest LED and collect the RSS for future computation.

After reviewing DTMF method, DTMF provide a good immunity for inter-cell interferences because all DTMF symbols have different frequency and each LEDs have unique DTMF symbol ID. Besides, DTMF method also not required information from background light intensity which may eliminate the interference from flicking background light that causes by Fluorescent Lamp. Moreover, DTMF system required constant sampling time and Fourier Transform calculation to convert the received signal to frequency domain for analysis which required better performance microcontroller. Furthermore, each transmitter required to transmit its ID at the same time periodically and require LEDs synchronization which increase system complexity.

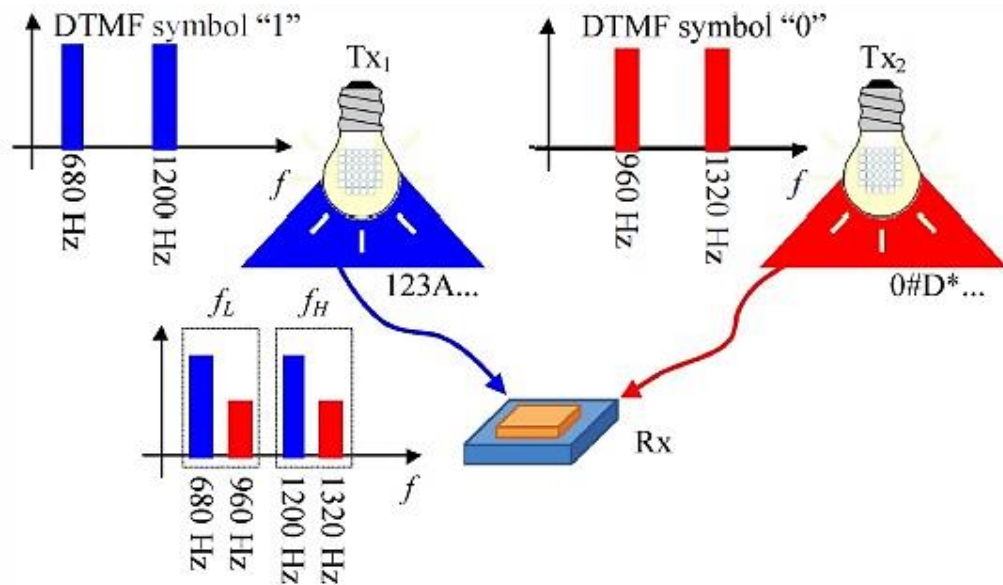


Figure 2.7: DTMF System with Two LEDs (Luo et al., 2014)

### 2.5.3 Unique Frequency Address (F-ID)

Unique Frequency Address (F-ID) method, each LEDs transmitter was assigned with a unique frequency as represented as its address. According to Jung et al. (2011) F-ID design, three transmitter LEDs is assigned with frequency of 1 MHz, 3 MHz and 5 MHz to represent as its coordinates. In order reduce inter-cell interference, transmitter LEDs frequency assignation need to be  $LED_{f_2} = 3LED_{f_1}$  and  $LED_{f_3} = 5LED_{f_1}$ . Since, the F-ID is used with Time Different of Arrival (TDOA) system. The synchronization needed for all the transmitters. Retrieve the transmitted F-ID signal, the output of the photodiode receiver can send into a band-pass filter to filter out all unwanted frequency and remain the needed F-ID frequency. For example, to retrieve of 1MHz F-ID signal, a band-pass filter with 1MHz passband is needed. Figure 2.8 show the block diagram of an F-ID transmitter system.

After reviewing the F-ID method, F-ID method is easier as compared with Dual-Tone Multiple Frequency (DTMF) method because it only used a desired frequency to represent as coordinate of the transmitter whereas DTMF system required two frequency and a DTMF address to represent a transmitter. Besides, F-ID also would not require the intensity information of backlight hence it also immune to the

flicking backlight that caused by Fluorescent Light. Moreover, the F-ID may require transmitter synchronization when TDOA detection method is use. The F-ID method also required a time-frequency domain conversion algorithm or digital filter which may load the processor and reduce the response rate. Further, F-ID may have limited number of unique address as compare with DTMF method because single frequency is only assigned to one transmitter and repeated of frequency is not permitted.

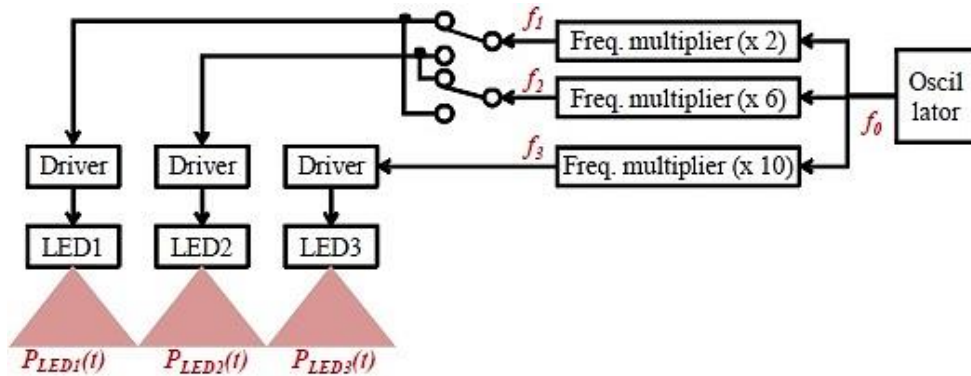


**Figure 2.8: F-ID Transmitter Block Diagram (Jung et al., 2011)**

#### 2.5.4 Carrier Allocation (CA)

Carrier Allocation (CA) method, a different radio frequency (RF) is begin used for signal modulation as to prevent the inter-cell interferences. According to Kim et al. (2013) CA-VLC system, three transmitter LED cells is modulated with different RF of 2 MHz, 2.5 MHz and 3 MHz respectively to prevent inter-cell interference. Further, PSK RF modulation technique is used for data modulation because the average signal power for PSK modulation technique will among remain the same hence it will not cause flicking effect while data transmission is occurring. The received RF power is then extracted and determine the distance. Figure 2.9 and Figure 2.10 show the RF modulation of LED transmitter and CA-VLC system respectively.

After reviewing CA-VLC system, the CA-VLC system have the advantages of reducing inter-cell interference due to different carrier frequency is allocation for each LEDs cells hence each cells data can be extracted. Besides that, CA-VLC system also

used with PSK modulation method as to enable for data transfer. Because of that, it enable each LEDs cell to broadcast its coordinate and allow the receiver to calculate the distance by using the coordinate data received and received signal strength. CA-VLC with PSK modulation method used is useful but it will increase the system complexity as compare to TDMA, F-ID and DTMF method due to the extra PSK modulator and demodulator involved. Thus, more stages needed to process the receive signal.

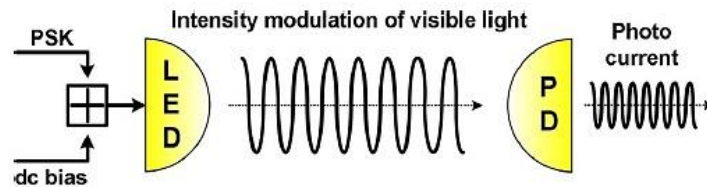


Figure 2.9: RF Modulation for LED Transmitter (Kim et al., 2013)

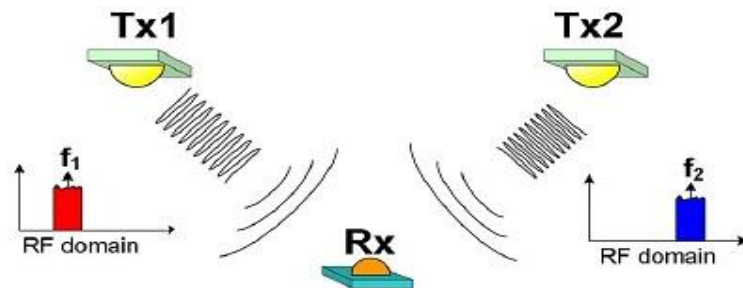


Figure 2.10: CA-VLC System (Kim et al., 2013)

## CHAPTER 3

### METHODOLOGY

#### 3.1 Proposed VLC-IPS System Overview

Light Emitting Diode (LED) and Photodiode are the two major hardware components in VLC-IPS. The Unique Frequency Address (F-ID) method is proposed as a modulation method for the LED transmitter to prevent inter-cell interference whereas Received Signal Strength (RSS) method and Trilateration method are proposed as distance and coordinate estimation of the receiver. Figure 3.1 shows the basic block diagram to explain the flow of the system. The major hardware and technique will be discussed in the next section. The practical simulation model is shown in Figure 3.2. The procedures and the method of constructing the simulation model will be discussed in Section 3.2 and Section 3.3.

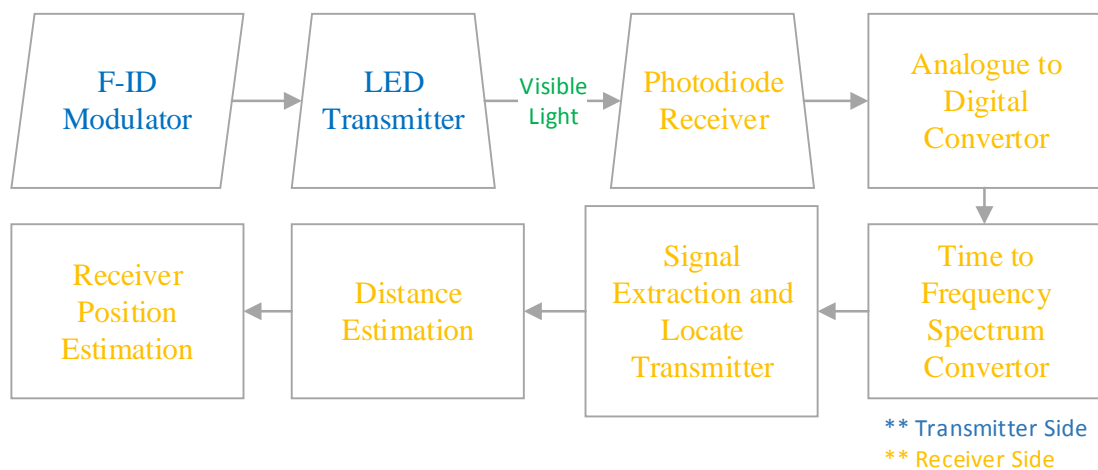


**Figure 3.1: Basic Block Diagram of Proposed VLC-IPS**

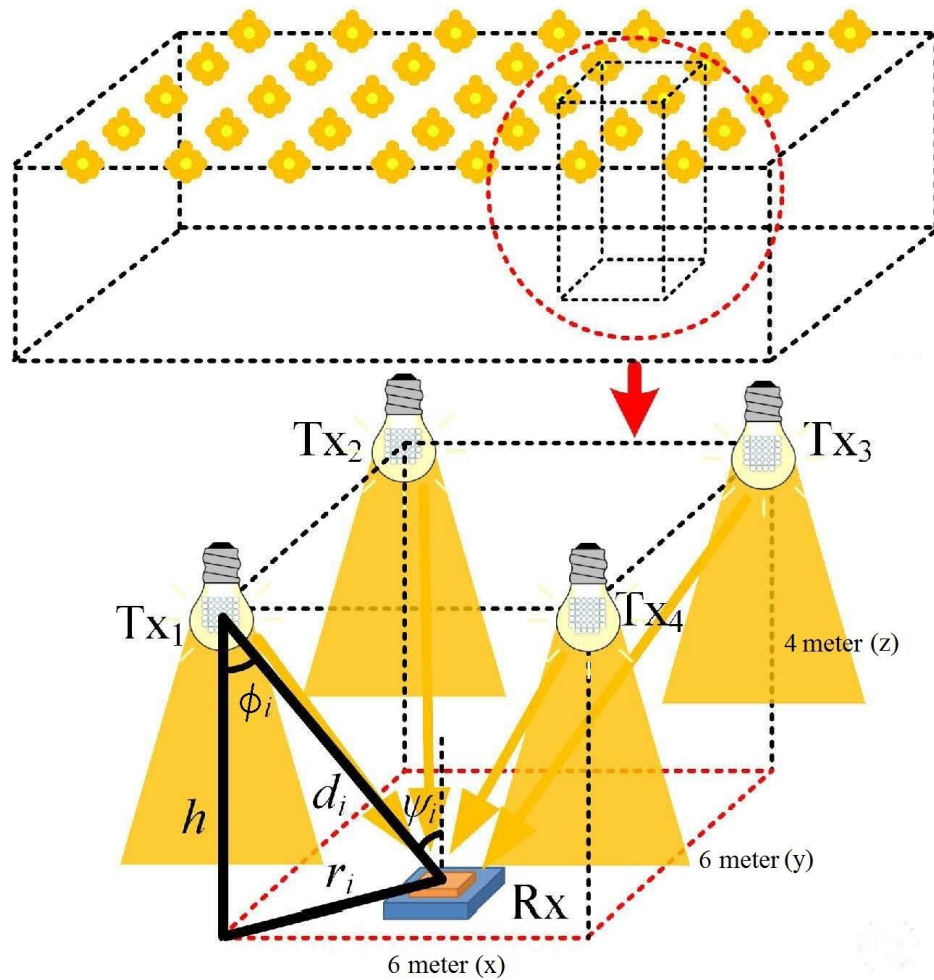


**Figure 3.2: Practical Model of the proposed VLC-IPS**

## 3.2 Details of Proposed VLC-IPS

### 3.2.1 Unique Frequency Modulator (F-ID)

In the F-ID method proposed by Jung et al. (2011), three LEDs that modulated at frequency of 1 MHz, 1.5 MHz and 2 MHz were used as transmitter. In this proposed system four LEDs are used and modulated in frequency of 1 kHz, 1.25 kHz, 1.75 kHz and 2 kHz.

Each of the LEDs transmitter has connected to a frequency generation module with high precision and high stability capability. In F-ID method, small variation in frequency will create another new unique frequency address which result unrecognizable frequency. Lastly, all the LEDs are place far away from each an others. Hence, F-ID is the most suitable and asynchronous method to be used.

### 3.2.2 LED Transmitter

Light Emitting Diode (LED) is used to convert F-ID modulated electrical signal into visible light spectrum that carries identity information. Four LEDs bulb are installed. BRIDGEFLUX LEDs BXRC-30E2000-C-03 were installed at the four corner of the ceiling. The LEDs are able to emit 2000 lumens with the input power of 16.4W at Correlated Colour Temperature (CCT) of 3000 Kelvin.

### 3.2.3 Photodiode Receiver

Photodiode is used to convert the optical intensity into electrical current. In another word the higher the optical intensity, the higher the current flows through the photodiode. In this proposed system, the photodiode is used to receive the optical signal that transmitted by LEDs. Photodiode OPT101 which have a peak sensitivity on visible light at the spectrum of 650nm at red colour region is used in the proposed system. This photodiode have half sensitivity at titled angle of 75°.

The relationship between the incoming light intensity, the output current and output voltage can be determined in Eq. 3.1 and Eq. 3.2.

$$I_{PD}(A) = 0.45 \times Lumens (W) \quad (3.1)$$

$$V_{PD}(V) = 0.45 \times Lumens (\mu W) \quad (3.2)$$

where  $I_{PD}$  represents the photodiode output current and  $V_{PD}$  represents the photodiode output voltage. The transfer function is shown in Eq. 3.3.

$$R_{ext}(M\Omega) = V_{PD} \times 10^6 / I_{PD}A \quad (3.3)$$

where  $R_{ext}$  is the external resistor connected as feedback gain of the amplifier. Substituting Eq. 3.1 into Eq. 3.3, a new equation, Eq. 3.4 is generated as follow.

$$V_{PD}'(V) = 0.45 \times Lumens (W) \times R_{ext}(\Omega) \quad (3.4)$$

Equation 3.4 shows the relationship between the photodiode voltage output, the optical input in lumens and the external resistor which connected in close-loop amplifier.

The radiant sensitive area for the photodiode is  $5.2\text{mm}^2$  which required in distance calculation in the section 3.2.5.

### 3.2.4 ADC Sampling and Signal Extraction

Analog Digital Converter (ADC) is used for converting the analogue signal into digital form. This proposed system, common microcontroller 12-bits ADC is used for sampling the output signal of the photodiode in the simulation environment. Further, The ADC is configured to sampling at the speed of 8192 Hz. Since the Radix-2 transformation method based Fast Fourier Transform (FFT) requires  $2^n$  data, sampling frequency of 8192 Hz is chosen. The proposed design, the LED transmitters is transmitting frequency of 1 kHz, 1.25 kHz, 1.75 kHz and 2 kHz.

### 3.2.5 Received Signal Strength (RSS) Distance Estimation

Received Signal Strength (RSS) is the method to estimate the distance between transmitter and receiver. Lambertian equation is used to estimate the distance between transmitter and receiver. Eq. 2.1, can be further simplified to suit the proposed design, where Eq. 3.5 shows the simplified equation that suit the proposed design in simulation environment.

$$G_{LOS} = \frac{(m+1)A}{2\pi d^2} \cos^m(\phi) \cos^M(\psi) \quad (3.5)$$

where the filter gain,  $T(\phi)$  and concentrator gain,  $g(\psi)$  are equal to 1.

The LEDs transmitters, BXRC-30E2000-C-03 and photodiode receiver, OPT101 having a half-angle of  $60^\circ$  and  $75^\circ$  respectively. Hence,  $m$  and  $M$  in Eq. 3.5 can be simplified as below.

$$m = \frac{-\log 2}{\log(\cos(\frac{\phi_1}{2}))} = \frac{-\log 2}{\log(\cos(60))} = 1$$

$$M = \frac{-\log 2}{\log(\cos(\frac{\psi_1}{2}))} = \frac{-\log 2}{\log(\cos(75))} = 0.512825$$

A new equation, Eq. 3.6 is formed from the value of  $m$  and  $M$ .

$$G_{LOS} = \frac{A}{\pi d^2} \cos(\phi) \cos(\psi)^{0.512825} \quad (3.6)$$

where  $\cos(\phi) = \cos(\psi) = \frac{h}{d}$ ,  $h$  is the system height and  $d$  is the distance between transmitter and receiver. Eq. 3.7 shows the changes. The relationship between the transmitter signal and the receiver signal with added Gaussian Noise is shown in Eq. 3.8.

$$G_{LOS} = \frac{Ah^{(1+0.512825)}}{\pi d^{(3+0.512825)}} \quad (3.7)$$

$$R_{lx}(t) = G_{LOS} T_{lx}(t) + N(t) \quad (3.8)$$

where  $R_{lx}(t)$  is the received signal illuminate,  $G_{LOS}$  is the Lambertian characteristic,  $T_{lx}(t)$  is the transmit signal illuminate and  $N(t)$  is the Adaptive White Gaussian Noise. The distance information, Eq. 3.9 is obtained by solving the Eq. 3.7 and the Eq. 3.8.

$$R_{lx}(t) = \frac{Ah^{(1+0.512825)}}{\pi d^{(3+0.512825)}} T_{lx}(t) + N(t)$$

$$\frac{R_{lx}(t) - N(t)}{Ah^{(1+0.512825)} T_{lx}(t)} = \frac{1}{\pi d^{(3+0.512825)}}$$

$$\frac{Ah^{(1+0.512825)} T_{lx}(t)}{R_{lx}(t) - N(t)} = \pi d^{(3+0.512825)}$$

$$d = \frac{(3+0.512825) \sqrt{Ah^{(1+0.512825)} T_{lx}(t)}}{\pi (R_{lx}(t) - N(t))} \quad (3.9)$$

The simplified distance equation (Eq. 3.9) is determined by the signal strength received from the photodiode.

### 3.2.6 Trilateration Coordinate Estimation

Using the distance data (Eq. 3.10) from the Received Signal Strength (RSS) algorithm. Trilateral is used to determine the coordinate of an object. As in the proposed design, four trilateral equations are used to represent four transmitter (Eq. 3.11 to Eq. 3.14).

$$(x_e - x_1)^2 + (y_e - y_1)^2 + (z_e - z_1)^2 = d_{c_1}^2 \quad (3.11)$$

$$(x_e - x_2)^2 + (y_e - y_2)^2 + (z_e - z_2)^2 = d_{c_2}^2 \quad (3.12)$$

$$(x_e - x_3)^2 + (y_e - y_3)^2 + (z_e - z_3)^2 = d_{c_3}^2 \quad (3.13)$$

$$(x_e - x_4)^2 + (y_e - y_4)^2 + (z_e - z_4)^2 = d_{c_4}^2 \quad (3.14)$$

All LEDs transmitter have the same height which lead to  $z_1 = z_2 = z_3 = z_4$ . Equation 3.11 to Eq. 3.14 are simplified to Eq. 3.15.

$$A = \begin{bmatrix} x_2 - x_1 & y_2 - y_1 \\ x_3 - x_1 & y_3 - y_1 \\ x_4 - x_1 & y_4 - y_1 \end{bmatrix}, X = \begin{bmatrix} x_e \\ y_e \end{bmatrix} \quad (3.15)$$

$$B = \begin{bmatrix} (d_{c_1}^2 - d_{c_2}^2 + x_2^2 + y_2^2 - x_1^2 - y_1^2)/2 \\ (d_{c_1}^2 - d_{c_3}^2 + x_3^2 + y_3^2 - x_1^2 - y_1^2)/2 \\ (d_{c_1}^2 - d_{c_4}^2 + x_4^2 + y_4^2 - x_1^2 - y_1^2)/2 \end{bmatrix}$$

Using linear least square method, the receiver coordinate  $(x_e, y_e)$  is located by  $X = BA^{-1}$ .

### 3.2.7 Noise for Visible Light Communication (VLC) System

According to Komine and Nakagawa (2004), Gaussian Noise is appeared in VLC system. It have a variances of  $N$ . The variance is the sum of shot noise, thermal noise and intersymbols interference (Eq. 3.16).

$$N = \sigma_{shot}^2 + \sigma_{thermal}^2 + \gamma^2 P_{ISI}^2 \quad (3.16)$$

where  $\sigma_{shot}^2$  is the variance of shot noise,  $\sigma_{thermal}^2$  is the thermal noise,  $\gamma^2$  is the responsivity of photodiode and  $P_{ISI}$  is the intersymbols interference. As each of the LED has its own unique frequency in F-ID modulation, intersymbol interferences among the LEDs are ignored to form Eq. 3.17.

$$N = \sigma_{shot}^2 + \sigma_{thermal}^2 \quad (3.17)$$

Komine and Nakagawa (2004) defined the variance of shot noise as

$$\sigma_{shot}^2 = 2q\gamma(P_{r\ signal})B + 2qI_{bg}I_2B \quad (3.18)$$

where  $q$  is the electron charge ( $1.602 \times 10^{-19}$ ),  $P_{r\ signal}$  is the reflected signal,  $B$  is the bandwidth of the system,  $I_{bg}$  is the current for background light and  $I_2$  is the noise bandwidth factor. The variance of thermal noise can be represented by Eq. 3.19.

$$\sigma_{thermal}^2 = \frac{8\pi kT_k}{G} \eta A I_2 B^2 + \frac{16\pi^2 kT_k \Gamma}{g_m} \eta^2 A^2 I_3 B^3 \quad (3.19)$$

where  $k$  is the Boltzmann Constant,  $T_k$  is the temperature,  $\eta$  is the fixed capacitance per unit area of photodiode,  $A$  is the photodiode effective area,  $G$  is the open-loop voltage gain,  $\Gamma$  is the FET channel noise factor,  $g_m$  is the FET transconductance and  $I_3$  is equal to 0.0868.

Zhang et al. (2014) defined reflected light,  $P_{r\ signal} = \sum_{i=1}^4 H_i(0)P_i$ , where  $H_i(0)$  is the DC gain and  $P_i$  is the instantaneous emitting power,  $I_2 = 0.562$  and  $I_{bg} = 740\mu A$  with indirect sunlight exposure with the photodiode responsivity of  $0.54A/W$  (Moreira et al., 1995). These bring the Eq. 3.18 to Eq. 3.20

$$\sigma_{shot}^2 = 2(1.602 \times 10^{-19})\gamma(\sum_{i=1}^4 H_i(0)P_i)B + 2(1.602 \times 10^{-19})I_{bg}(0.562) \quad (3.20)$$

In the proposed VLC-IPS, the system bandwidth  $B = 1kHz$ , the photodiode responsivity,  $\gamma = 0.45A/W$  and the power of the LEDs  $16.4W$  are used. 50% duty cycle is used in F-ID modulation. This give the DC gain,  $H_i(0) = 0.5$ . In an ideal condition, the power transmitted by the LEDs will all received by photodiode. Thus, the summation of all LEDs,  $\sum_{i=1}^4 H_i(0)P_i = 32.8W$  where  $H_i(0) = 0.5$ ,  $P_i = 32.8W$ . The background current,  $I_{bg}$  for indirect sunlight without optical filter is  $740 \times 10^{-6}A$  at  $0.54A/W$  photodiode responsivity (Moreira et al., 1995). In the proposed VLC-IPS, photodiode responsivity of  $0.45A/W$  was used. Therefore, by caring the linear relation, the new  $I'_{bg}$  is obtained at follow where the value of 2000 is the gain of the photodiode internal amplifier.

$$I'_{bg} = \frac{740 \times 10^{-6}A}{0.54A/W} \times \frac{(0.45 \times 2000)A}{W} = 1.25A \quad (3.21)$$

The shot noise (Eq. 3.18) can be further simplified to Eq. 3.22.

$$\sigma_{shot}^2 = 2(1.602 \times 10^{-19})(0.45 \times 2000)(32.8W)(1000) + 2(1.602 \times 10^{-19})(1.25)(0.562)$$

$$\sigma_{shot}^2 = 9.4582 \times 10^{-12} \quad (3.22)$$

The variance for thermal noise can be derived by using Eq. 3.19. Based on Zhang et al. (2014), the following value are used. Open-loop voltage gain,  $G = 10$ , the FET channel noise factor,  $\Gamma = 1.5$ , the FET transconductance,  $g_m = 30mS$ ,  $\eta A = 1200pF$  ( $\eta$  is the fixed capacitance per unit area,  $A$  is the photodiode effective area) with obtained from the photodiode specification manual. The ambient temperature,  $T_k = 298.15K(25^\circ C)$ .

$$\begin{aligned} \sigma_{thermal}^2 &= \frac{8\pi(1.3807 \times 10^{-23})(298.15)}{10} (1200 \times 10^{-12})(0.562)(1000)^2 \\ &\quad + \frac{16\pi^2(1.3807 \times 10^{-23})(298.15)(1.5)}{30 \times 10^{-3}} (1200 \\ &\quad \times 10^{-12})^2(0.0868)(1000)^3 \\ \sigma_{thermal}^2 &= 6.9812 \times 10^{-24} \end{aligned} \quad (3.23)$$

The variance of Gaussian Noise can be determined as follow,  $N = \sigma_{shot}^2 + \sigma_{thermal}^2$

$$\begin{aligned} N &= 9.4582 \times 10^{-12} + 6.9812 \times 10^{-24} \\ N &= 9.4594 \times 10^{-12} \end{aligned} \quad (3.24)$$

The Signal to Noise Ratio (SNR) of each LED can be calculated using Eq. 3.25 (Yasir et al., 2014).

$$SNR(dB) = 10 \log \frac{(R_p \frac{P_{LOS}}{A})^2}{\sigma_{noise}^2} \quad (3.25)$$

where  $R_p$  is the responsivity photodiode,  $P_{LOS}$  is the line-of-sight power,  $A$  is the effective area in photodiode and  $\sigma_{noise}^2$  is the Gaussian Noise variance,  $P_r$  is the power received by photodiode. SNR is used to determine the quality of the signal in VLC-IPS.

### **3.3 Simulation Environment**

MATLAB and Simulink version R2014b was used as a simulation environment to carry out the experiment on VLC-IPS model. In order to stimulate the proposed system, the VLC-IPS model need to be construct as Figure 3.1. All the input, output and systems such as F-ID modulator, LEDs, Photodiode, RSS and Trilateral are modelled as a mathematical transfer function and build inside the MATLAB Simulink environment. Figure 3.3 show the complete simulation model that build in MATLAB Simulink.

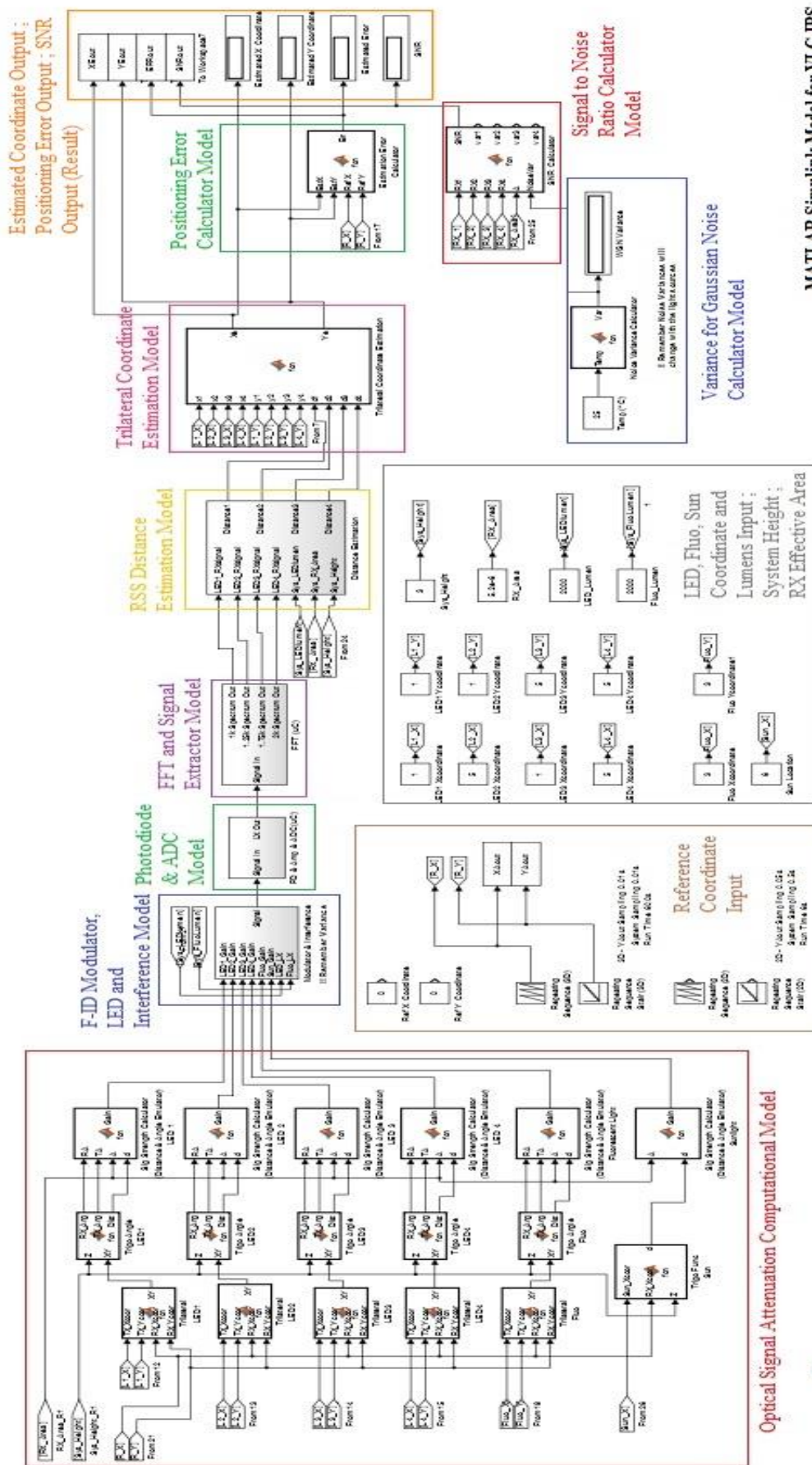


Figure 3.3: Complete VLC-IPS Simulation Model in Simulink

MATLAB Simulink Model for VLC-IPS

### 3.3.1 F-ID Modulator, LED and Interferences

Unique Frequency Address (F-ID) is a frequency generator and the selected frequency is used to represent each individual LED. Sine wave generator is the tool in MATLAB which used to model F-ID. By default the sine wave generator is operated as continuous step. This will be reconfigured to discrete step which operated at 8192Hz. The discrete square wave generator and pulse generator are not suitable to be used in this project as the generated square wave is according the sampling number. Therefore, it's difficult to generate on accurate frequency using F-ID modulator method. Four Discrete Sine Wave generator are used to generate 1 kHz, 1.25 kHz, 1.75 kHz and 2 kHz of frequency for the four LEDs that used in the proposed system. These are shown in Figure 3.4 (a), (b), (c).

The output of the sine wave generator is converted into square wave where the negative cycle of the square wave is removed. Figure 3.5 shows the system setup where the sine wave is converted into square wave with negative components is removed. The output signal amplitude is normalized to 1 lumen. Additional multiplier is used to convert the normalized value to 2000 lumens. Figure 3.6 shows the simulation model for F-ID and LEDs. The "LED\_LX" input is the input to configure the LED lumens. This shown in Figure 3.6. The "LED1\_Gain" is the attenuation parameters and the "Manual Switch8" is used to enable or disable the signal into the system.

The simulation model for fluorescent bulb is constructed as shown in Figure 3.7. The frequency of the conventional fluorescent light is 100 Hz and 20 kHz for electronic ballast fluorescent light (Moreira et al., 1995). Interference that causes by sunlight is also considered in this project. The sunlight interference is modelled as a constants and its lumens is assumed to be 5 times greater than the lumens of the proposed LED. According to Komine and Nakagawa (2004), Gaussian Noise is affected the VLC-IPS performance, therefore Gaussian Noise is necessary to be modelled with the variance that calculated in Eq. 3.17. Figure 3.8 shows Gaussian Noise model in MATLAB.

Figure 3.9 shows the final outline of the transmitter model in Simulink. However, Figure 3.10 shows the complete transmitter model in Simulink.

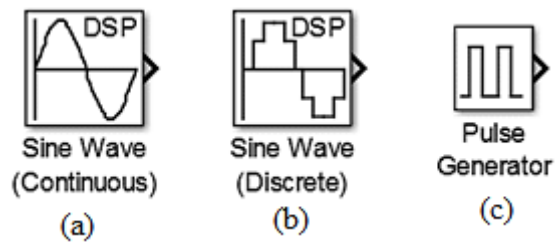


**Figure 3.4 (a), (b) and (c): Continuous Sampling Sine Wave Generator, Discrete Sampling Sine Wave Generator and Square Wave Generator.**

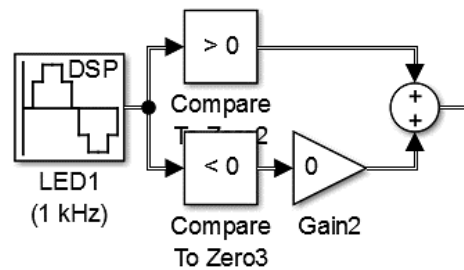


**Figure 3.5: System for Sine to Square and Negative Components Elimination**

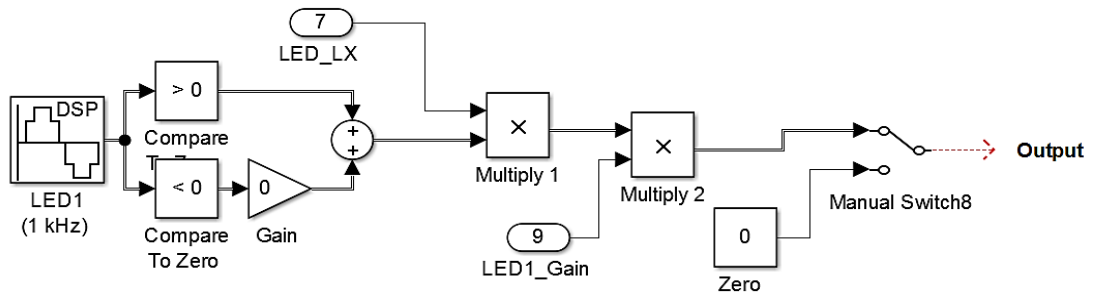


**Figure 3.6: Simulation Model for F-ID and LED module**

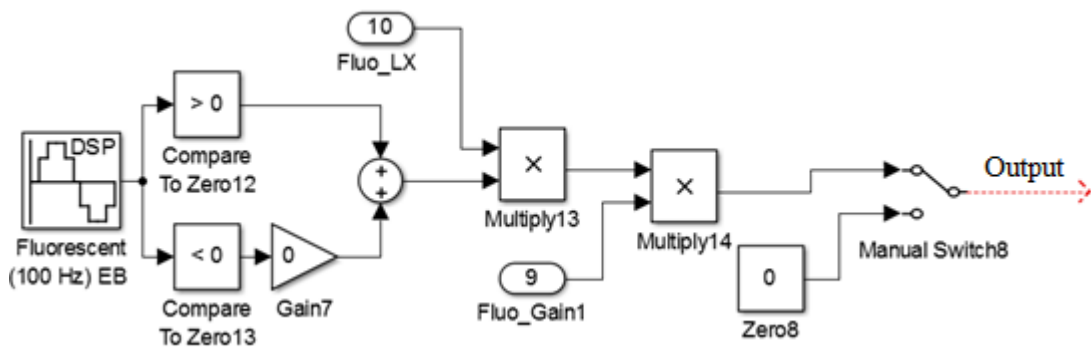


**Figure 3.7: Simulation Model for Fluorescent Interference**

Gaussian Noise



Figure 3.8: Gaussian Noise Block Diagram in MATLAB

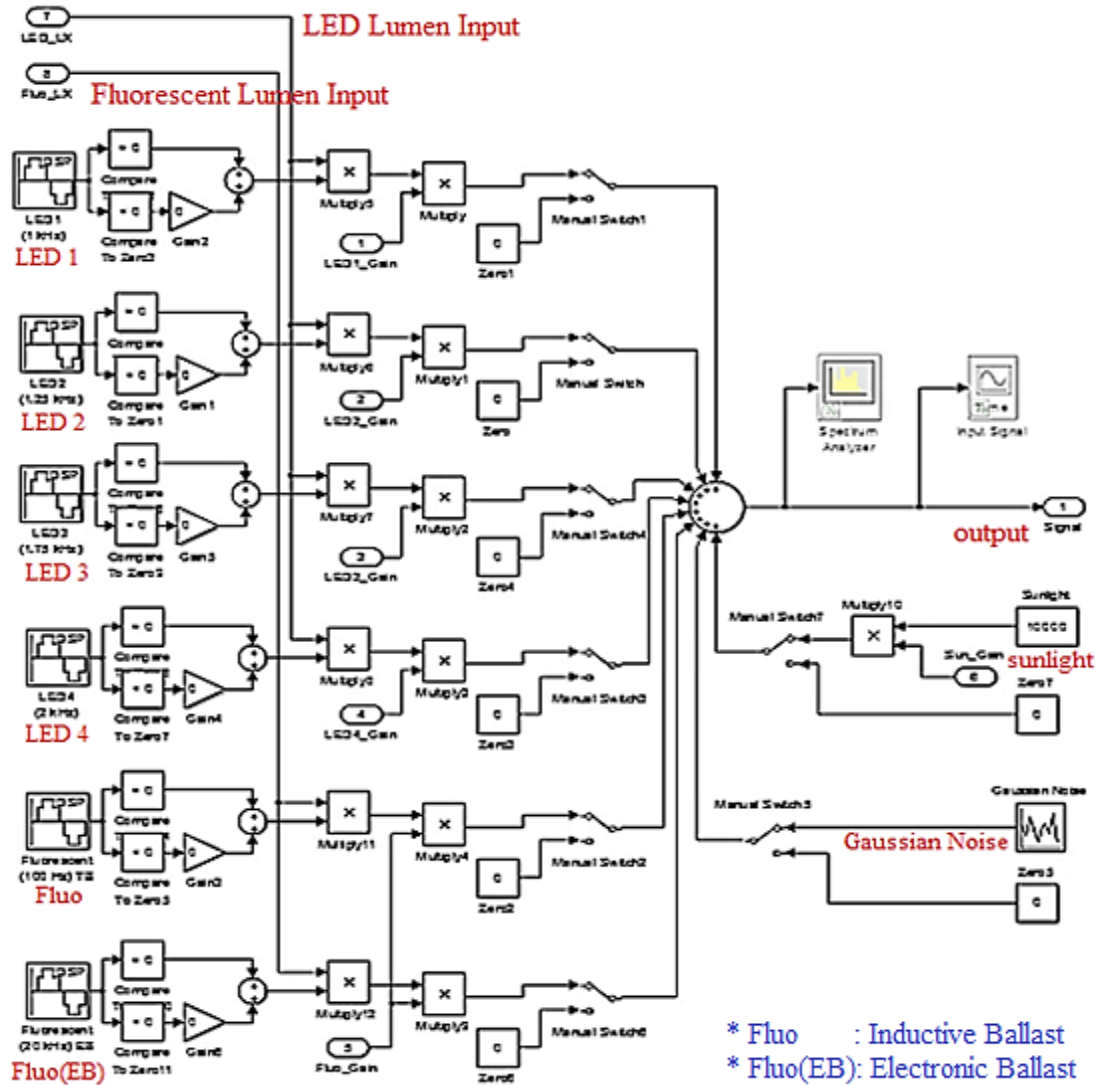
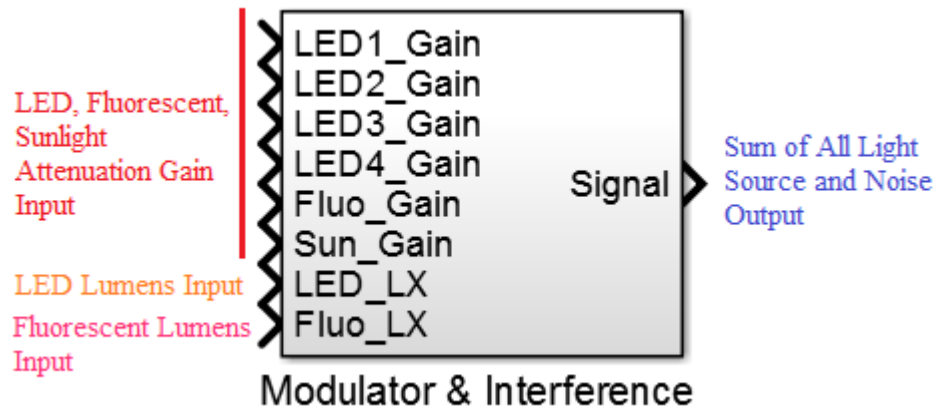


Figure 3.9: Overall Optical Transmitter Model for Proposed System



**Figure 3.10: Complete Transmitter Model in Simulink**

### 3.3.2 Photodiode (PD) and Analogue to Digital Convertor (ADC)

Photodiode (PD) is used as an optical receiver to receive frequency modulated signals. The “Gain” block diagram that prebuilt in Simulink is used to model the transfer function of the PD which shown in Figure 3.11. The transfer function for photodiode in Eq. 3.4 is filled into the “Gain” block diagram to act as PD. Referring to the section 3.3.1, the input light source are from the four LEDs, fluorescent light and sunlight. By assuming, a 40W fluorescent tube emit 4000 lumens and sunlight intensity is 5 times greater than LED intensity, 10000 lumens. Avoid ADC saturation, by consider attenuation, angle effect, the resistor controlling the gain of PD amplifier computed as 2kΩ. The transfer function for PD can be computed as shown in Eq. 3.26 by reference from Eq. 3.4.

$$V_{PD}(V) = 0.45 \times Lumens (W) \times 2000\Omega$$

$$V_{PD}(V) = 900 \times Lumens (W) \quad (3.26)$$

Quantization Noise and Saturation Effect in ADC will affect the performance of the whole system. Figure 3.12 shows the block diagram. As shown in Eq. 3.27, the ADC step of 0.8567mV is used on 12-bits ADC with  $V_{ref}$  of 3.3V. This estimated the quantization noise to be 0.4284mV.

$$ADC \text{ Step} = \frac{V_{ref}}{2^{(no. \text{ of bits})}} \quad (3.27)$$

$$ADC \text{ Step} = \frac{3,3V}{2^{12}} = \frac{3,3V}{4096} = 8.05664 \times 10^{-4} V$$

A compensator that convert the ADC sampling value back to the optical power in lumens which is needed by the Lambertian Distance Estimation. However, in this case, same “Gain” model is used for modelling the transfer function for the Compensator. Figure 3.13 shows the overall connection of PD receiver. Figure 3.14 shows the simplified PD and ADC model in Simulink.

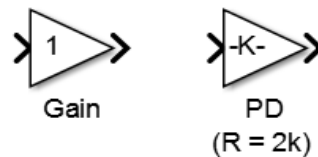


**Figure 3.11: Default “Gain” model in MATLAB (left) and Photodiode Model in MATLAB (right)**

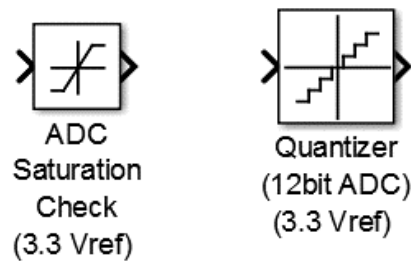


**Figure 3.12: Simulation Model for ADC Saturation (left) and ADC Quantizer (right)**

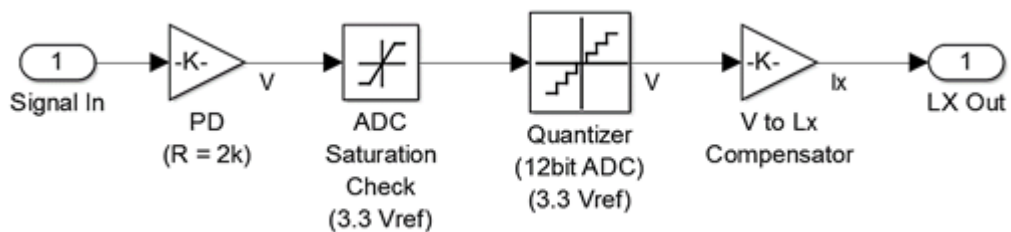


**Figure 3.13: Overall System for Photodiode Receiver**

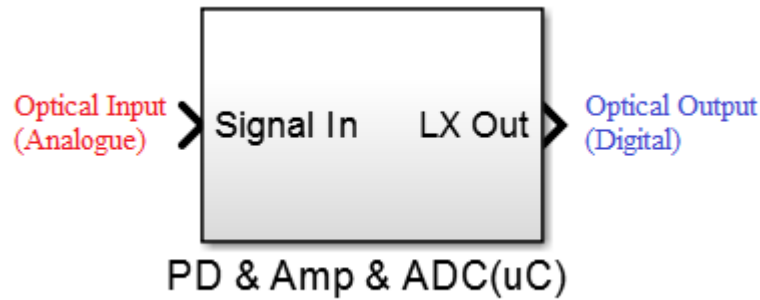


**Figure 3.14: Combine PD and ADC Model in Simulink**

### 3.3.3 Signal Extracting or Fast Fourier Transform (FFT)

The Fast Fourier Transform (FFT) is used to extract the useful data, time spectrum data into frequency spectrum data and four frequencies: 1 kHz, 1.25 kHz, 1.75 kHz and 2 kHz will be extracted. The FFT block is shown in Figure 3.15 (a). The data output from the FFT convertor is in complex form. Hence, a connection from FFT to Complex to Magnitude convertor is used to extract the magnitude of components from the system. Figure 3.15 (b) shows the Complex to Magnitude block diagram. The FFT is configured into Radix-2 because this type of conversion is commonly found in ARM uC DSP library.

Since, output from FFT convertor is an array consists of 8192 members with the sampling rate of 8192Hz. Based on the results, each members of the array represent each single Hz of frequency. For example, let the array to be 'x' and 11<sup>th</sup> array member, x[10] represents the amplitude components in 10Hz. In addition, according to Nyquist rate, the maximum recognisable frequency for 8192 Hz of sampling rate is 4096 Hz and the FFT output array contains 8192 members. In order to clarify that, the FFT output array starts from 0Hz with array member of 1, x[0] until 4095Hz with array member of 4096, x[4095] and it repeats from 0Hz to 4095Hz with array member from x[4096] to x[8191].

Although, all the frequencies in each Hertz can be extracted but the useful data only located at 1 kHz, 1.25 kHz, 1.75 kHz and 2 kHz. Thus, demultiplexor (demux)

that in built at Simulink are used to extract the required four components from the FFT output array which contain 8192 members. The demux is shown in Figure 3.16. The FFT output array from the member of  $x[4096]$  to  $x[8191]$  is the repetition from  $x[0]$  to  $x[4095]$  hence a demux is used to extract signal from  $x[0]$  to  $x[4095]$ . The reason of cascading the first demux with another demux is to extract the four necessary frequencies. The second demux need to be configured its output as “[1000 1 249 1 499 1 249 1 2095]”. The first ‘1000’ means the FFT outputs data from  $x[0]$  to  $x[999]$ . The second ‘1’ mean output, 1 kHz signal is outputted at the second output port. Third, ‘249’ means outputs from  $x[1001]$  to  $x[1249]$  are outputted at the third output port. The fourth, ‘1’ mean output from  $x[1250]$ , 1.25kHz signal is outputted at the fourth output port. The sequence is repeated and these frequency are link to the dedicated output port from the demux. Figure 3.17 shows the frequency extracting process and can be represented in a simpler FFT model in Figure 3.18.

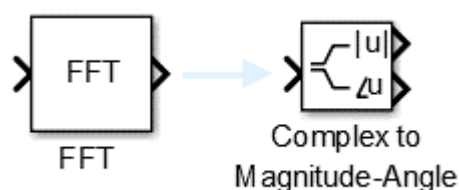


**Figure 3.15 (a) and (b): Fast Fourier Block Diagram (left) and Complex to Magnitude or Angle Block Diagram (right)**

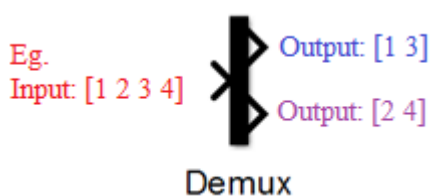


**Figure 3.16: One to Two Demultiplexor in Simulink**

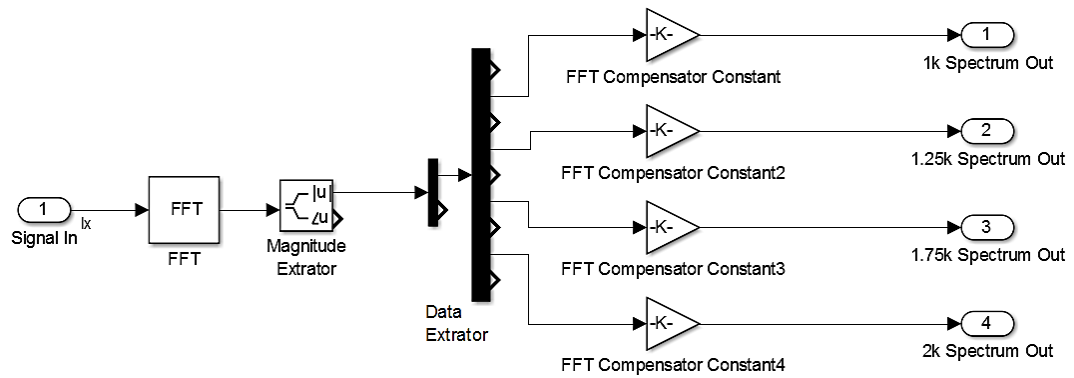


**Figure 3.17: Full Diagram of Signal Conditioning and Extracting Process**

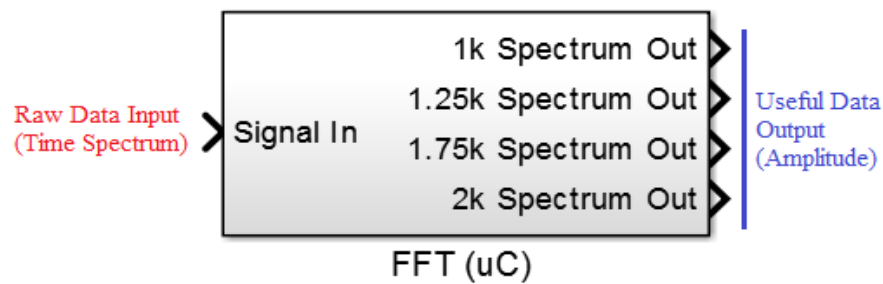


**Figure 3.18: Combined FFT Model in Simulink**

### 3.3.4 Distance Estimation

Distance estimation is used to compute the distance between LEDs transmitter and photodiode receiver. Simplified Lambertian equation in Eq. 3.28 is modelled in Simulink to compute the distance between transmitter and receiver. The MATLAB Function will engaged with distance estimation feature after the insertion of simplified Lambertian equation (Eq. 3.29).

In the proposed system, four LEDs are used as transmitter, hence, four sets of distance estimation blocks are needed. Figure 3.20 shows the final layout of the distance estimation block. Referring to the Figure 3.20, “Sys\_LEDlumen” is the LED lumen input, “Sys\_RX\_Area” is the photodiode effective area input, “Sys\_Height” is the system height input, “LED1\_RXsignal”, “LED2\_RXsignal”, “LED3\_RXsignal” and “LED4\_RXsignal” are the received signal strength input of the four LEDs.

However, “Distance1”, “Distance2”, “Distance3” and “Distance4” are the estimated distance for all four LEDs. The four sets of distance estimation model can be simplified into a block as shown in Figure 3.21.

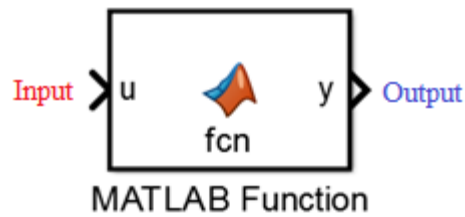


**Figure 3.19: MATLAB Function in Simulink Environment**

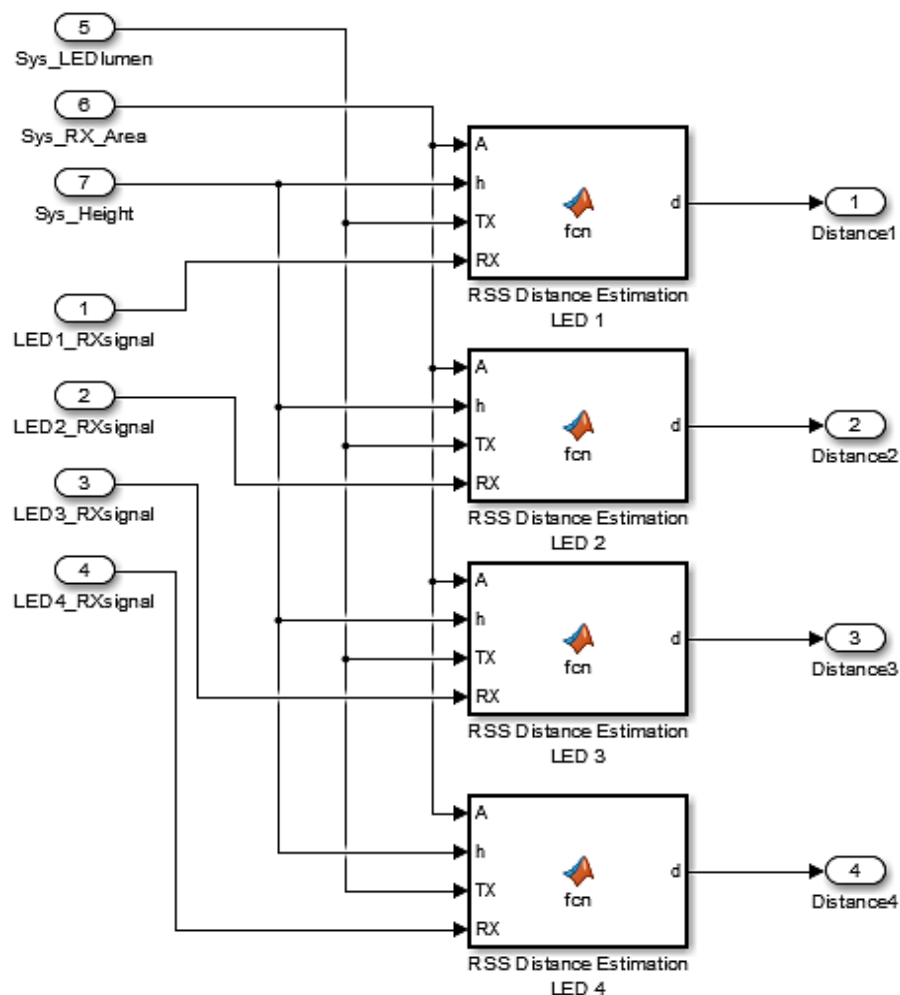


**Figure 3.20: Schematic Layout for Distance Estimation Block**

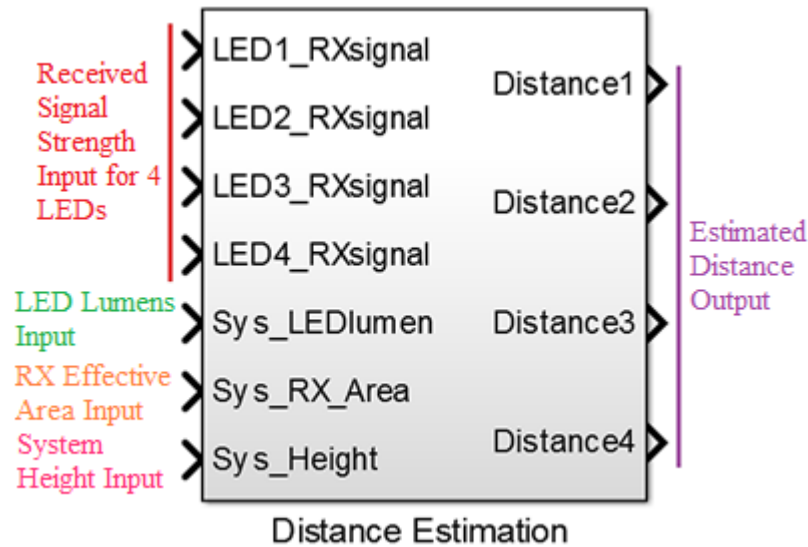


**Figure 3.21: Combined Distance Estimation Model**

### 3.3.5 Trilateral Coordinate Estimation

Trilateral equation is used to estimate the coordinate of the receiver. The trilateral coordinate estimation model input the estimated distance from the distance estimation model of the four LED transmitters. The receiver coordinate computation is based on the estimated distance and the coordinate of each LEDs. The “MATLAB Function” is used to perform this estimation. This is shown in Figure 3.19. The modified and simplified trilateral equation in Eq. 3.15 and linear least square method are inserted into the “MATLAB Function” to perform the coordinate estimation. Figure 3.22 shows the Trilateral Coordinate Estimation Model. The input  $x_1, x_2, x_3 \dots y_3$  and  $y_4$  are the LED X and Y coordinates and the input  $d_1, d_2, d_3$  and  $d_4$  are the estimated distance input. The  $X_e$  and  $Y_e$  are the estimated output coordinate output. In other words, the  $X_e$  and  $Y_e$  output are the X and Y coordinate of the photodiode receiver.

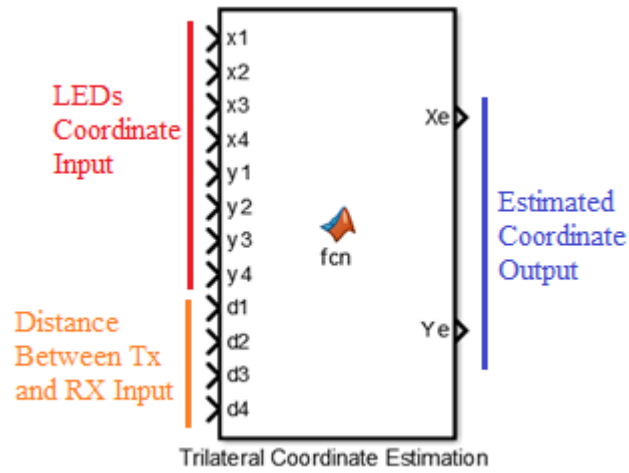


**Figure 3.22: Trilateral Coordinate Estimation Model**

### 3.3.6 Optical Signal Attenuation Computational Model

The attenuation of the optical signal is based on the distance and incident angle. This is computed by using Optical Signal Attenuation Computational Model. This model is using Lambertian equation to compute the attenuation of the signal. LED-photodiode “MATLAB Function” block is used to model the attenuation computation system by inserting the Lambertian equation (Eq. 3.6). The attenuation of the signal is based on the distance between the transmitter and the receiver,  $d$ , angle between transmitter and receiver,  $\cos(\phi)$  and  $\cos(\psi)$  respectively. Hence, the trilateral equation is used to compute the distance and trigonometric equation is used to compute the angle. Eq. 3.30, Eq. 3.31 and Eq. 3.32 shows the trilateral equation and the trigonometric equation.

$$d = \sqrt{(X_{LED} - X_{PD})^2 + (Y_{LED} - Y_{PD})^2 + (Z_{LED} - Z_{PD})^2} \quad (3.30)$$

$$\text{Angle, } \phi (TX) = \tan^{-1} \left( \frac{\sqrt{(X_{LED} - X_{PD})^2 + (Y_{LED} - Y_{PD})^2}}{Z_{LED} - Z_{PD}} \right) \quad (3.31)$$

$$\text{Angle, } \psi (RX) = 90^\circ - \text{Angle, } \phi (TX) \quad (3.32)$$

The obtained results  $(d, \phi, \psi)$  are fed into attenuation model to calculate the attenuation value. The computed attenuation gain is sent to the “F-ID modulation, LED and Interference” model and then multiplied with the transmitted signal. These are shown in the Optical Signal Attenuation Computational Model in Figure 3.23.

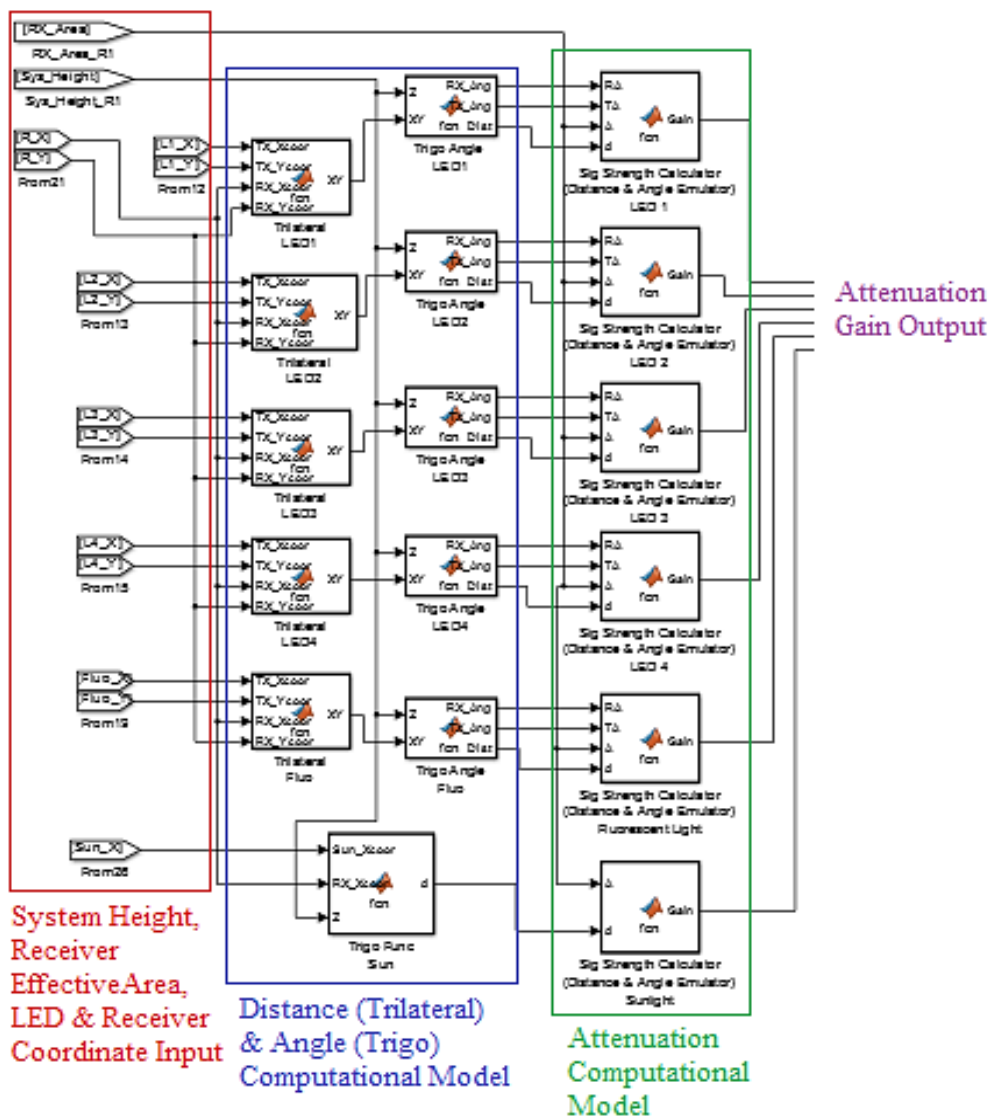


Figure 3.23: Optical Signal Attenuation Computational Model

### 3.3.7 Others Models in Simulink

Sub-model such as positioning error calculator, SNR calculator and SNR variance calculator are included in the Simulink. These models are built by using “MATLAB Function” model.

Since, the output from the Trilateral Coordinate Estimation model is the predicted coordinate of the system. A “positioning error calculator” is used to make

comparison between estimated and reference coordinate. The “SNR calculator” model is used to compute the Signal to Noise Ratio and determine the noise level in a given coordinate. The “SNR variance calculator” model is used to calculate the Variance for Gaussian Noise. The obtained variance value is to be inserted into the Gaussian Noise generator located in the “F-ID Modulation, LED and Interference” model.

Similarity, trilateral equation that used to calculate the distance between the transmitter and the receiver (Eq. 3.30) is used in the “positioning error calculator” model. This equation is modified as shown in Eq. 3.33.

$$\text{Positioning Error} = \sqrt{(X_{Est} - X_{Ref})^2 + (Y_{Est} - Y_{Ref})^2} \quad (3.33)$$

where  $X_{Est}$  is the estimated X coordinate,  $X_{Ref}$  is the reference X coordinate,  $Y_{Est}$  is the estimated Y coordinate and  $Y_{Ref}$  is the reference Y coordinate. The “SNR calculator” model is used (Eq. 3.25) to compute the Signal to Noise Ratio in given coordinate. The “SNR variance calculator” is used (Eq. 3.17) to compute the Gaussian Noise Variance. Figure 3.24 shows the sub-model to calculate Positioning Error, SNR and Noise Variance.

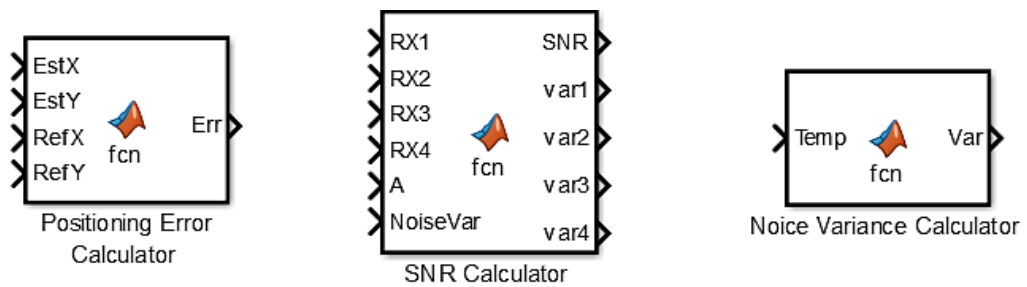


**Figure 3.24: Sub-model in Simulink**

## CHAPTER 4

### RESULTS AND DISCUSSION

#### 4.1 Result and Discussion of Individual Module

##### 4.1.1 Signal Generation

Based on the Section 3.3.1, four F-ID modulators were built by using sine wave model in MATLAB and the output from the F-ID modulator with sampling rate of 8192Hz is shown in Figure 4.1.

Logic 1 represents that the LED light is at on state; whereas, logic 0 represents the LED light is at off state. In the experiment, each frequency have different samples, for example, 8 samples are used for 1 kHz frequency, 4 samples are used for 2 kHz frequency. Frequency spectrum graph is generated to determine the fundamental and harmonic components of the F-ID modulated frequency. This are shown in Figure 4.2 (a) – (d). According to the Figures, frequency of 1 kHz, 1.25 kHz, 1.75 kHz and 2 kHz are chosen to prevent inter-cell interference. For example in Figure 4.2 (a), there are a few harmonic components, only the fundamental frequency, 1 kHz is useful to this experiment. It is important to ensure that the amplitude of the harmonic components do not affect the fundamental frequency (1 kHz, 1.25 kHz, 1.75 kHz, 2 kHz). If the signal does interfere each other, frequency used for the F-ID modulator need to revised again.

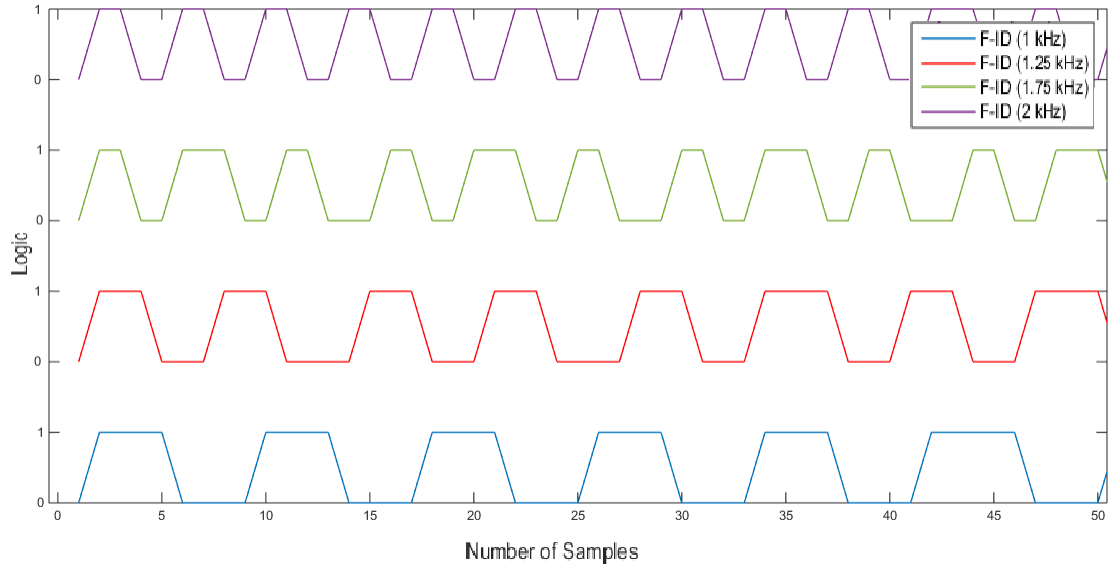
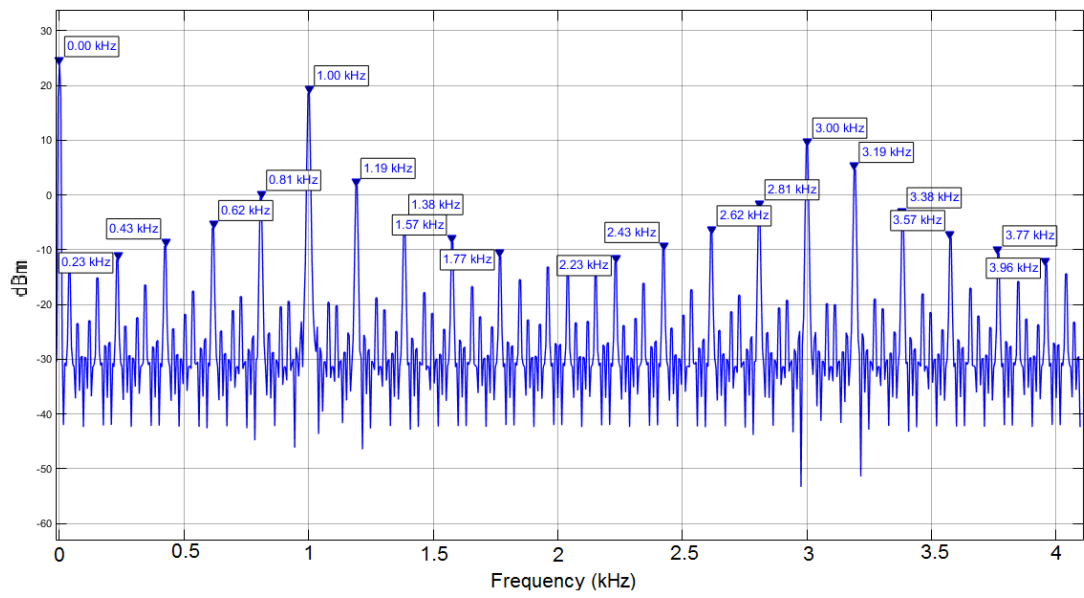
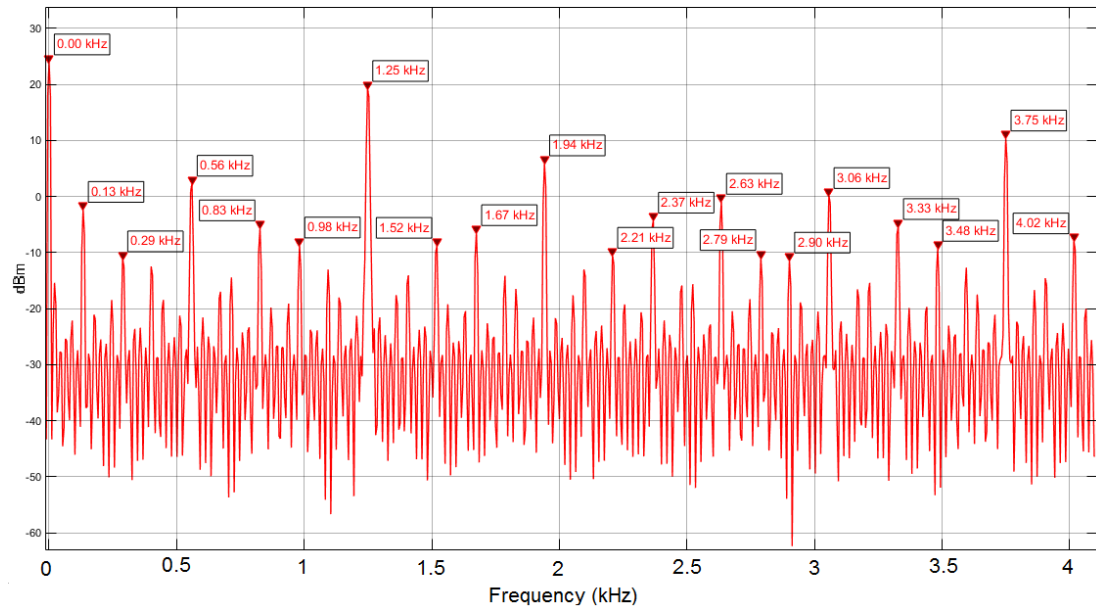


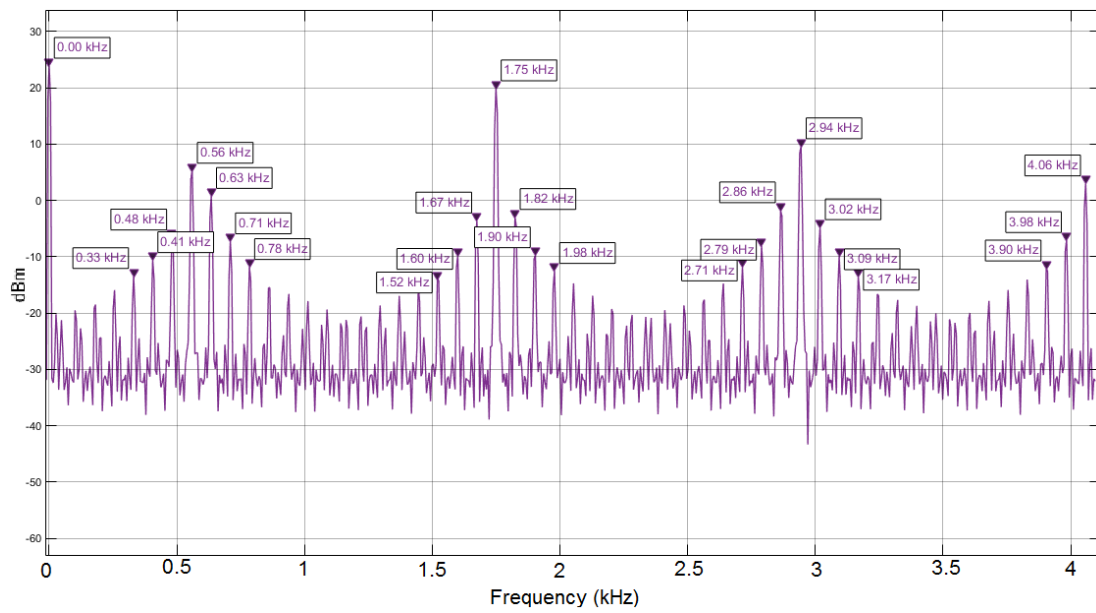
**Figure 4.1: Time Spectrum for the four F-ID generator**



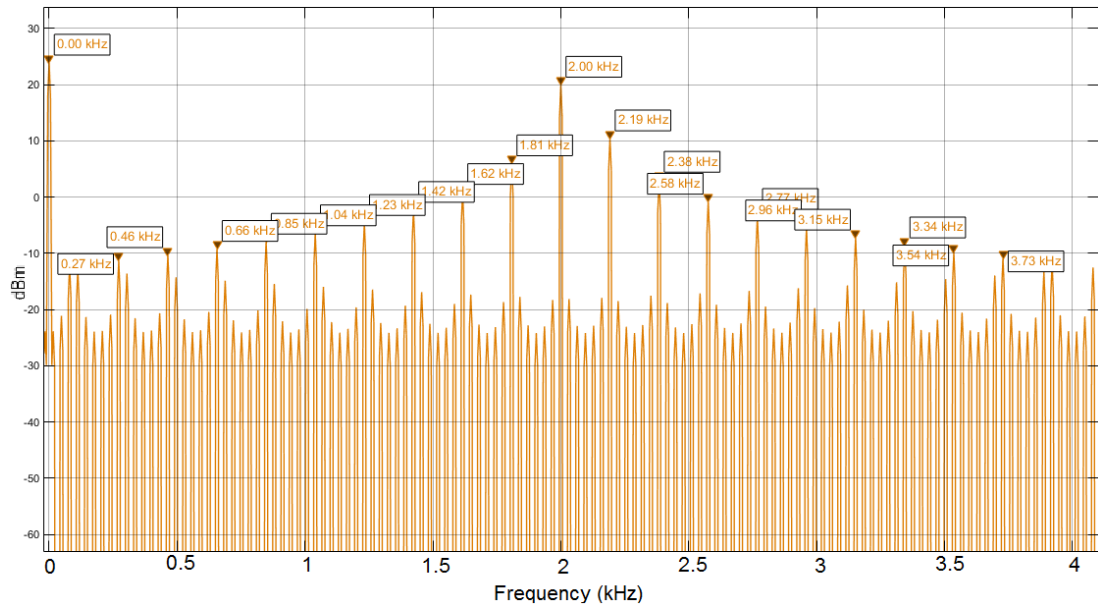
**(a) Frequency Spectrum of 1 kHz**



**(b) Frequency Spectrum of 1.25 kHz**



**(c) Frequency Spectrum of 1.75 kHz**

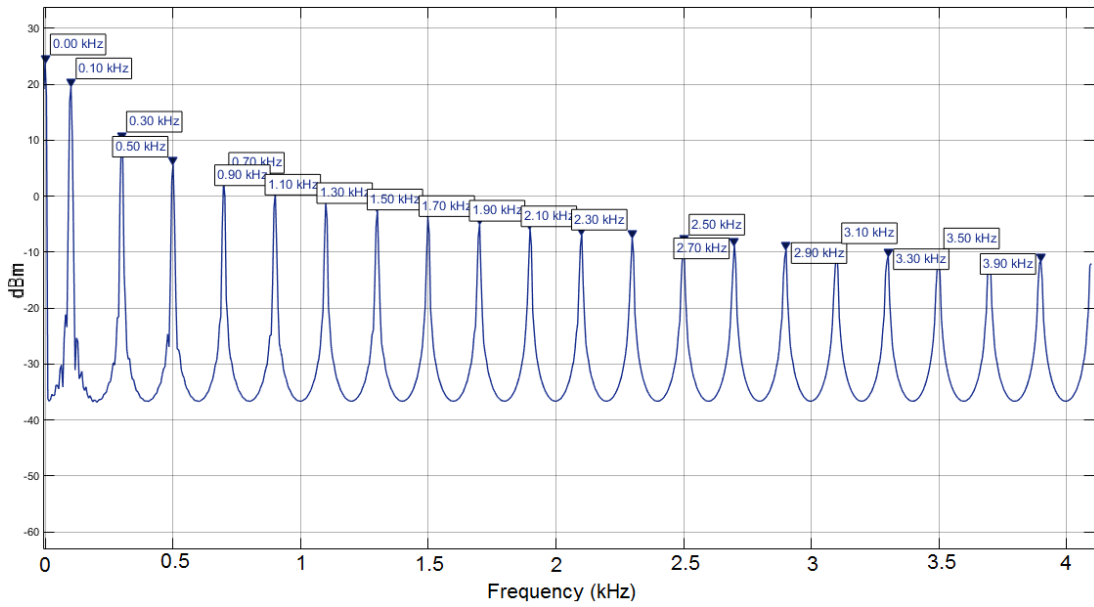


**(d) Frequency Spectrum of 2 kHz**

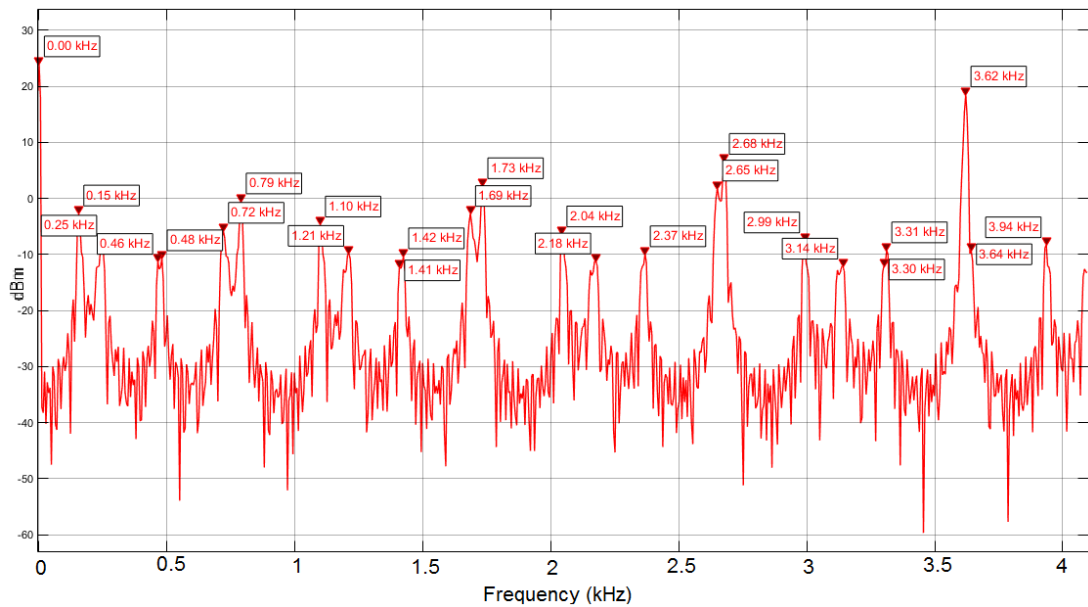
**Figure 4.2 (a) – (d): Frequency Spectrum of 1 kHz, 1.25 kHz, 1.75 kHz and 2 kHz F-ID Modulator**

In this proposed design, fluorescent light interference is used. Hence, the fundamental and harmonic frequencies components of the inductive / electronic ballast powered fluorescent light need to be determined. The used frequency for the F-ID modulator need to be revised if the fluorescent light affecting the F-ID modulator frequency (1 kHz, 1.25 kHz, 1.75 kHz, 2 kHz). The purpose of determine the fluorescent light spectrum and the revise F-ID modulator frequency is to minimize the interference cause by fluorescent light. Revise of F-ID modulator frequency is a process to change the modulated frequency to others frequency which no light source would affect the fundamental frequency amplitude in the chosen F-ID modulator frequency.

Figure 4.3 (a) – (b) shows the frequency spectrum of the fluorescent light that discussed in Section 3.3.1. Figure 4.3 (a) shows the frequency spectrum of fluorescent lighting with inductive ballast; whereas, Figure 4.3 (b) shows the frequency spectrum of fluorescent lighting with electronic ballast. Based on the results, there are no overlapping of harmonic frequencies with the fundamental frequencies of the F-ID modulators as shown in Figure 4.2 (a) – (d). Therefore, the F-ID modulator frequencies (1 kHz, 1.25 kHz, 1.75 kHz, 2 kHz) are suitable in the proposed system.



(a) Frequency Spectrum of Fluorescent (Inductive, 100Hz)



(b) Frequency Spectrum of Fluorescent (Electronic, 20 kHz)

**Figure 4.3 (a) – (b): Frequency Spectrum for Fluorescent Lamp with Inductive / Electronics Ballast**

Electrical noise and thermal noise exist in photodiode can be modelled as Gaussian Noise. The variance of the Gaussian Noise is computed in Section 3.2.7 and substituted into Gaussian Noise Generator. The simulated Gaussian Noise is analysed using Frequency Spectrum Analyser and the spectrum is shown in Figure 4.4. The

Gaussian Noise will affect the F-ID signal in the VLC-IPS. The amplitude of the Gaussian Noise are changed with respect to the time and there will affect the performance of the VLC-IPS.

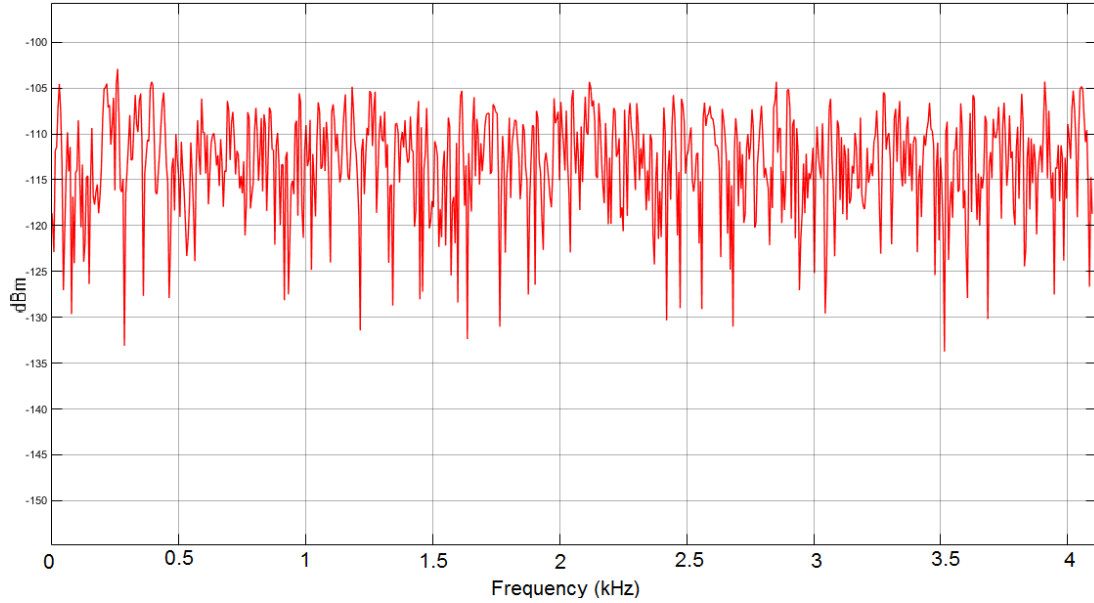


**Figure 4.4: Gaussian Noise Spectrum**

#### 4.1.2 Signal Received

The optical signals such as F-ID modulated signals, fluorescent and Sunlight signals and Gaussian Noise are received by photodiode and converted into electrical signal. The photodiode receiver is located at the centre of the system (3, 3, 1) as shown in Figure 4.5. The time spectrum and frequency spectrum of the photodiode were retrieved. These are shown in Figure 4.6 and Figure 4.7 respectively. According to Figure 4.7, the received signal components are located among all frequencies. The F-ID modulator frequencies (1 kHz, 1.25 kHz, 1.75 kHz, 2 kHz) are needed frequencies. According to Lambertian Equation, the amplitude components of the modulator frequencies should be the same when the receiver is at the centre of the simulation environment (Figure 4.5). However, in Figure 4.7, the amplitudes of the frequencies (1 kHz, 1.25 kHz, 1.75 kHz, 2 kHz) are different from each other because of the Gaussian Noise. Thus, the accuracy of the VLC-IPS is varied with the Gaussian Noise.

The frequency components from the sunlight and fluorescent light components do not interfere the amplitude of the modulated frequencies. This mean, the sunlight and fluorescent light only cause slight rise in Shot Noise which have low impact on the system.

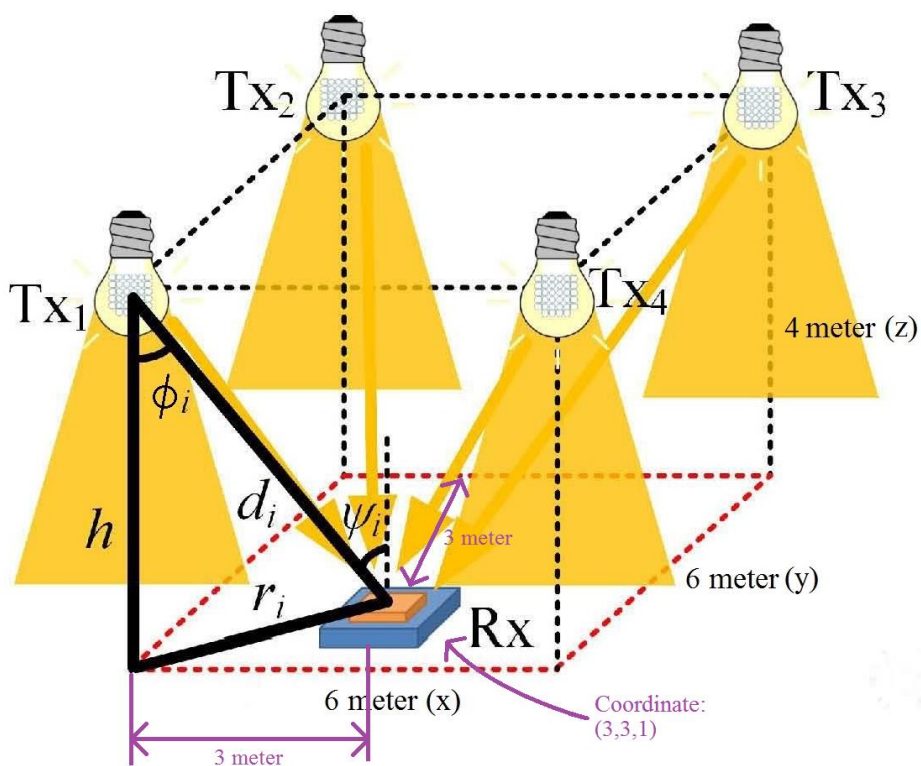


Figure 4.5: Photodiode at Coordinate (3, 3, 1)

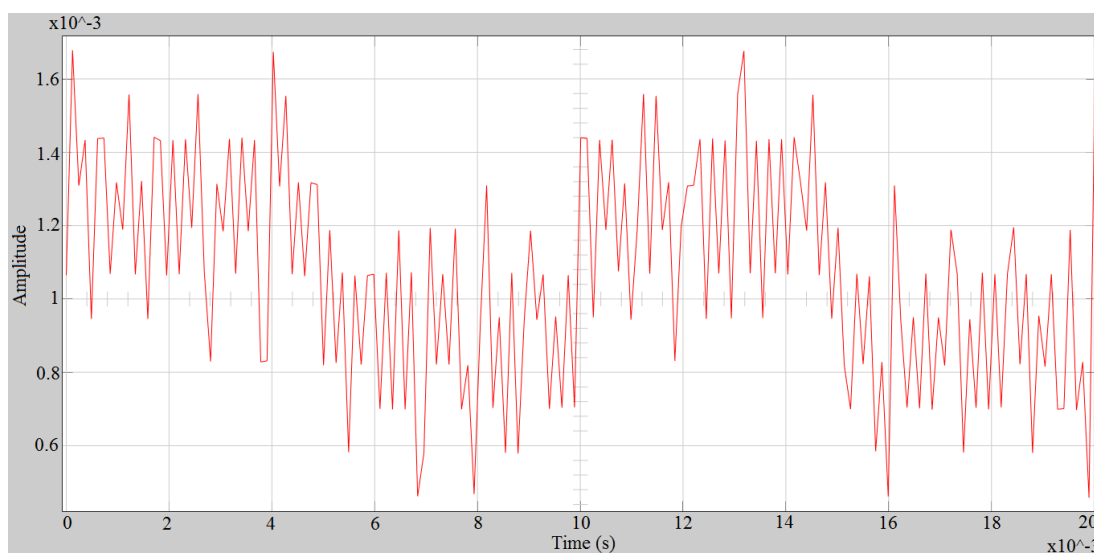
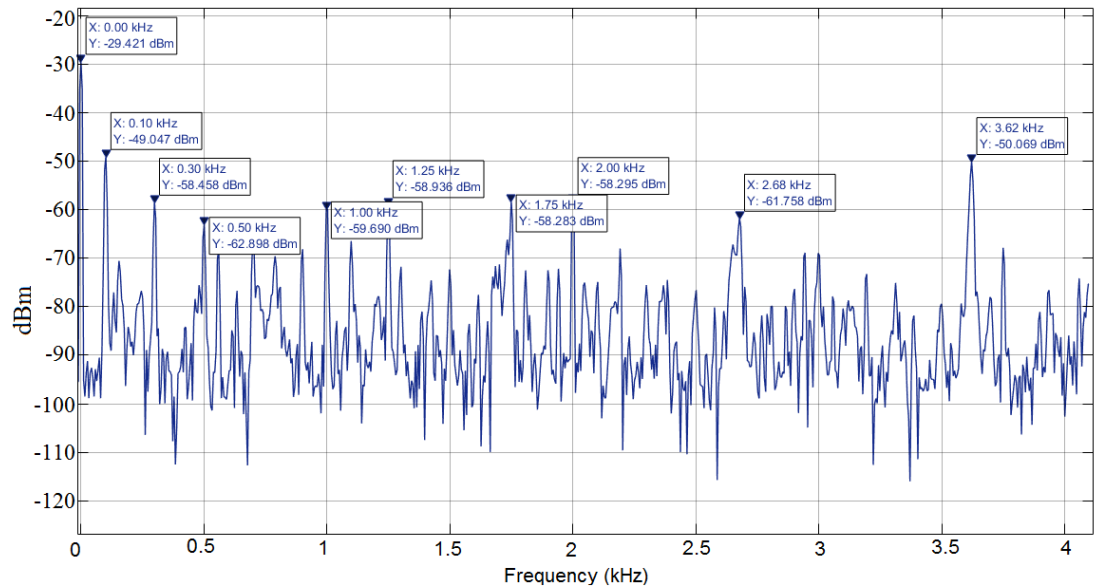


Figure 4.6: Photodiode Received Signal in Time Spectrum



**Figure 4.7: Photodiode Received Signal in Frequency Spectrum**

### 4.1.3 Signal Filtering and Selection

The received signals from photodiode are sampled to form an array of 8192 members at every second. The sampled array is converted into frequency spectrum using FFT. As discussed in section 3.3.3, the 1 kHz modulated signal is located at 1001 member, 1.25 kHz modulated signal is located at 1251 member, 1.75 kHz modulated signal is located at 1751 member and 2 kHz modulated signal is located at 2001 member. The photodiode receiver is placed at the coordinate (3, 3, 1) as shown in Figure 4.5. The raw data is sent to FFT for time to frequency spectrum conversion. The operation is shown in Figure 4.8. The amplitude and the location of the modulated signal are shown in Figure 4.8. The receiver is located at the centre of the simulation environment (Figure 4.5). Therefore, the amplitude of the four modulated signal (1 kHz, 1.25 kHz, 1.75 kHz, 2 kHz) are having value which approximately equal to each other. Furthermore, the amplitude of the modulated signal from FFT output array is converted to lumen for distance estimation computation.

|      |        |
|------|--------|
| 999  | 0.0017 |
| 1000 | 0.0029 |
| 1001 | 0.3145 |
| 1002 | 0.0036 |
| 1003 | 0.0011 |
| 1749 | 0.0036 |
| 1750 | 0.0011 |
| 1751 | 0.3117 |
| 1752 | 0.0017 |
| 1753 | 0.0018 |
| 1249 | 0.0164 |
| 1250 | 0.0175 |
| 1251 | 0.3099 |
| 1252 | 0.0013 |
| 1253 | 0.0022 |
| 1999 | 0.0016 |
| 2000 | 0.0012 |
| 2001 | 0.3132 |
| 2002 | 0.0023 |
| 2003 | 0.0014 |

**Figure 4.8: 1 kHz, 1.25 kHz, 1.75 kHz and 2 kHz in FFT Result Array**

#### 4.1.4 Distance Estimation

Distance Estimation model was used to compute the distance by the given amplitude of the modulated signal. The distance estimation model is modelled using Lambertian equation (Eq. 4.1). Figure 4.9 shows the transmitter and receiver setup for the Lambertian characteristic determination. In Figure 4.9, a transmitter and a receiver are separated from each other with 1 meter height. The transmitter location is fixed; whereas, the receiver is moved along the x-axis. The result from receiver was shown in Figure 4.10.

In Figure 4.10, the graph shows that the Lambertian gain fall exponentially as the distance between TX and RX increases from 1 meter to 6 meter. Thus, Lambertian gain will become smaller when the distance is increased. According to the Lambertian equation (Eq. 4.2), the VLC-IPS performance can be improved when there is an increase in the half-angle of the transmitter or the receiver. Increase in the half angle will reduce the power in distance,  $d$  and the system height,  $h$  variables in Lambertian equation (Eq. 3.7) from power of 3.5 to a smaller value. Thus, this in turn will reduce the SNR of the system. Besides that, reducing the distance between transmitter and receiver by reducing the system height is another way to improve the VLC-IPS performance; however, it is not a good and practical solution.

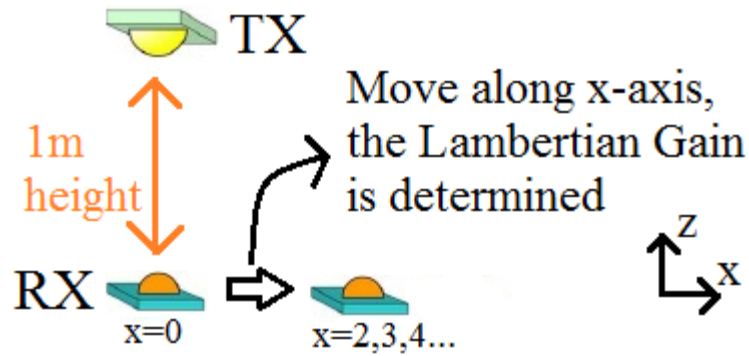


**Figure 4.9: Setup for Lambertian Characteristic Determination**

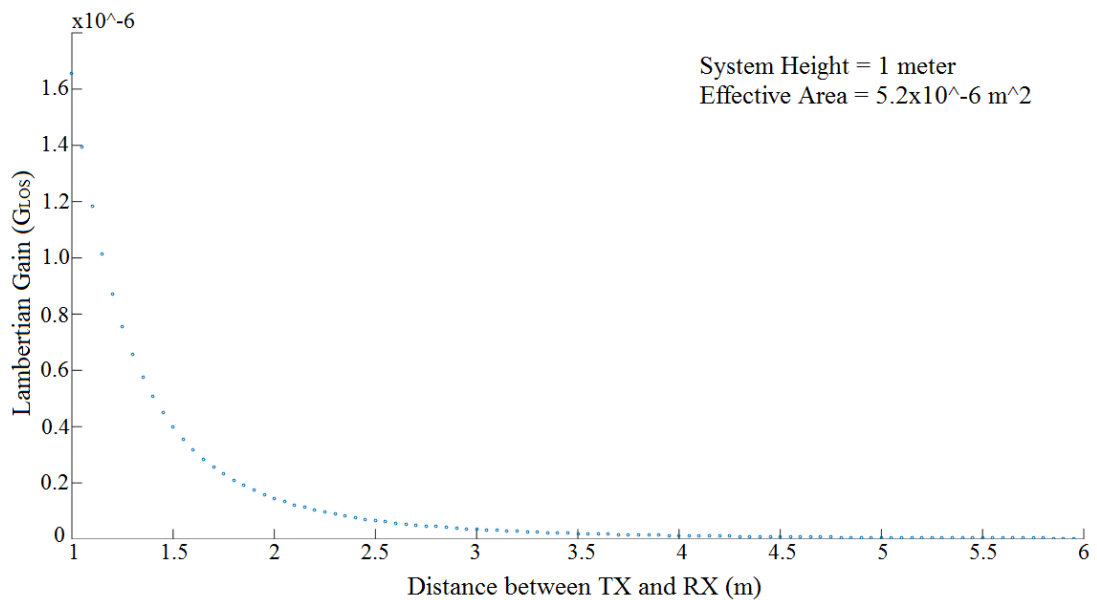


**Figure 4.10: Lambertian Gain with Different Distance between TX and RX**

## 4.2 VLC-IPS Performance

### 4.2.1 Performance with All Interference

In VLC-IPS, the error between estimated coordinates and reference coordinates are used to study the performance of the VLC-IPS. The system is shown in Figure 3.3 is built with all the interference such as fluorescent light, sunlight and Gaussian noise are taken into consideration when gathering the result. The VLC-IPS will be setup as shown in Figure 4.11. The photodiode receiver is simulated to move around the x-axis and y-axis (reference coordinates input) with 1 m height from ground and the estimated

coordinates are computed according to the position of the receiver. The positioning error between estimated coordinates and receiver coordinates (reference coordinate) is used to determine the performance of the VLC-IPS. Figure 4.12 shows the result of the estimated coordinates and the reference coordinates of VLC-IPS in 2-D plane.

In Figure 4.12, the estimated coordinates follows the receiver coordinates (reference coordinates) when the receiver moves around x-axis and y-axis. The positioning error is minimal when the receiver is at the centre area of the simulation environment. However, the accuracy of the estimated coordinates begin to drop when the receiver reaches the corner of the simulation environment which is described in Figure 4.13. In Figure 4.14, the photodiode receiver is move along x-axis and y-axis. The positioning error at each coordinate (1 cm resolution) is determined and shown in Figure 4.14.

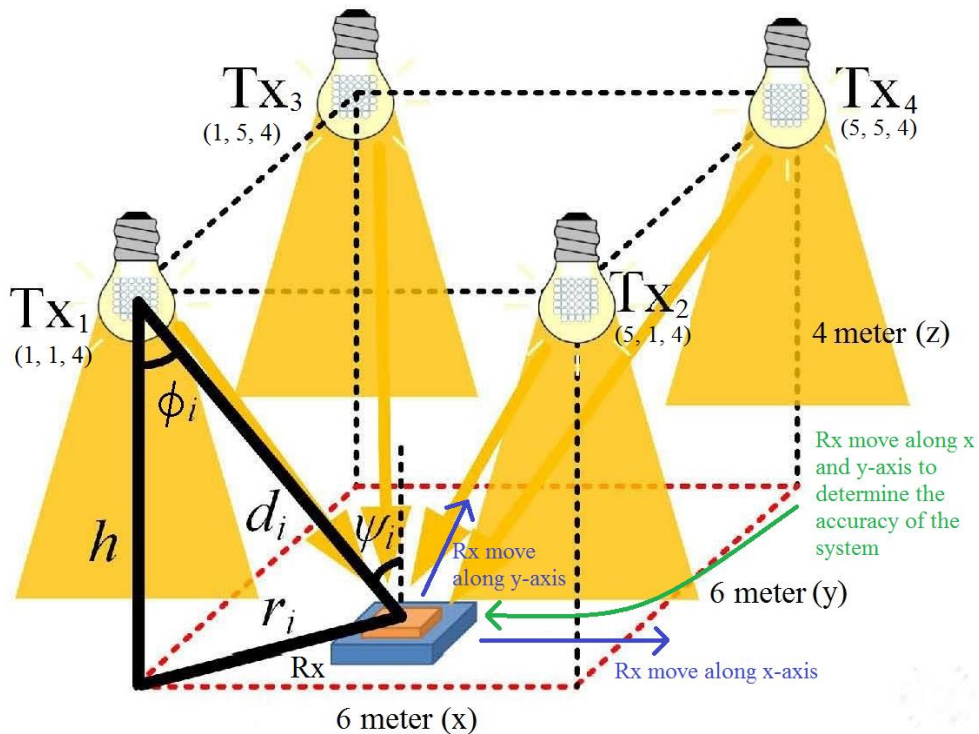


**Figure 4.11: VLC-IPS Setup for Performance Testing**

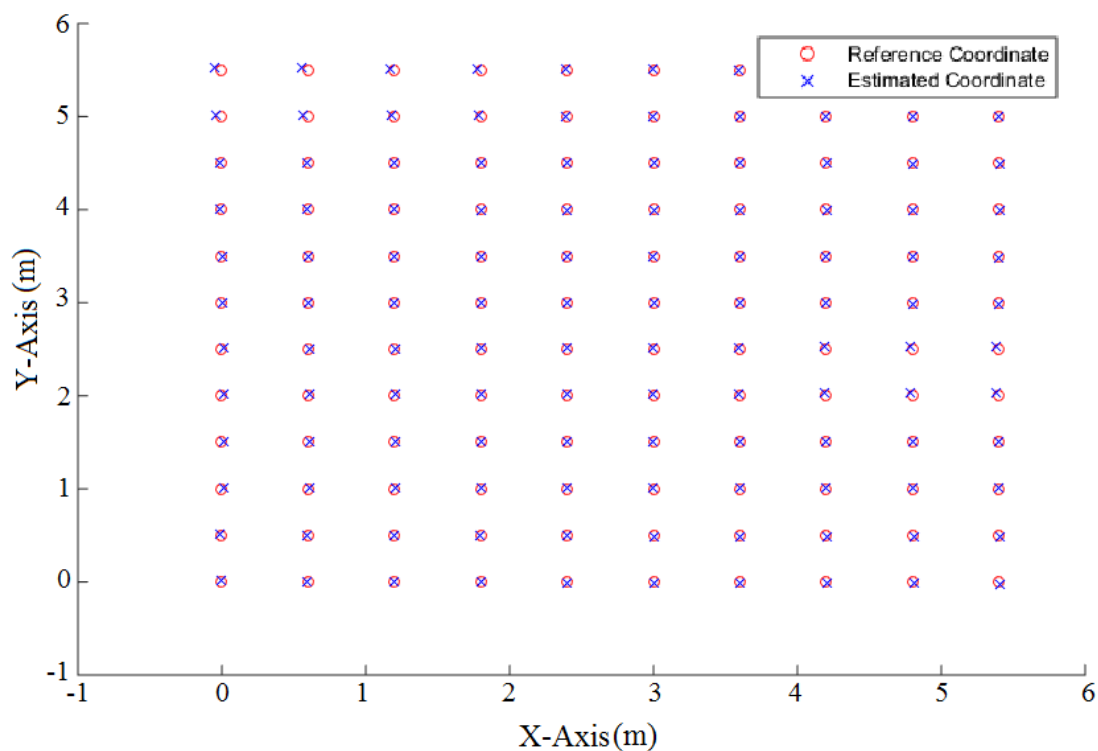


**Figure 4.12: Result of Estimated and Reference Coordinate in XY plane**

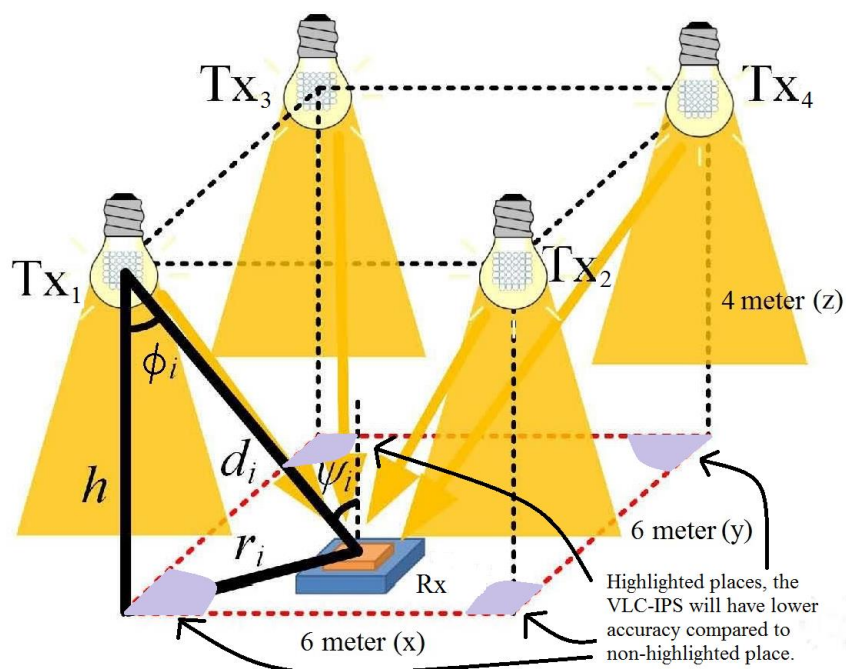


**Figure 4.13: Image on VLC-IPS Accuracy Description**

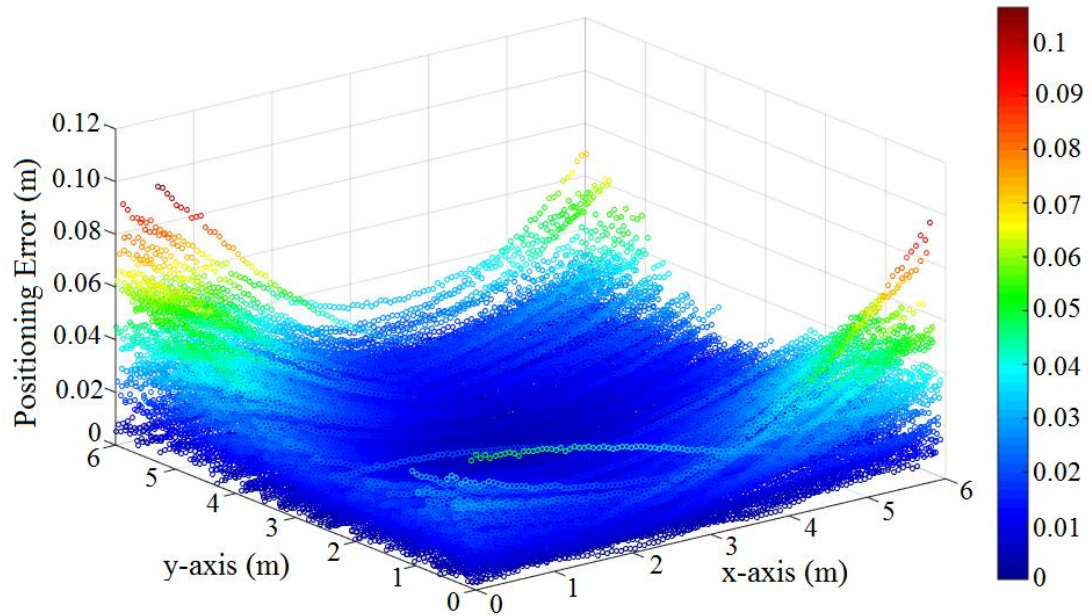


**Figure 4.14: Positioning Error of VLC-IPS**

In Figure 4.14, points in dark blue colour mean the coordinate has the lowest positioning error; however, dark red coloured points mean the coordinate has the highest positioning error. In other words, VLC-IPS performs better at the dark blue coloured region. In Figure 4.12 and Figure 4.14, the VLC-IPS perform the best at the centre region where the four LEDs transmitters are located. However, the positioning error is still considered low if the receiver stays inside the four LEDs transmitter bounded region. For example, the four LEDs transmitter are installed at position of (1, 1, 4), (5, 1, 4), (1, 5, 4), (5, 5, 4). If the photodiode receiver stays inside the bounded region (x-axis from 1 to 5 and y-axis from 1 to 5), the positioning error is still considered to perform well. However, the positioning error is increased rapidly once the receiver is moved out of the LEDs transmitters bounded region. For example, the photodiode receiver is located at (0, 6, 1) while all the LEDs transmitter are installed as mentioned.

Larger positioning errors are normally located at the four corners in the simulation environment because the average distance from all four LEDs transmitters to Photodiode receiver is the longest. The longer the distance the modulated signal needs to travel, its amplitude is attenuated dramatically as described in Section 4.1.4 and Figure 4.10. Thus, higher noise levels are introduced causing lower SNR. In Figure 4.15, the SNR graph of the photodiode receiver with respect to LED 1 (1, 1) is shown.

In the Figure 4.15, the SNR drops significantly when the distance between transmitters and receiver is increased. It is similarly seen in the photodiode receiver with respect to the other three LEDs transmitters as shown in Figure 4.16, Figure 4.17 and Figure 4.18. The average SNR of the photodiode receiver for the VLC-IPS is shown in Figure 4.17. Based on the average SNR graph, the four corners in the simulation environment have the lowest SNR compared to the centre. Hence, this explains the larger positioning error that occurs at the corner.

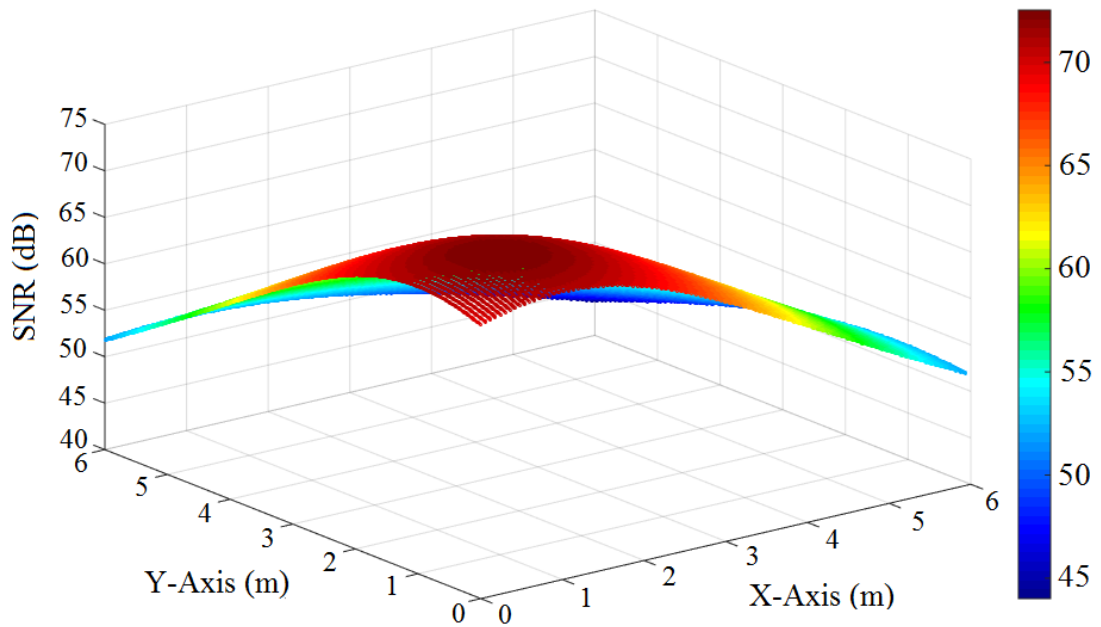


**Figure 4.15: SNR graph of PD Receiver with respect to LED 1 (1, 1)**

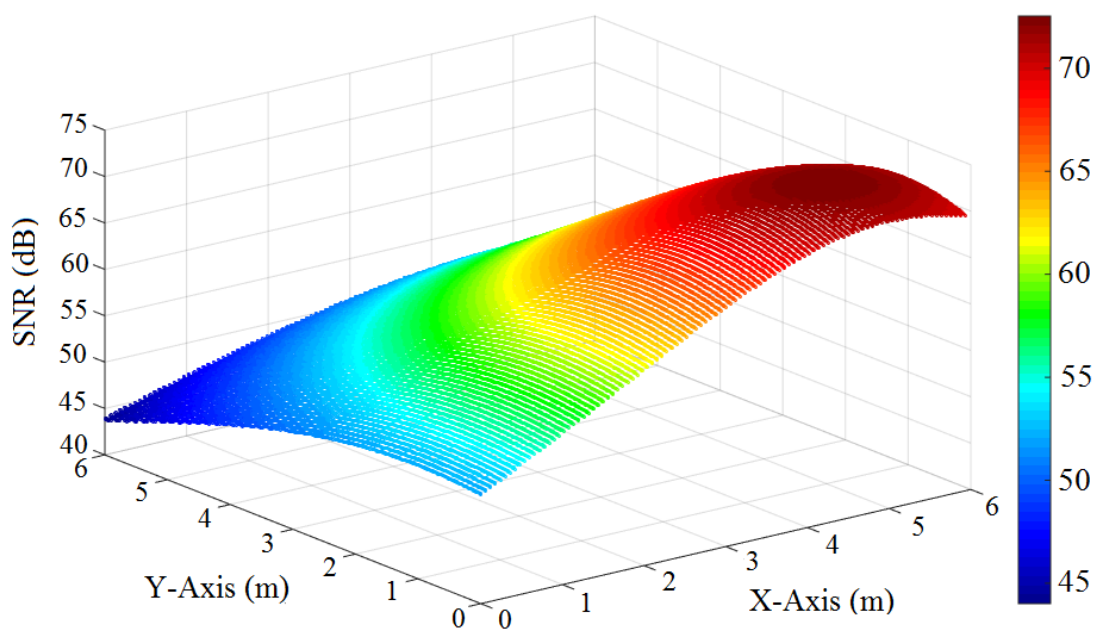


**Figure 4.16: SNR graph of PD Receiver with respect to LED 2 (1, 5)**

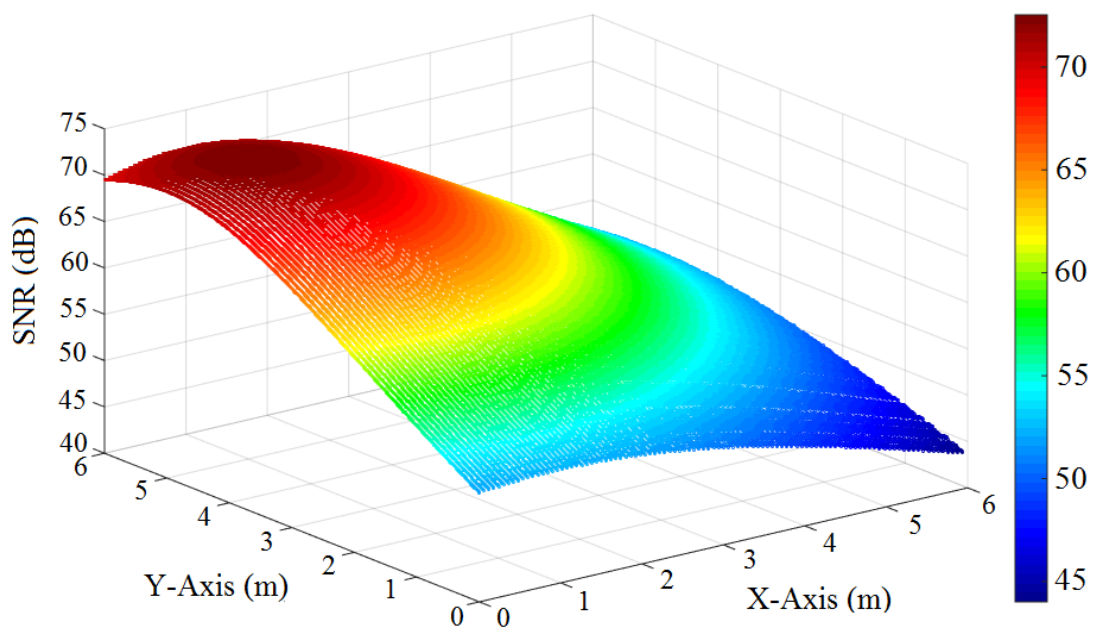


**Figure 4.17: SNR graph of PD Receiver with respect to LED 3 (5, 1)**

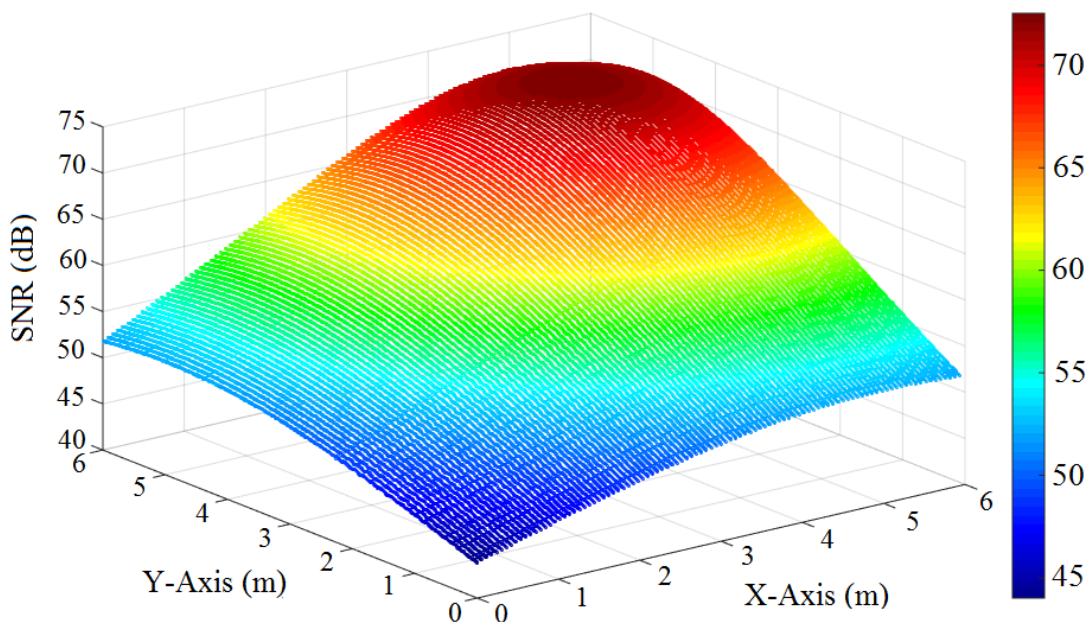


**Figure 4.18: SNR graph of PD Receiver with respect to LED 4 (5, 5)**

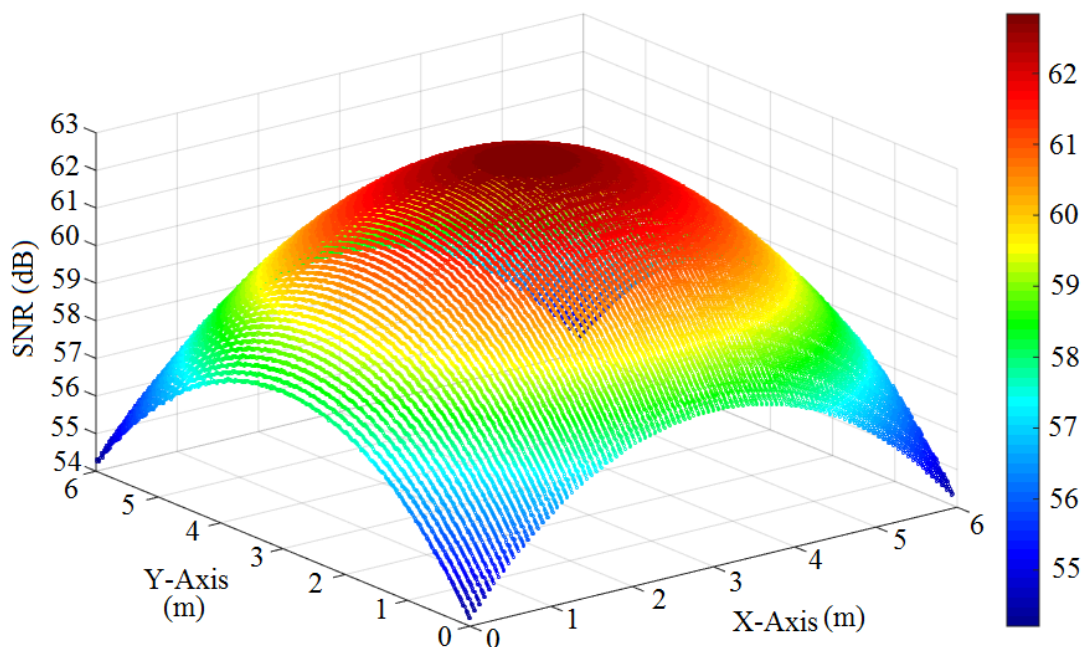


**Figure 4.19: SNR graph (Average) of PD receiver in VLC-IPS**

In the Figure 4.14, sixty thousand results are computed for 6m x 6m x 4m room with 1 cm resolution. The positioning error in the form of Histogram and Cumulative Distribution Function (CDF) result is shown in Figure 4.20 and Figure 4.21 respectively. According to the histogram graph, the highest point has a positioning error of 5 mm. Most of the estimated coordinates have positioning error that less than

0.02 m. However, as the positioning error increased, the number of samples (estimated coordinate) drop exponentially.

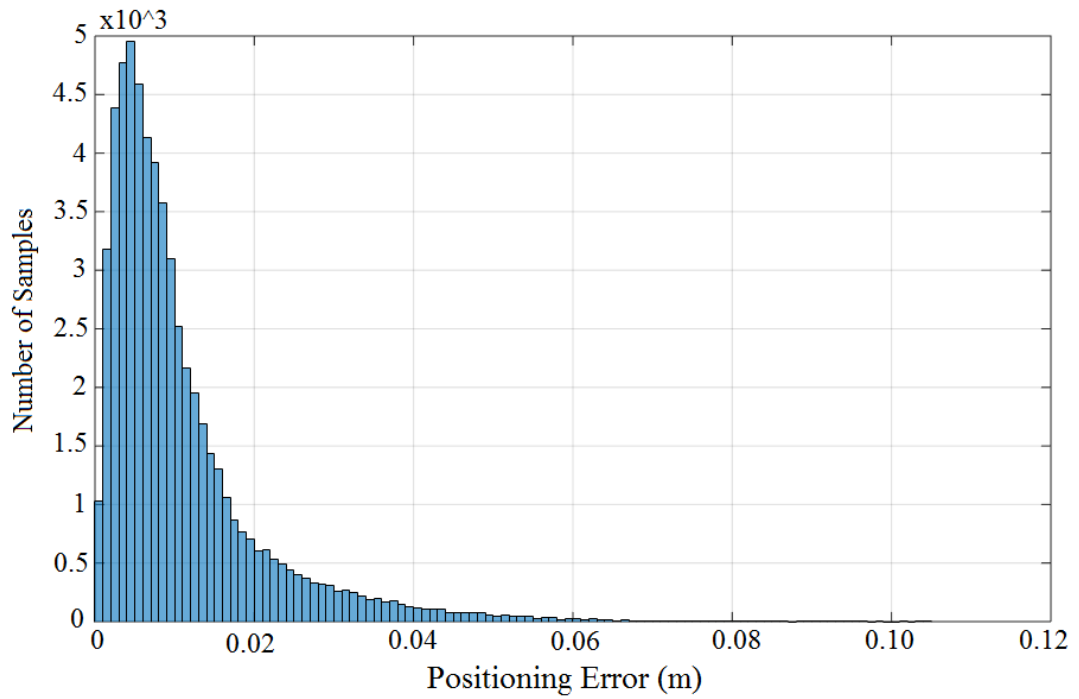


**Figure 4.20: Histogram of Positioning Error**

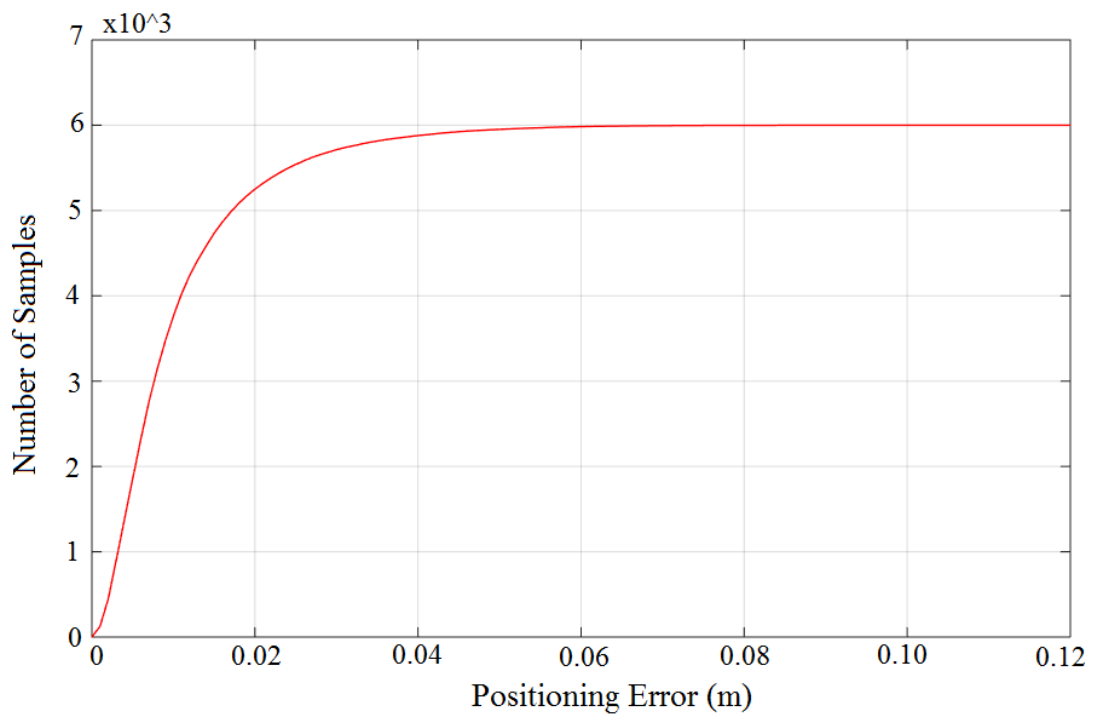


**Figure 4.21: Cumulative Distribution Function (CDF) of Positioning Error**

In a nutshell, this proposed design has **average positioning error of 0.0105 m (1 cm)** and **the average SNR of 59.8678 dB**. With this small positioning errors, appliances such as Robot Navigation, Indoor Navigation are suitable to be used.

#### 4.2.2 Performance without Fluorescent Light Interference

The effect of fluorescent light on the modulated signal is important to be studied in this project. During the result retrieving process, the fluorescent light is switched off and the receiver is moved along x-axis and y-axis (Figure 4.11) with 1 m height to collect the estimated coordinate data. The positioning error without fluorescent light interference is plotted in Figure 4.22. Compare between the graph of positioning error without fluorescent light (Figure 4.22) and the graph of positioning error with interference (Figure 4.14), it is found that the one without fluorescent light, the VLC-IPS is able to estimate the coordinate more accurately (lower positioning error).

Signal to Noise Ratio (SNR) for VLC-IPS without fluorescent light is shown in Figure 4.23. VLC-IPS without fluorescent light, gives higher SNR than the VLC-IPS with all interference. According to the SNR graph w/o fluorescent light (Figure 4.23), the maximum SNR is about 64 dB and the minimum SNR is about 56 dB. However, the SNR graph with interference (Figure 4.19), the maximum and minimum SNR are 62 dB and 54 dB respectively.

Histogram and Cumulative Distribution Function (CDF) are plotted and shown in Figure 4.24 and Figure 4.25 respectively. In Figure 4.24, the highest point has a positioning error of 2 mm. Most of the estimated coordinates have the positioning error of about 0.09 m (0.9 cm). As the positioning error increase, the number of estimated coordinate drop exponentially.

In conclusion, the **average positioning error w/o fluorescent light interference is 0.0084 m (0.84 cm)** and the **average SNR w/o fluorescent light interference is 61.6284 dB**.

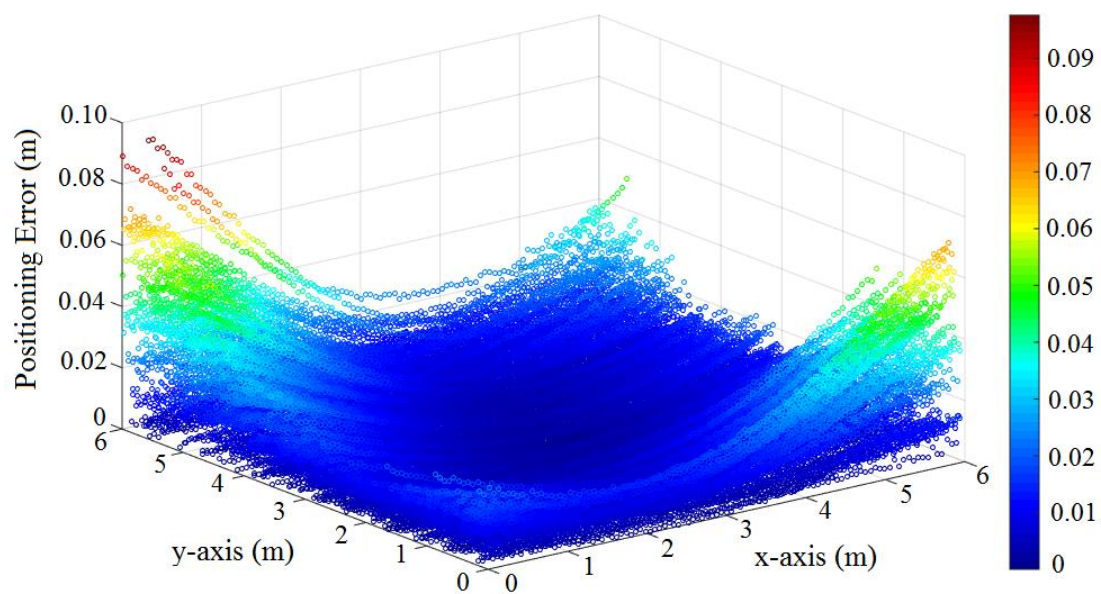


**Figure 4.22: Positioning Error w/o Fluorescent Light**

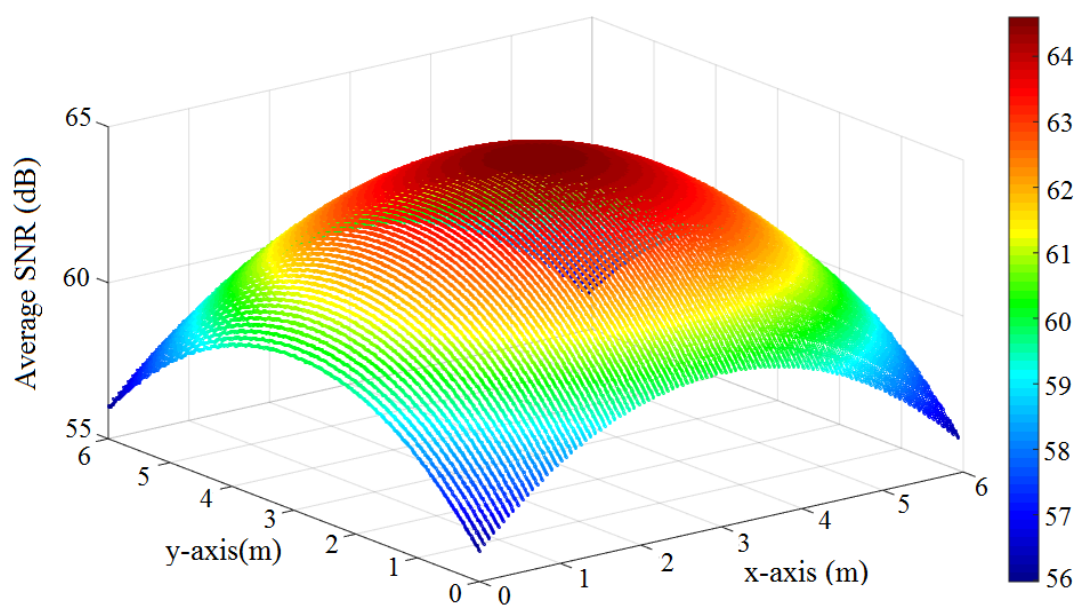


**Figure 4.23: Average SNR w/o Fluorescent Light**

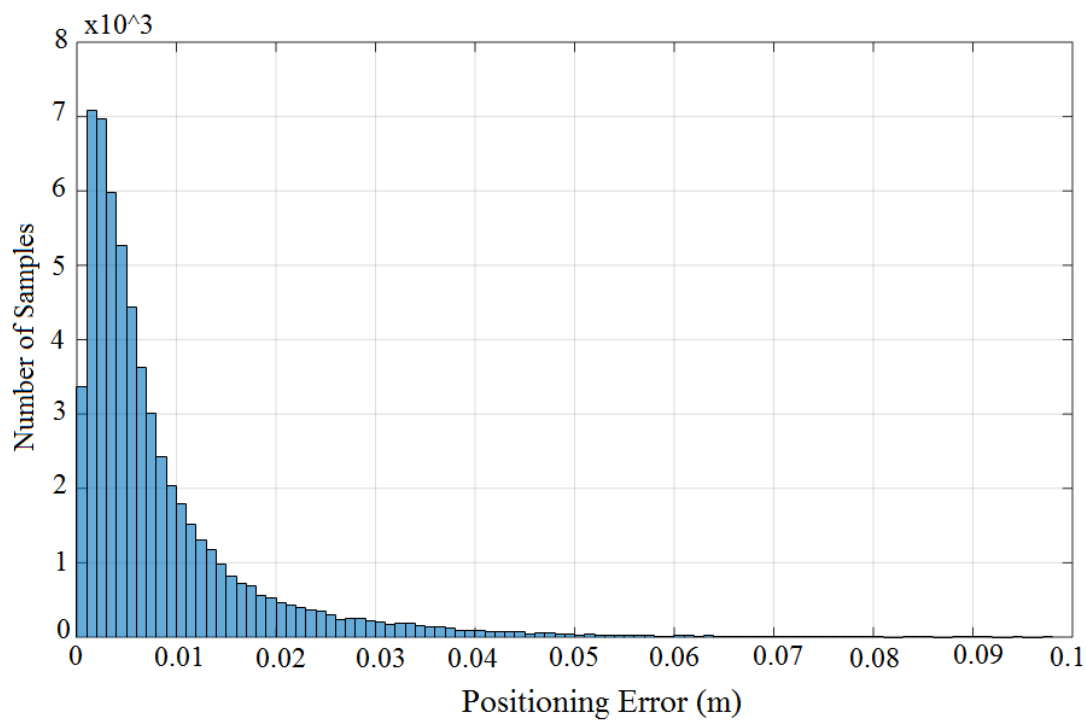


**Figure 4.24: Histogram of Positioning Error w/o Fluorescent Light**

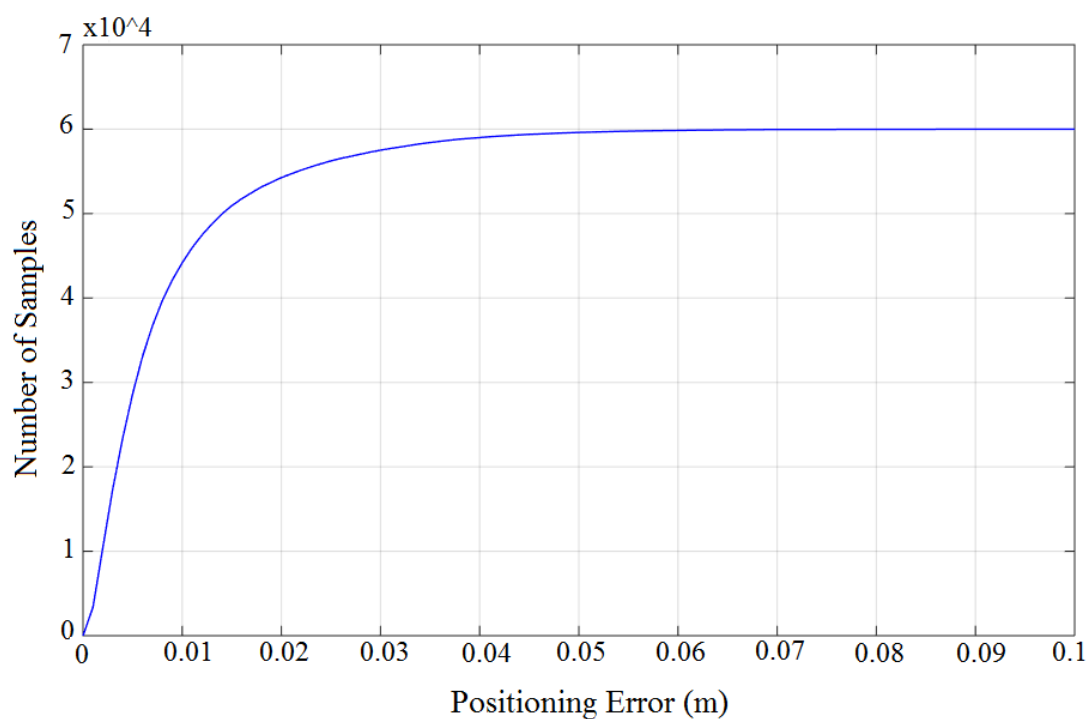


**Figure 4.25: Cumulative Distribution Function (CDF) of Positioning Error w/o Fluorescent Light**

### 4.2.3 Comparison between the Performance with Fluorescent and without Fluorescent

The performance different between with fluorescent and without fluorescent light interference is studied in this section. The average positioning error and SNR for both cases are tabulated in Table 4.1. The Cumulative Distribution Function (CDF) of positioning error for both cases are plotted in Figure 4.26.

**Table 4.1: Comparison Table for with or w/o Fluorescent**

|                   | All Interference Included (X) | Without Fluorescent Interference (Y) | $ X-Y $<br>$(\frac{X-Y}{X} \times 100\%)$ |
|-------------------|-------------------------------|--------------------------------------|---|
| Positioning Error | 0.0105 m                      | 0.0084 m                             | 0.0021 m (20%)                            |
| SNR               | 59.8678 dB                    | 61.6284 dB                           | 1.7606 dB (2.94%)                         |

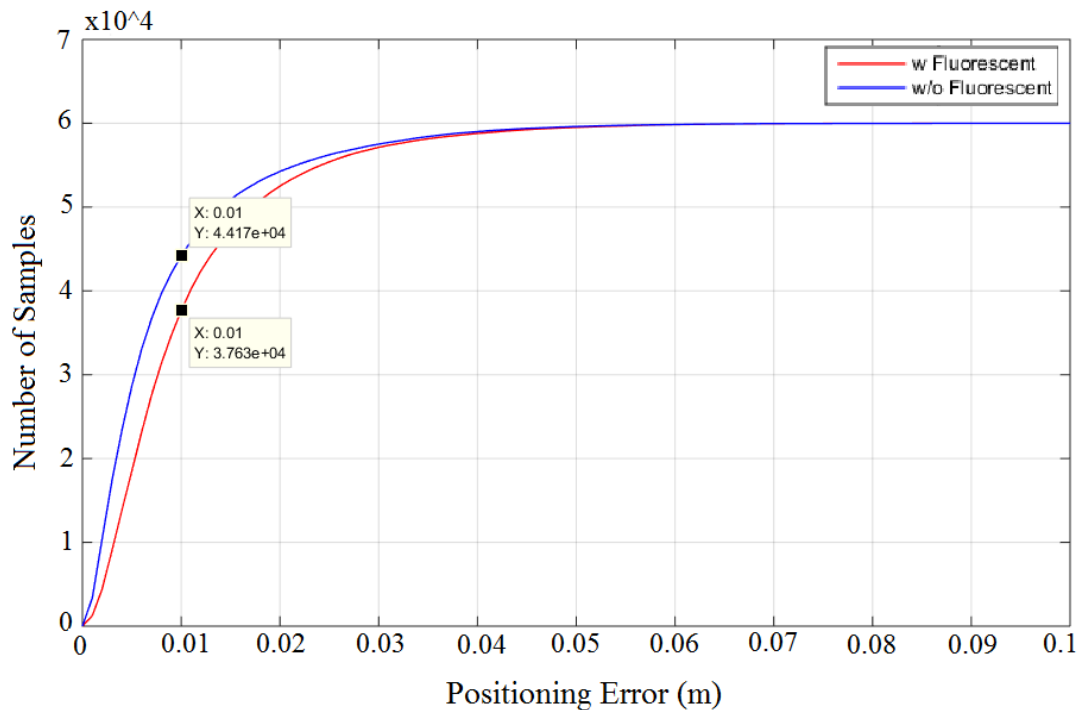


**Figure 4.26: Cumulative Distribution Function (CDF) for Positioning Error with and w/o Fluorescent**

According to Table 4.1, the VLC-IPS with interference included, the average positioning error is 0.0105 m (1 cm) and the average SNR is 59.8678 dB; however in

the VLC-IPS w/o fluorescent light interference, the average positioning error is 0.0084 m (0.84 cm) and the average SNR is 61.6284 dB. As compare between the positioning error and the SNR for both cases, the average positioning error for VLC-IPS w/o fluorescent interference is about 2mm (20%); whereas the SNR drops about 2dB (2.94%). In a nutshell, the fluorescent light does cause small interference to the modulated signal. As discussed in Section 4.1.1, theoretically the inductive ballast and electronic ballast powered fluorescent light have different spectrum with F-ID modulated frequency (1 kHz, 1.25 kHz, 1.75 kHz, 2 kHz) but it gives higher positioning error and lower SNR (Table 4.1). That is because, the fluorescent light increases the total intensity of light. Therefore, it introduces higher shot noise, and Gaussian noise to the system, hence reduces the SNR and the accuracy of the system. The electronic ballast powered fluorescent light is operated at 20 kHz and sampling rate of the system is 8192Hz, hence the operating frequency of electronic ballast introduces multiple fundamental and harmonic frequency (Figure 4.3(b)). A few of this fundamental and harmonic frequencies have same frequency with F-ID modulated frequencies. Therefore, error in the received signal amplitude is introduced to the system by the summation of this fundamental and harmonic frequencies with the F-ID modulated frequency. The amplitude error in the received signal, introduces higher positioning error to the system.

Based on the CDF graph (Figure 4.26), the VLC-IPS w/o Fluorescent Light Interference have higher samples (estimated coordinate) at 0.01 positioning error than VLC-IPS with all interference.

#### **4.2.4 Performance Comparison with Others Work**

In Zhang et al. (2014) work, the Basic Framed Slotted Additive (BFSA) is used for LED modulation and the RSS method is used for distance estimation. The simulation environment used by Zhang et al. (2014) is 6m x 6m x 4m. Four LEDs are placed accordingly at coordinates (2, 2, 4), (4, 2, 4), (2, 4, 4) and (4, 4, 4). Photodiode receiver is lifted up 1 m from ground. The average positioning error of 0.0179m is reported.

The setup in Zhang et al. (2014) work is summarise into Table 4.2. The positioning error for Zhang et al. (2014) work is shown in Figure 4.27.

**Table 4.2: Methods and Environment Setup (Zhang et al., 2014)**

|                                  |                 |
|----------------------------------|-----------------|
| Modulation Method                | BFSA            |
| Distance Estimation Method       | RSS             |
| Environment Dimension            | 6m x 6m x 4m    |
| LEDs Transmitter Coordinate      |                 |
| 1. LED 1                         | 2, 2, 4         |
| 2. LED 2                         | 4, 2, 4         |
| 3. LED 3                         | 2, 4, 4         |
| 4. LED 4                         | 4, 4, 4         |
| Modulation Bandwidth             | 640 kHz         |
| <b>Average Positioning Error</b> | <b>0.0179 m</b> |

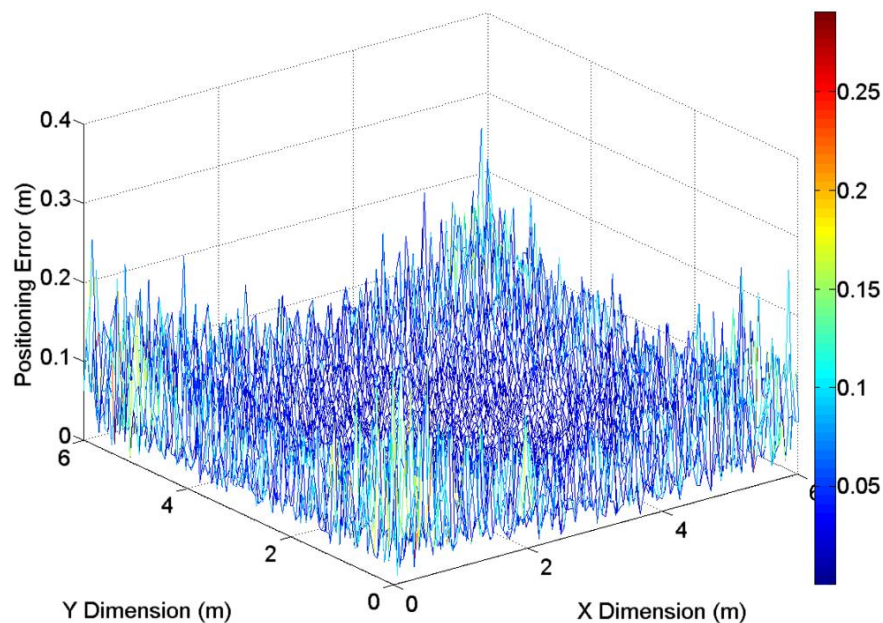


**Figure 4.27: Positioning Error (Zhang et al., 2014)**

However, in the proposed VLC-IPS, the average **positioning error is 0.0068 m** and the positioning error in XY-plane is shown in Figure 4.28.

The proposed VLC-IPS provides better accuracy. In the proposed design, the F-ID modulation have the advantages of immunity towards the interference causes by

others light source when the modulated frequency is configured correctly. However, the BSFA modulation scheme did not have such immunity. In BSFA modulation method, it subjects to frequency modulated light interference such as inductive ballast powered fluorescent light. In another hands, BSFA provides a simpler modulation method and it can support more LEDs with a smaller modulation bandwidth. According to Komine and Nakagawa (2004), higher modulation bandwidth introduce higher shot noise into the system. In Zhang et al. (2014), the modulation bandwidth of 640 kHz is used whereas in this proposed project, 1 kHz modulation bandwidth is used. Therefore, the proposed design is having a smaller shot noise, and Gaussian noise gives a lower positioning error and better accuracy in coordinate estimation. In conclusion, the proposed system provide better accuracy but at the same time it increases the complexity of the system. The proposed system and Zhang et al. (2014) work is tabulated in Table 4.3.

**Table 4.3: Summary of Proposed System and Zhang et al. (2014) System**

|                                  | <b>Proposed System</b> | <b>Zhang et al. (2014) system</b> |
|----------------------------------|------------------------|-----------------------------------|
| Modulation Method                | FDM                    | BFSA                              |
| Distance Estimation Method       | RSS                    | RSS                               |
| Environment Dimension            | 6m x 6m x 4m           | 6m x 6m x 4m                      |
| Number of LEDs used              | 4                      | 4                                 |
| 1. LED 1 Coordinate              | 2, 2, 4                | 2, 2, 4                           |
| 2. LED 2 Coordinate              | 4, 2, 4                | 4, 2, 4                           |
| 3. LED 3 Coordinate              | 2, 4, 4                | 2, 4, 4                           |
| 4. LED 4 Coordinate              | 4, 4, 4                | 4, 4, 4                           |
| Modulation Bandwidth             | 1 kHz                  | 640 kHz                           |
| <b>Average Positioning Error</b> | <b>0.0068m</b>         | <b>0.0179m</b>                    |

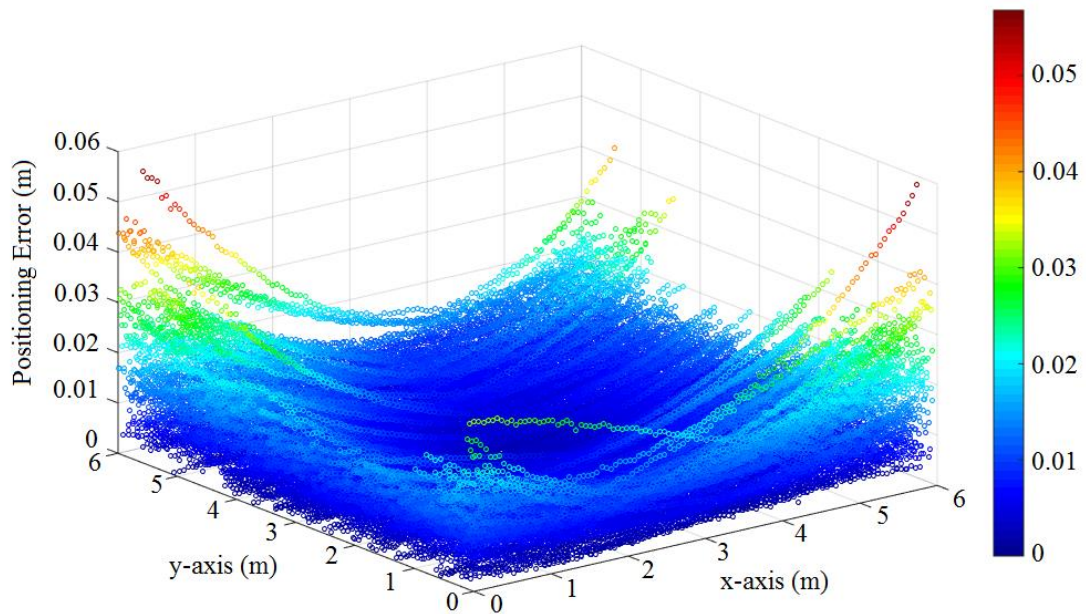


**Figure 4.28: Positioning Error of Proposed System with Zhang et al. (2014) Environment Setup**

In Nadeem et al. (2014) work, the frequency division multiplex (FDM) is used as the LEDs transmitter modulation method and time different of arrival (TDOA) is used for distance estimation. The simulation environment dimension is 5m x 5m x 3m and five LEDs are installed at coordinate of (2.5, 2.5, 3), (1.5, 3.5, 3), (1.5, 1.5, 3), (3.5, 1.5, 3) and (3.5, 3.5, 3). The average accuracy of Nadeem et al. (2014) VLC-IPS is  $2.0599 \times 10^{-5}$  m. The summary of Nadeem et al. (2014) work and positioning error figure was shown in Table 4.4 and Figure 4.29 respectively.

**Table 4.4: Method and Environment Setup (Nadeem et al., 2014)**

|                                  |   |
|----------------------------------|---|
| Modulation Method                | FDM   |
| Distance Estimation Method       | TDOA  |
| Environment Dimension            | 5m x 5m x 3m                                |
| LEDs Transmitter Coordinate      |   |
| 1. LED 1                         | 2.5, 2.5, 3                                 |
| 2. LED 2                         | 1.5, 3.5, 3                                 |
| 3. LED 3                         | 1.5, 1.5, 3                                 |
| 4. LED 4                         | 3.5, 1.5, 3                                 |
| 5. LED 5                         | 3.5, 3.5, 3                                 |
| <b>Average Positioning Error</b> | <b><math>2.0599 \times 10^{-5}</math> m</b> |

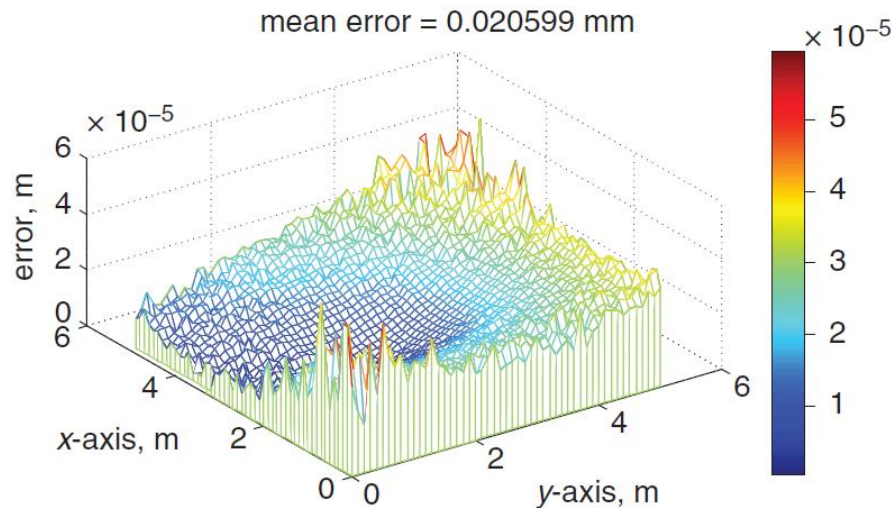


**Figure 4.29: Positioning Error (Nadeem et al., 2014)**

The average positioning error for the proposed design under similar environment as Nadeem et al. (2014) work is 0.0054m and the positioning error in XY-plane is shown in Figure 4.30.

The proposed system provide poorer accuracy as compared to Nadeem et al. (2014) work. This is because, in the proposed system, RSS distance estimation is used and it is prone to the Gaussian noise compared with the TDOA method. In the TDOA method, the phase shift of the modulated signals is used for distance computation hence the change in amplitude of the modulated signal that caused by Gaussian noise is not affecting the system performance. In the RSS method, the amplitude of the modulated signals is used for distance computation. These noise that causes small changes in the amplitude of the modulated signal which affects the accuracy, positioning error of the proposed RSS based VLC-IPS. However, in Nadeem et al. (2014), the TDOA distance estimation method have an advantage of immunity to Gaussian noise but it requires higher sampling frequency and processing rate. However, the proposed method, RSS method is subject to Gaussian noise but it does not required high sampling frequency. Nadeem et al. (2014) system is tabulated as Table 4.5.

**Table 4.5: Summary of Proposed System and Nadeem et al. (2014) System**

|                            | Proposed System | (Nadeem et al. (2014))<br>system |
|----------------------------|-----------------|----------------------------------|
| Modulation Method          | FDM             | FDM                              |
| Distance Estimation Method | RSS             | TDOA                             |
| Environment Dimension      | 5m x 5m x 3m    | 5m x 5m x 3m                     |
| Number of LEDs used        | 4               | 5                                |
| 1. LED 1 Coordinate        | 1.5, 1.5, 3     | 2.5, 2.5, 3                      |
| 2. LED 2 Coordinate        | 3.5, 1.5, 3     | 1.5, 3.5, 3                      |
| 3. LED 3 Coordinate        | 1.5, 3.5, 3     | 1.5, 1.5, 3                      |
| 4. LED 4 Coordinate        | 3.5, 3.5, 3     | 3.5, 1.5, 3                      |
| 5. LED 5 Coordinate        | -               | 3.5, 3.5, 3                      |
| Modulation Bandwidth       | 1 kHz           | Not stated                       |
| Average Positioning Error  | 0.0054m         | $2.0599 \times 10^{-5}$ m        |

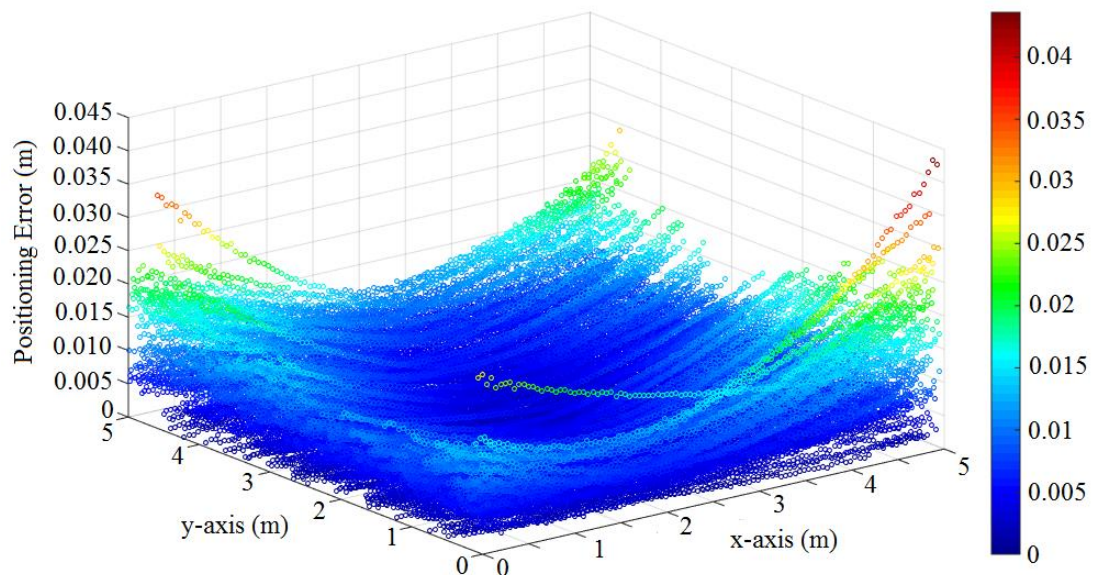


**Figure 4.30: Positioning Error of Proposed System with Nadeem et al. (2014) Environment Setup**

## CHAPTER 5

### CONCLUSION AND RECOMMENDATIONS

#### 5.1 Conclusion

The use of LED will become more popular in future due to cost efficiency. This drives the research on VLC-IPS system. In this proposed project, simulation software MATLAB, is use to simulate the feasibility of the proposed VLC-IPS system through Unique Frequency Modulation (F-ID). Firstly, the Frequency Division Multiplexing (FDM) is used for LEDs transmitter modulator to prevent interference from inter-cell or others light source such as sunlight and fluorescent. Secondly, the photodiode is used to retrieve the transmitter signal and processed by FFT to extract the amplitude of the modulated signal. Thirdly, the Received Signal Strength (RSS) is used to estimate the distance between transmitters and receiver by applying the Lambertian equation. Lastly, the trilateral method is used to estimate the receiver coordinate based on the distance information from RSS system.

The VLC-IPS simulation is modelled at the environment dimension of 6m x 6m x 4m with LEDs transmitters coordinate of (1, 1, 4), (5, 1, 4), (1, 5, 4), (5, 5, 4) and photodiode receiver lifted from ground by 1m. The average positioning error in VLC-IPS with all interference is 0.0105 m (1 cm) and average SNR is 59.8678 dB; however, for VLC-IPS system without fluorescent interference is 0.0084 m (0.84 cm) and average SNR without fluorescent light interference is 61.6284 dB. In a nutshell, the accuracy of the proposed system is having a good performance with RSS distance estimation method but it has lower performance compared with TDOA distance estimation method.

## 5.2 Recommendation

In F-ID method, only frequency is transmitted to represent the address of the transmitters, hence it have limited number of transmitters can be installed in a particular bandwidth. The transmitter modulation can be improved by using better modulation method such Dual-Tone Multiple Frequency (DTMF). By doing so, the number supported transmitter in a particular bandwidth will increase. This is because, DTMF is using transmitted data to represent address instead of using frequency. The more data bits are used for the address, the higher the number of transmitters can be supported.

Fast Fourier Transform (FFT) is used as signal extractor in this proposed project. Multiple number of IIR filter can be constructed to replace the FFT to provide faster response time. FFT have 1 second of data acquisition time; however IIR filter will process every sampling data immediately and shorten the processing time. Hence, using IIR filter will increase the responsive of the VLC-IPS.

## REFERENCES

- BARRIOS, C. & MOTAI, Y. 2011. Improving Estimation of Vehicle's Trajectory Using the Latest Global Positioning System With Kalman Filtering. *Instrumentation and Measurement, IEEE Transactions on*, 60, 3747-3755.
- BYTELIGHT. 2015. *ByteLight Homepage* [Online]. Available: <http://www.bytelight.com/about> 2015].
- CHANG, N., RASHIDZADEH, R. & AHMADI, M. 2010. Robust indoor positioning using differential Wi-Fi access points. *Consumer Electronics, IEEE Transactions on*, 56, 1860-1867.
- DRANE, C., MACNAUGHTAN, M. & SCOTT, C. 1998. Positioning GSM telephones. *Communications Magazine, IEEE*, 36, 46-54, 59.
- GU, Y., LO, A. & NIEMEGERES, I. 2009. A survey of indoor positioning systems for wireless personal networks. *Communications Surveys & Tutorials, IEEE*, 11, 13-32.
- HARUYAMA, S. Visible light communication using sustainable LED lights. ITU Kaleidoscope: Building Sustainable Communities (K-2013), 2013 Proceedings of, 2013. IEEE, 1-6.
- JUNG, S.-Y., HANN, S. & PARK, C.-S. 2011. TDOA-based optical wireless indoor localization using LED ceiling lamps. *Consumer Electronics, IEEE Transactions on*, 57, 1592-1597.
- KIM, H.-S., KIM, D.-R., YANG, S.-H., SON, Y.-H. & HAN, S.-K. 2013. An indoor visible light communication positioning system using a RF carrier allocation technique. *Lightwave Technology, Journal of*, 31, 134-144.
- KOMINE, T. & NAKAGAWA, M. 2004. Fundamental analysis for visible-light communication system using LED lights. *Consumer Electronics, IEEE Transactions on*, 50, 100-107.
- LEE, B.-J. S. K.-W., KIM, S.-H. C. J.-Y. & KIM, W. J. L. H. S. Indoor WiFi positioning system for Android-based smartphone. 2010. Information and Communication Technology Convergence (ICTC), 2010 International Conference on.
- LUO, P., GHASSEMLOOY, Z., LE MINH, H., KHALIGHI, A., ZHANG, X., ZHANG, M. & YU, C. Experimental demonstration of an indoor visible light communication positioning system using dual-tone multi-frequency technique. Optical Wireless Communications (IWOW), 2014 3rd International Workshop in, 2014. IEEE, 55-59.
- MOREIRA, A. J., VALADAS, R. T. & DE OLIVEIRA DUARTE, A. Characterisation and modelling of artificial light interference in optical wireless communication systems. Personal, Indoor and Mobile Radio Communications, 1995. PIMRC'95. Wireless: Merging onto the Information Superhighway., Sixth IEEE International Symposium on, 1995. IEEE, 326-331.

- NADEEM, U., HASSAN, N., PASHA, M. & YUEN, C. 2014. Highly accurate 3D wireless indoor positioning system using white LED lights. *Electronics Letters*, 50, 828-830.
- OWEN COMSTOCK, K. J. 2014. LED bulb efficiency expected to continue improving as cost declines. Annual Energy Outlook 2014 Early Release: U.S. Energy Information Administration.
- TANAKA, Y., KOMINE, T., HARUYAMA, S. & NAKAGAWA, M. 2003. Indoor visible light data transmission system utilizing white LED lights. *IEICE transactions on communications*, 86, 2440-2454.
- WANG, T. Q., SEKERCIOGLU, Y. A., NEILD, A. & ARMSTRONG, J. 2013. Position Accuracy of Time-of-Arrival Based Ranging Using Visible Light With Application in Indoor Localization Systems. *Journal of Lightwave Technology*, 31, 3302-3308.
- YASIR, M., HO, S.-W. & VELLAMBI, B. N. 2014. Indoor positioning system using visible light and accelerometer. *Journal of Lightwave Technology*, 32, 3306-3316.
- YAZICI, A., YAYAN, U. & YUCEL, H. An ultrasonic based indoor positioning system. Innovations in Intelligent Systems and Applications (INISTA), 2011 International Symposium on, 2011. IEEE, 585-589.
- ZHANG, W., CHOWDHURY, M. S. & KAVEHRAD, M. 2014. Asynchronous indoor positioning system based on visible light communications. *Optical Engineering*, 53, 045105-045105.

## **APPENDICES**

The softcopy of the FYP report will be include in the CD during final report submission.